Limits of Control Performance for Networked Control Systems with Random Communication Delays

by

Guoyang Yan

A thesis submitted in partial fulfillment of the requirements for the degree of

Doctor of Philosophy

in

Process Control

Department of Chemical and Materials Engineering

University of Alberta

© Guoyang Yan, 2020

Abstract

Networked control systems (NCSs) and distributed networked control systems (DNCSs) increasingly appear in the modern process industry due to continuous expansion of system scales, physical setups and functionalities. Control loops in a NCS are closed through information exchange between the spatially distributed controller and system components over a shared network, while local information in a DNCS is transmitted between different subsystems through a communication network to compensate for plant-wide interaction. However, the inevitable and time-varying network-induced communication delays degrade the system control performance and lead to a non-stationary behavior of the closed-loop system, which pose great challenges in the design of automatic control systems over network. On the other hand, control performance assessment is an asset-management technology aiming at optimal control performance and cost effectiveness. The key to control performance assessment is first to find the limit of control performance and then to estimate this benchmark control performance from routine operating data. This thesis extends the first step of centralized control performance assessment techniques to distributed networked control and networked control cases with random communication delays.

Input and output communication delays between different subsystems are posed as the controller and observer structure constraints in DNCSs. In order to handle random communication delays, the limits of control performance in terms of variance for DNCSs is proposed as a bounded performance region with respect to the range of communication delays. Then, the same idea is extend to characterize the limits of linear quadratic Gaussian (LQG) control

performance for DNCSs with the upper and lower LQG tradeoff curves.

Controller-to-actuator and sensor-to-controller communication delays are both considered as random values or first order Markov chains in NCSs. A practical linear time-varying (LTV) minimum variance benchmark is proposed for NCSs by using order of the interactor matrix (OIM) and relative degree of the interactor matrix (RIM). It is shown that the obtained benchmark terms can be estimated from routine operating data. Further, an explicit solution to time-varying model predictive control (MPC) is derived for NCSs, based on which the limits of control performance for networked model predictive control systems is proposed as the time-varying MPC performance tradeoff curve. The applicability and effectiveness of the proposed approaches are illustrated via their applications to different numerical and chemical process examples.

Preface

This thesis is an original work by Guoyang Yan under the supervision of Dr. Biao Huang and Dr. Jinfeng Liu, and is funded in part by Natural Sciences and Engineering Research Council (NSERC) of Canada. Most of materials have been published in peer-reviewed journals and a conference proceeding, listed below:

1. Guoyang Yan, Jinfeng Liu, and Biao Huang. Limits of control performance for distributed networked control systems in presence of communication delays. *International Journal of Adaptive Control and Signal Processing*, 2018 Sep 32(9): 1282-93. (*Chapter 2*)

   Authors' contributions: G. Yan conceived the original idea. This was also discussed with B. Huang and J. Liu. Mathematical derivations and algorithm programming were done by G. Yan. J. Liu provided many helpful suggestions on solving the problem numerically. G. Yan performed the simulation and drafted the manuscript. B. Huang and J. Liu provided critical feedback and helped shape the manuscript. All authors read and approved the final manuscript.

2. Guoyang Yan, Jinfeng Liu, Yousef Alipouri, and Biao Huang. Performance assessment of distributed LQG control subject to communication delays. *International Journal of Control*, 2020 May 28: 1-23. (*Chapter 3*)

   Authors' contributions: G. Yan conceived the presented idea in discussions with B. Huang, J. Liu and Y. Alipouri. G. Yan developed the main mathematical derivations,

programmed the algorithm and completed the simulation. J. Liu contributed to the selection of distributed observer structure. Y. Alipouri provided a method on choosing an initial stabilizing controller. B. Huang encouraged G. Yan to investigate the applicability of separation principle in distributed networked control and supervised the findings of this work. G. Yan wrote the manuscript. B. Huang and J. Liu revised it critically for important intellectual contents.

3. Guoyang Yan, Jinfeng Liu, and Biao Huang. MV benchmark for networked control systems with random communication delays. *IFAC-PapersOnLine*, 52(1): 970 C 975, 2019. 12th IFAC Symposium on Dynamics and Control of Process Systems, including Biosystems DYCOPS 2019. (*Chapter 4 - Short version*)

   Authors' contributions: G. Yan conceived the original idea. B. Huang provided many valuable suggestions on assessing control performance in the presence of non-stationary characteristics in routine operating data. G. Yan completed the mathematical derivations and verified it through the simulation. G. Yan wrote the manuscript with input from J. Liu and B. Huang. All authors discussed the results and approved the final manuscript.

Acknowledgements

First and foremost, it gives me great pleasure to express sincere gratitude to my supervisors, Dr. Biao Huang and Dr. Jinfeng Liu, for all their patience and support during my entire Ph.D. life. This thesis would have remained a dream had it not been for their guidance. I would like to show my admiration to their enthusiasms for work, creativeness in research and encouraging views to life, which are significant in assisting to build up my long-time career goals and experiences. Through my frequent interactions with them, I have been inspired by their insightful understandings of research and encouraged by their trusts when I got trapped. All of these bring me consistent encouragements and make me always keep passion and curiosity to explore the fields that I am working on. Ph.D. is indeed a tough and long journey, and I am so fortunate to be accompanied by the guidance from Dr. Huang and Dr. Liu.

It has been such a great honor to join the Computer Process Control Group at the Department of Chemical and Materials Engineering. The camaraderie and the cooperative spirit within the group has allowed me to debate and discuss my ideas freely with the talented group members. I would like to especially thank my former group member Dr. Yousef Alipouri for his academic supports to make me grow and learn faster. And I truly enjoy the friendship with group members including but not limited to: Lei Fan, Mengqi Fang, Yanjun Ma, Jingyi Wang, Xunyuan Yin, An Zhang. Additionally, I would also like to thank Liya Dong for her company and concern during the past year. Please wait for me to show up in front of you with the ring and the love.

I would like to thank the Alberta Innovates and National Science and Engineering Research Council of Canada for the financial supports and the University of Alberta to provide great opportunity for my Ph.D. experiences.

Special thanks to my beloved parents on the other side of the pacific for their encouragement and devotion. They have been always tolerating my willfulness and supporting me unconditionally, especially for the past five years. It is their love that gives me the courage and makes me stronger.

Contents

1 Introduction **1**

1.1 Motivation 1

1.2 Literature review 2

1.2.1 An overview of control performance assessment techniques 3

1.2.2 Multivariate minimum variance benchmark 6

1.2.3 LQG tradeoff curve 10

1.3 Contributions of this thesis 11

1.4 Organization of this thesis 12

2 Limits of Minimum Variance Control Performance for DNCSs with Random Communication Delays **15**

2.1 Introduction 15

2.2 Preliminaries 17

2.2.1 System description 17

2.2.2 Modeling of communication network 17

2.2.3 Controller structure 18

2.2.4 Main objective 19

2.3 Limits of distributed minimum variance control performance considering time-invariant communication delays 20

2.3.1 Problem formulation 21

2.3.2 Best achievable control performance 26
2.4 Limits of distributed minimum variance control performance considering random communication delays 27
2.5 Simulations 29
2.5.1 Case of time-invariant communication delays 29
2.5.2 Case of random communication delays 32
2.6 Conclusions 33

3 Limits of LQG Control Performance for DNCSs with Random Communication Delays 34

3.1 Introduction 34
3.2 Preliminaries 35
3.2.1 System description 35
3.2.2 Modeling of communication network 36
3.3 Objective and proposed approach 37
3.3.1 Structure of subsystem controllers 38
3.3.2 Structure of subsystem observers 39
3.3.3 Lower and upper LQG tradeoff curves 42
3.4 Limits of distributed LQG control performance 45
3.4.1 Distributed state feedback control 46
3.4.2 Distributed state feedback control combined with distributed state estimation 52
3.5 Simulations 57
3.6 Conclusions 63

4 Practical Solutions to LTV Minimum Variance Benchmark for NCSs with Random Communication Delays 64

4.1 Introduction 64

4.2 Preliminaries . . . 67
4.2.1 System description . . . 67
4.2.2 Illustrative example . . . 67
4.3 Control performance assessment of NCSs with random communication delay 72
4.3.1 Calculation of LTV transfer function matrices . . . 72
4.3.2 LTV minimum variance benchmark for NCSs with the simple interactor matrix . . . 74
4.3.3 Solutions to LTV minimum variance benchmark for NCSs with the general interactor matrix . . . 77
4.3.4 Practical considerations . . . 82
4.4 Application to a reactor-separator example . . . 85
4.5 Conclusions . . . 91

5 Limits of Control Performance for Networked Model Predictive Control Systems with Random Communication Delays 92

5.1 Introduction . . . 92
5.2 Preliminaries . . . 94
5.3 Time-varying MPC performance tradeoff curve for networked model predictive control systems . . . 95
5.3.1 Subspace matrices . . . 95
5.3.2 Time-varying MPC design . . . 100
5.3.3 Time-varying MPC performance tradeoff curve . . . 106
5.4 Simulations . . . 109
5.5 Conclusions . . . 114

6 Concluding Remarks and Future Works 115

6.1 Concluding remarks . . . 115
6.2 Recommendations for future works . . . 117

Appendix A Mathematical Backgrounds and Derivations of Chapter 4 **128**

A.1 Calculation of LTV transfer function matrices 128

A.2 Detailed derivations of LTV minimum variance benchmark for NCSs with the simple interactor matrix 131

A.3 Parameters of the reactor-separator process 135

Appendix B Detailed Derivations of Chapter 5 **136**

B.1 Proof of positive semi-definite matrix 136

List of Tables

4.1 Control performance assessment results of the pilot-scale process 71

A.1 Steady state values, system parameters and controller parameters of the reactor-separator process 135

List of Figures

1.1 The LQG tradeoff curve [1]. 10

2.1 Network topology design for DNCSs with random communication delays. . 18

2.2 Closed-loop system with separation of the interactor matrix. 21

2.3 Comparison of minimum achievable output variance under centralized control and distributed networked control with time-invariant communication delays. 30

2.4 Comparison of minimum achievable output variance under centralized control and its lower and upper bounds under distributed networked control with random communication delays. 31

3.1 Network topology design for DNCSs with random communication delays. . 37

3.2 The lower and upper LQG tradeoff curves. 43

3.3 Schematic of the closed-loop system. 46

3.4 Schematic of the closed-loop system. 53

3.5 Control actions and state estimation errors for two cases: 1) controller designed for $\lambda = 2$ combined with observer designed for $\lambda = 2$; 2) controller designed for $\lambda = 2^{-4}$ combined with observer designed for $\lambda = 2$. 60

3.6 LQG control performance for two cases: 1) controller designed for $\lambda = 2^{-4}$ combined with observer designed for $\lambda = 2^{-4}$; 2) controller designed for $\lambda = 2^{-4}$ combined with observer designed for $\lambda = 2$. 61

3.7 Comparison of best achievable LQG control performance under state feedback control combine with state estimation in case of centralized control and distributed networked control. 62
3.8 Optimal control efforts for the LQG cost function with different weights. . . 62

4.1 Schematic of NCSs with random communication delays. 66
4.2 Schematic diagram of the pilot-scale process. 68
4.3 Sequences of communication delays. 70
4.4 Closed-loop test of the IMC controller. 70
4.5 Schematic of the reactor-separator process. 86
4.6 Sequences of communication delays. 88
4.7 Closed-loop test of the PID controller 89
4.8 Lower and upper bounds of the LTV minimum variance benchmark. 90
4.9 Performance indexes of the PID controller. 90

5.1 Schematic of NCSs with random communication delays. 94
5.2 Sequences of communication delays. 110
5.3 Output trajectories for the two control cases. 112
5.4 Output and input trajectories for current control system. 113
5.5 The time-varying MPC performance tradeoff curves for different time intervals. 114

List of Abbreviations and Notations

Abbreviations

NCS	Networked control system
DNCS	Distributed networked control system
LQG	Linear quadratic Gaussian
OIM	Order of the interactor matrix
RIM	Relative degree of the interactor matrix
MPC	Model predictive control
LTV	Linear time-varying
ARMA	Autoregressive moving average
BMI	Bilinear matrix inequality
LTI	Linear time-invariant
IMC	Internal model control
PID	Proportional-integral-derivative

Notations

a_t	White noise sequence
A, B, C	Dynamic state space system matrices
$A_{cl}, B_{cl}, C_{cl}, D_{cl}$	Dynamic state space system matrices of the closed-loop system
A_c, B_c, C_c, D_c	Dynamic state space system matrices of the controller
A_e, B_e, C_e, D_e	Dynamic state space system matrices of the observer
$C(q^{-1}, k)$	LTV output feedback controller
d_{ij}	Communication delay between the i^{th} and the j^{th} subsystems
d_{min}	Maximum communication delay in DNCSs
d_{max}	Minimum communication delay in DNCSs
d_s	Order of the interactor matrix
$d_s - v_s$	Relative degree of the interactor matrix
$d_{ca}(k)$, δ_t	Controller-to-actuator communication delays
$d_{sc}(k)$, τ_t	Sensor-to-controller communication delays
$\bar{d_{ca}}$, $\bar{\delta}$	Maximum controller-to-actuator communication delays
$\bar{d_{sc}}$, $\bar{\tau}$	Maximum sensor-to-controller communication delays
$D(q^{-1})$	The interactor matrix
$diag(\cdot)$	Diagonal matrix operator
$E(\cdot)$	Expectation operator
F	Controller gain matrix
$F(q^{-1})$	Matrix polynomial

$G_{cl}(q^{-1}, k)$	Transfer function matrix representation of the closed-loop system
$H_f^N\|_{\tau_t}$	Subspace matrix corresponding to the deterministic inputs
I	Identity matrix
L	Observer gain matrix
$L_w^N\|_{\tau_t}$	Subspace matrix corresponding to the past inputs and outputs
$N(q^{-1})$	Disturbance transfer function matrix
q^{-1}	Backshift operator
$Q(q^{-1}, t)$	LTV output feedback controller
$R(q^{-1})$	Rational transfer function matrix
t, k	Time instants
$tr(\cdot)$	Trace of matrix
$T(q^{-1})$	Process transfer function matrix
$\tilde{T}(q^{-1})$	Delay-free process transfer function matrix
U_t, U_k	Manipulated inputs
$var(\cdot)$	Variance operator
Y_t, Y_k	Measured outputs
$\tilde{Y}_t, \tilde{Y}_k$	Interactor-filtered outputs
$Y_t\|_{mvc}$	Output under centralized minimum variance control
$Y_t\|_{mvd}$	Output under distributed minimum variance control
Z_t	Controlled output

$\|\cdot\|$	H_2 norm
λ, ω	Weighting factors
Λ_τ	Transition probability matrix of τ_t
Λ_δ	Transition probability matrix of δ_t
Δ	Communication delay sequence of δ_t
η_c	Performance index of centralized case
$\eta_n^{lower}(k)$	Lower performance index of networked control case
$\eta_n^{upper}(k)$	Upper performance index of networked control case
$\Phi_{mv}^{lower}(k)$	Lower bound of the LTV minimum variance benchmark
$\Phi_{mv}^{upper}(k)$	Upper bound of the LTV minimum variance benchmark

Chapter 1

Introduction

1.1 Motivation

NCS has been one of the most attractive topics in both industry and academia due to continuously expanding physical setups and functionalities in modern industrial processes [2, 3, 4, 5]. A typical NCS consists of spatially distributed controller and system components (physical plants, actuators, sensors, etc.). Control loops in a NCS are closed through information exchange between the spatially distributed controller and system components over a shared network. The elimination of unnecessary wiring in NCSs reduces overall cost for the installation of control systems and provides ease in maintenance. In addition, by connecting cyber to physical space through communication network, NCSs are able to fuse global information and operate systems across long distance [6, 7]. On the other hand, large-scale processes typically can be decomposed into several operating subsystems that interact with each other through materials, energy and information networks. Design of automatic control systems from the distributed and the networked perspectives has gained popularity [8, 9]. In a DNCS, which denotes NCS with a number of spatially distributed subsystems, local information is transmitted between different subsystems through a communication network to compensate for plant-wide interaction. Different subsystems efficiently cooperate with

each other through the information exchange to achieve a desired control performance and to reduce the computation cost. This feature makes DNCS more structurally flexible and favorable for fault tolerance.

However, the inevitable and time-varying network-induced communication delays degrade the system control performance and lead to a non-stationary behavior of the closed-loop system, which pose great challenges in the design of automatic control systems over network [10, 11]. Therefore, for better regulation of systems, the design of advanced control algorithms for NCSs and DNCSs has largely preoccupied the control researchers' efforts; the authors are referred to [12, 13, 14, 15] for results on distributed networked control and [16, 17, 18, 19, 20, 21] for results on networked control. Although a variety of control design techniques have been proposed, the literature is relatively sparse on studies concerned with control performance assessment of NCSs and DNCSs. Control performance assessment is an important asset-management technology with a goal towards achieving optimal control performance [22, 23], in which the limit of control performance for an existing control system is determined and used to evaluate the potential for control performance improvement. Finding the limit of control performance is helpful on maintaining control performance of a NCS or a DNCS. Comparing with the theoretically best achievable one, the potential for further control performance improvement indicates the needs for the tuning of controller and observer or the improvement of communication network topology. In this thesis, for control performance assessment purpose, the limits of control performance for DNCSs and NCSs with random communication delays is derived.

1.2 Literature review

In this section, literature review of control performance assessment is first presented. Then, the main mathematical techniques and concepts employed throughout this thesis is illustrated. Starting from the definition of the unitary interactor matrix, the algorithm of the

multivariate minimum variance benchmark is explained. Further, the idea of the LQG trade-off curve is introduced.

1.2.1 An overview of control performance assessment techniques

The notable work of the minimum variance benchmark for univariate processes laid the theoretical foundation for control performance assessment [24], where the control objective was to minimize output variance and the feedback controller-invariant term was proposed as a benchmark to assess control loop performance. This contribution was significant due to the fact that only the *a priori* knowledge of univariate system time delay is required for the estimation of the benchmark term from routine operating data. Another related performance assessment statistic defined as the normalized performance index was proposed in [25]. Then, the idea of minimum variance benchmark was extend to unstable and non-minimum phase univariate processes in [26].

The concept of univariate system time delay, which denotes delay between a pair of input and output, is important in determining univariate minimum variance control. This idea was extended to multivariate minimum variance control, where delay between a set of inputs and outputs is termed as the interactor matrix. The interactor matrix was first proposed in [27] with a lower triangular form. The multivariate minimum variance control law designed based on this form of the interactor matrix is output-order dependent [28]. Then, the unitary interactor matrix is proposed in [29] as a special form of the interactor matrix. The unitary interactor matrix is an all-pass factor, and factorization of such interactor matrix retains the spectral property of the underlying system and is ideal for the design of multivariate minimum variance control [1]. By introducing the unitary interactor matrix, the works of Huang [30] and Harris [31] extended the minimum variance benchmark to multivariate processes, where the minimum variance control law is shown to be unique.

The algorithm for factoring the lower triangular interactor matrix as proposed in [27] requires a complete knowledge of the process model. However, a large-scale process typically

consists of thousands of control loops, where process dynamics and disturbances may vary with time. Identification and on-line update of such a process model are demanding requirements. Moreover, control performance assessment should be carried out with disturbing the running system as less as possible. Thus, factoring the interactor matrix from process model is not a desirable approach. An algorithm for directly estimating the unitary interactor matrix from closed-loop data was proposed in [32] to promote the use of multivariate minimum variance control as a benchmark for control performance assessment.

In the work of Huang [30], the minimum variance benchmark for multivariate processes was introduced by considering system time delays (the unitary interactor matrix) as the most fundamental performance limitation. Some extensions of this work were proposed to cover more realistic performance limitations. In [1], the generalized unitary interactor matrix was proposed to factorize both the non-minimum phase zeros and the infinite zeros from process model, based on which the control performance assessment algorithm for multivariate non-minimum phase processes was provided. User-specified benchmarks were proposed in [33, 34] to include design specifications of the closed-loop system dynamics. In [35], the minimum feedforward plus feedback control variance was shown estimable from routine operating data, and can then be used as a benchmark for performance assessment of feedforward plus feedback controllers.

Although the unitary interactor matrix can be estimated from closed-loop data [32] with perturbations, the obtained unitary interactor matrix is generally not accurate enough and not easily understood for practical application. Hence, reducing the complexity of the requirement to develop the interactor matrix is of interest [36]. Ko and Edgar [37] proposed a method to estimate the multivariate minimum variance benchmark using routine operating data, which does not require the intermediate interactor matrix. McNabb and Qin [38] developed an algorithm for assessing control performance from routine operating data using subspace projection and state space formulation. Although these attempts reduced the complexity of the *a priori* knowledge to some extent, they all require certain information that is

fundamentally equivalent to the interactor matrix. Then, practical solutions to multivariate feedback control performance assessment were introduced in [39] by using OIM and RIM. In [40], estimation of the upper and lower bounds of the multivariate minimum variance benchmark from routine operating data is proposed with known I/O delay matrix.

So far, various control performance assessment methods exist for stationary systems. But there are only few results available for assessing control performance in the presence of non-stationary characteristics in routine operating data. Control performance assessment techniques developed for processes with time-varying disturbance dynamics were introduced in [41, 42]. Li and Evans [43] proposed a d-step ahead minimum variance control algorithm for LTV processes in the form of autoregressive moving average (ARMA) models. Huang [44] developed a general framework for the minimum variance benchmark of LTV univariate processes, and the industrial applications of this work were presented in [45].

Minimum variance control provides useful information for control performance assessment, as no other controller can achieve a lower output variance. However, tighter requirements on output variance result in stronger disturbance rejection, and typically requires larger variation in control action (more control effort) [46]. Minimum variance control is usually not practical for real process operation due to its demand for excessive control effort and poor robustness. One may be interested in knowing how far away the real system output variance is from the best achievable system output variance with the same control effort. Grimble [47] proposed the generalized minimum variance benchmark for univariate processes by considering control effort penalty, and this work was further extended to multivariate processes in [48]. Huang [1] proposed the use of the LQG benchmark for control performance assessment, where the LQG tradeoff curve was introduced to show the limit of control performance in terms of the best achievable input and output variances. As recommended in [1], the LQG solution can be achieved with the infinite generalized predictive control approach, or can be approximated by the generalized predictive control solution with a finite prediction horizon in practice. However, calculation of the LQG solution relies on a

complete knowledge of the process model. A simpler method for obtaining the LQG benchmark based on the Lyapunov equation and subspace matrices was proposed in [49]. Kadali and Huang [50] proposed a subspace identification based approach to directly estimate the LQG benchmark from routine operating data. A subspace method for LQG design and performance assessment of supervisory-regulatory control systems was proposed in [51].

In addition, MPC has been proven as one of the most effective advanced process control strategies to deal with constraint control problems and economic objectives. The LQG benchmark cannot handle the hard constraints and is an unattainable benchmark for commercial MPC algorithms. Julien, Foley and Cluett [52] pointed out that, unless the actual disturbance is a random walk, the best achievable MPC performance will never fall on the LQG benchmark even if the constraints are inactive. Then, several results for performance assessment of MPC were developed by considering constraints in control problems [53, 54, 55, 56]. Economic performance assessment methods of MPC were proposed in [57, 58] through the syntheses of variance control objectives and economic objectives using optimization-based approaches.

However, all of the aforementioned methods are concerned with performance assessment of centralized control systems. In NCSs and DNCSs, the time-varying network-induced communication delays degrade the system control performance and lead to a non-stationary behavior of the closed-loop system. The influence of communication delays on the best achievable system control performance has been seldom considered in existing control performance assessment methods. This fact motivates the works of this thesis.

1.2.2 Multivariate minimum variance benchmark

The aim of the minimum variance benchmark for multivariate processes is first to design the benchmark term (output with minimum variance), then estimate this benchmark term from routine operating data by multivariate time series analysis. In the following, we will adopt the algorithm developed in [30] to illustrate this procedure. Unless otherwise illustrated, a

standard multivariate process model

$$Y_t = T(q^{-1})U_t + N(q^{-1})a_t \tag{1.1}$$

is used throughout the thesis, where $T(q^{-1})$ and $N(q^{-1})$ are proper, rational transfer function matrices in the backshift operator q^{-1}; Y_t, U_t and a_t are the output, input and disturbance vectors of dimensions n_y, n_u and n_a, respectively. For simplification purposes, we make the following assumptions without loss of generality:

1. $T(q^{-1})$ and $N(q^{-1})$ are square transfer function matrices and contain no non-minimum phase zeros except for infinite zeros;

2. a_t is white noise with zero mean and unit variance.

Non-minimum phase zeros in $N(q^{-1})$ can be factored out by an all pass factor without affecting the noise spectrum. Further, when $E[a_t a_t^T] \neq I$, the disturbance model $N(q^{-1})$ can always be scaled to satisfy this assumption. For the sake of brevity, in the rest of this thesis, the backshift operator q^{-1} is dropped in the expression of all transfer function matrices unless circumstances necessitate its presence.

The system time delays of multivariate processes T can be factored as

$$T = D^{-1}\tilde{T} \tag{1.2}$$

where D is called the unitary interactor matrix [59] and can be served as the optimal generalization of univariate system time delay to the multivariate case. In equation (1.2), D^{-1} contains the infinite zeros of T, and $\tilde{T}$ is an invertible transfer function matrix which only contains the finite zeros of T.

Definition 1 *A non-singular polynomial matrix D is defined as the interactor matrix, if for a proper rational transfer function matrix T, such that*

$$\lim_{q^{-1}\to 0} DT = \lim_{q^{-1}\to 0} \tilde{T} = K \tag{1.3}$$

where K is a full rank constant matrix; $\tilde{T}$ is a delay-free (invertible) transfer function matrix of T. The matrix D can be written as

$$D = D_0 q^{d_s} + D_1 q^{d_s-1} + \cdots + D_{v_s} q^{d_s-v_s} \tag{1.4}$$

where d_s is OIM which is the maximum power of q in D; v_s is RIM which is the difference between the maximum and the minimum power of q in D; D_i $(i = 0, \cdots, v_s)$ is coefficient matrix. If the interactor matrix D satisfies $D^T(q^{-1})D(q) = I$, then this interactor matrix is further defined as the unitary interactor matrix, thus

$$D^{-1} = D_{v_s}^T q^{-d_s+v_s} + \cdots + D_1^T q^{-d_s+1} + D_0^T q^{-d_s} \tag{1.5}$$

There are three different forms for the interactor matrix D: 1) $D = q^{d_s} I$ is a simple interactor matrix; 2) $D = diag(q^{d_{s1}}, q^{d_{s2}}, \cdots, q^{d_{sn_y}})$ is a diagonal interactor matrix; 3) D is a general interactor matrix otherwise [60].

In stationary case, it has been shown that multiplying an unitary interactor matrix to the output does not change its variance, i.e.

$$E[\tilde{Y}_t^T \tilde{Y}_t] = E[Y_t^T Y_t] \tag{1.6}$$

where $\tilde{Y}_t = q^{-d_s} D Y_t$, which can be called as the interactor filtered output. Multiplying $q^{-d_s} D$

to both sides of equation (1.1) yields

$$\tilde{Y}_t = q^{-d_s} DY_t = q^{-d_s} \tilde{T} U_t + q^{-d_s} DNa_t \tag{1.7}$$

where using the Diophantine identity:

$$q^{-d_s} DN = F + q^{-d_s} R \tag{1.8}$$

where, F is the polynomial matrix consisting of the first d_s terms in $q^{-d_s} DN$, and R is the remaining transfer function matrix in $q^{-d_s} DN$. Then, $\tilde{Y}_t$ can be written as

$$\tilde{Y}_t = Fa_t + q^{-d_s}(\tilde{T} U_t + Ra_t) \tag{1.9}$$

Since the two terms on the right hand side of equation (1.9) are independent, as a result

$$E[\tilde{Y}_t^T \tilde{Y}_t] \geq E[(Fa_t)^T (Fa_t)] \tag{1.10}$$

Thus, for centralized control systems, $\tilde{Y}_t$ with minimum variance can be obtained as

$$\tilde{Y}_t|_{mvc} = Fa_t = F_0 a_t + \cdots + F_{d_s-1} a_{t-d_s+1} \tag{1.11}$$

where F_i $(i = 0, \cdots, d_s - 1)$ is the i_{th} coefficient matrix in F. The corresponding centralized minimum variance control law is given by

$$U(t)|_{mvc} = -\tilde{T}^{-1} R F^{-1} \tilde{Y}_t|_{mvc} \tag{1.12}$$

Due to the minimum variance benchmark term is independent of U_t as shown in equation (1.9), the coefficient matrices $F_0, \cdots, F_{d_s-1}$ can be estimated from the interactor filtered routine operating data of any stable process output Y_t by simple multivariate time series

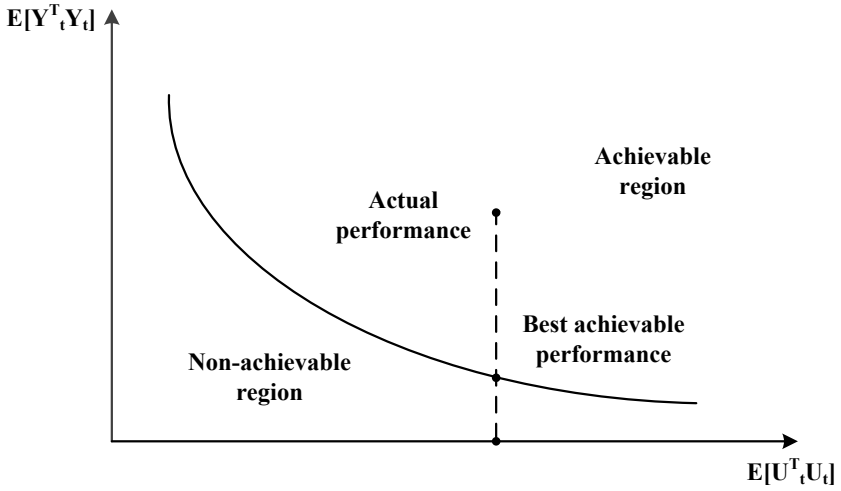

Figure 1.1: The LQG tradeoff curve [1].

analysis [30]. Then, the centralized control performance index can be calculated as

$$\eta_c = \frac{E[\tilde{Y}_t|_{mvc}^T \tilde{Y}_t|_{mvc}]}{E[Y_t^T Y_t]} = \frac{tr(F_0^T F_0 + \cdots + F_{d_s-1}^T F_{d_s-1})}{tr(var(Y_t))} \tag{1.13}$$

1.2.3 LQG tradeoff curve

In general, variation in a system arises from the disturbance. Tighter requirements on output variance result in stronger disturbance rejection, and typically requires larger variation in control action (more control effort) [50, 46]. Due to this tradeoff between output variance and control effort, one may be interested in knowing how far away the real system output variance is from the best achievable output variance with the same control effort.

In the control performance assessment based on the LQG benchmark, a tradeoff curve as shown in Figure 1.1 is used to solve this problem. The tradeoff curve is obtained from

solving the LQG problem with an objective function defined by

$$J(\omega) = E[Y_t^T Y_t] + \omega E[U_t^T U_t] \tag{1.14}$$

where ω is weighting factor. By varying ω, various LQG control solutions of control effort $E[U_t^T U_t]$ and output variance $E[Y_t^T Y_t]$ can be calculated. Then, the tradeoff curve can be determined from these solutions with the optimal $E[U_t^T U_t]$ as the x-axis and $E[Y_t^T Y_t]$ as the y-axis, respectively.

The whole control region is divided into the achievable region and the non-achievable region by the obtained LQG tradeoff curve. Any linear controller can only operate in the achievable region which is above the LQG tradeoff curve. With a given $E[U_t^T U_t]$ in real system, the best achievable value of $E[Y_t^T Y_t]$ can be found from this curve. The difference between the best achievable $E[Y_t^T Y_t]$ and the real $E[Y_t^T Y_t]$ can be used for control performance assessment.

1.3 Contributions of this thesis

The main contributions of this thesis are listed below:

1. Proposed the limits of control performance in terms of variance for DNCSs with random communication delays as a bounded performance region;

2. Proposed the lower and upper LQG tradeoff curves to characterize the limits of LQG control performance for DNCSs with random communication delays. Investigated and demonstrated the non-applicability of separation principle in distributed networked control;

3. Derived an explicit solution to LTV minimum variance control of NCSs with random communication delays. Developed a practical LTV minimum variance benchmark for

NCSs by using OIM and RIM, where the benchmark terms are shown to be estimable from routine operating data;

4. Derived an explicit solution to time-varying MPC of NCSs with random communication delays. Proposed the time-varying MPC performance tradeoff curve for control performance assessment of networked model predictive control systems.

1.4 Organization of this thesis

In Chapter 2, the limits of control performance in terms of variance for DNCSs with random communication delays is investigated. With a goal towards the best achievable control performance, a fixed network topology is designed for DNCSs where each subsystem in the network can communicate directly with all the other subsystems. Output communication delays and system time delays serve as the most fundamental performance limitations in distributed networked control, and are fully considered in the proposed distributed output feedback controller design. First, an optimization-based solution to minimum variance control of DNCSs with time-invariant communication delays is developed. The obtained output with minimum achievable variance is equal to the feedback controller-invariant term plus a polynomial term with its order equal to the maximum communication delay between different subsystems. Then, this result is extend to DNCSs with random communication delays, where the lower and upper bounds of the minimum achievable output variance are obtained by considering boundary values of random communication delays. Finally, a numerical case study is conducted to compare the best achievable performance between centralized control and distributed networked control in terms of the output variance.

In Chapter 3, the lower and upper LQG tradeoff curves are proposed to characterize the limits of LQG control performance for DNCSs with random communication delays. As an alternative to the work in Chapter 2, a distributed LQG control framework is developed by further considering input communication delays and control effort penalty. The opti-

mal structures of distributed state feedback controllers and distributed observers are first presented. Furthermore, a algorithm is proposed for designing distributed controllers and distributed observers simultaneously, based on which the lower and upper LQG tradeoff curves can be obtained. State estimation performance and control performance of the proposed algorithm are illustrated via a simulation study, and the non-applicability of separation principle in distributed networked control is tested.

In Chapter 4, practical solutions to the LTV minimum variance benchmark are developed for NCSs with random communication delays, where sensor-to-controller communication delay and controller-to-actuator communication delay are considered as independent random variables. The interactor matrix estimated from closed-loop data is generally not accurate enough in practice, especially when there are non-stationary characteristics in closed-loop data. Hence, the interactor matrix should be avoided when obtaining the control performance assessment benchmark for NCSs. To begin with, an explicit solution to the LTV minimum variance benchmark is derived for NCSs with the simple interactor matix. Furthermore, this result is extended to the development of practical solutions to the LTV minimum variance benchmark for NCSs with the general interactor matrix, where only OIM and RIM are assumed to be known as the *a priori* knowledge. Finally, a direct method is proposed to estimate the benchmark terms from routine operating data. The theoretical results are demonstrated through the application to a reactor-separator chemical process.

In Chapter 5, the time-varying MPC performance tradeoff curve is proposed to characterize the limits of control performance for networked model predictive control systems with random communication delays. Sensor-to-controller communication delay and controller-to-actuator communication delay are considered as first order Markov chains with known transition probabilities. In particular, an explicit solution to time-varying MPC of NCSs is derived by minimizing the expectation of a quadratic cost function over all possible future communication delays in the prediction horizon. Based on this control design, the time-varying MPC performance tradeoff curve is presented for control performance assessment of

networked model predictive control systems. Further, a strategy is provided for obtaining the time-varying MPC performance tradeoff curve from process model. The effectiveness of the proposed control design and the use of the time-varying MPC performance tradeoff curve in control performance assessment are illustrated via a simulation study.

In Chapter 6, the entire thesis is summarized and the future works are presented based on practical needs for further improvements.

This thesis has been written in a paper-format in accordance with the rules and regulations of the Faculty of Graduate Studies and Research, University of Alberta. Many of the chapters have appeared or are to appear in archival journals or conference proceedings. In order to link the different chapters, there is some overlap and redundancy of material. This has been done to ensure completeness and cohesiveness of the thesis material and help the reader understand the material easily.

Chapter 2

Limits of Minimum Variance Control Performance for DNCSs with Random Communication Delays[1]

2.1 Introduction

Nowadays, large-scale processes usually consist of several unit operations (subsystems) which interact with each other through networks of material, energy and information streams. A substantial increase of plant scale and complexity leads to high computation cost as well as reduced fault tolerance for centralized control system. Due to these concerns, the development of DNCSs has attracted much attention [5, 8]. In a DNCS, a local controller is designed for each subsystem, and different local controllers efficiently cooperate in achieving the desired control objectives. Information of local states, control actions and outputs is transmitted between different subsystems through the communication network to compensate for plant-wide interaction [9, 61]. In this way, computation cost can be reduced, and

[1] A shorter version of this chapter has been published in "Guoyang Yan, Jinfeng Liu, and Biao Huang. Limits of control performance for distributed networked control systems in presence of communication delays. International Journal of Adaptive Control and Signal Processing. 2018 Sep 32(9): 1282-93".

control performance can be guaranteed to a certain degree. Furthermore, because each local controller works separately, DNCS is more favorable in terms of fault tolerance as well as maintenance compared to the centralized one.

However, distributed networked control framework poses additional limitations on the best achievable control performance, where communication delays are the most fundamental one. In a DNCS, a communication network is needed for data exchange between different subsystems. Communication delays caused by wireless network, bandwidth limits, or triggered communication are one of the key factors that may affect control performance [14]. Hence, the overall control performance of a DNCS will be subpar compared to the one that can be achieved in the centralized case.

Motivated by the above discussions, to maintain highly efficient operation performance of DNCSs, this chapter is concerned with the limits of control performance in terms of variance for DNCSs with random communication delays. An explicit solution to distributed minimum variance control has great theoretical and practical value, but it is also equally difficult to obtain. The main difficulty arises due to the controller structure constraints caused by communication delays, as this yields a non-convex optimization problem. In this chapter, (i) communication delays are posed as the controller structure constraints; (ii) the gap between the minimum achievable output variance under centralized control and distributed networked control is proven to be a polynomial term with its order equal to the maximum communication delay between different subsystems. As a special case, when a DNCS has perfect communication, distributed networked control has the same best achievable performance as centralized control; (iii) minimum variance control for DNCSs with time-invariant communication delays is modeled as an optimization problem and solved using sums of squares programming; (iv) limits of minimum variance control performance for DNCSs with random communication delays is chosen as a region between the lower and upper bounds of minimum achievable output variance by selecting communication delays between all subsystems as the minimum and the maximum values, respectively; (v) a simulated

example is incorporated to show the results of the proposed work.

2.2 Preliminaries

2.2.1 System description

Consider a discrete-time linear time-invariant (LTI) system:

$$Y_t = TU_t + Na_t \tag{2.1}$$

where t indicates current time instant; T and N are proper rational transfer function matrices in the backshift operator q^{-1}; Y_t, U_t and a_t are output, input and disturbance vectors of appropriate dimensions. The whole system is divided into n subsystems. Y_{it} and U_{it} are the output and input vectors of subsystem i with proper dimensions, respectively. Thus, $Y_t = [Y_{1t}^T, \ldots, Y_{nt}^T]^T$ and $U_t = [U_{1t}^T, \ldots, U_{nt}^T]^T$.

2.2.2 Modeling of communication network

In this chapter, we consider a distributed networked control framework as shown in Figure 2.1, where a class of discrete-time LTI systems are composed of n interconnected subsystems. Measurements of the n subsystems are sampled synchronously and periodically at time instant t_k which is the starting time of the k^{th} sampling period. Each subsystem controller is assumed to have direct and immediate access to the measurements of its corresponding subsystem, and can transmit information of the local measurements to all other subsystem controllers through a communication network. Further, information is assumed to be transmitted (and received) by subsystem controllers once within each sampling period, and the exchange of information is subject to random communication delays. The delay of information transmission from subsystem j to subsystem i at time instant t_k is denoted as a positive integer $d_{ij}(t_k)$. If at time t_k, controller i receives the latest information of controller j sent

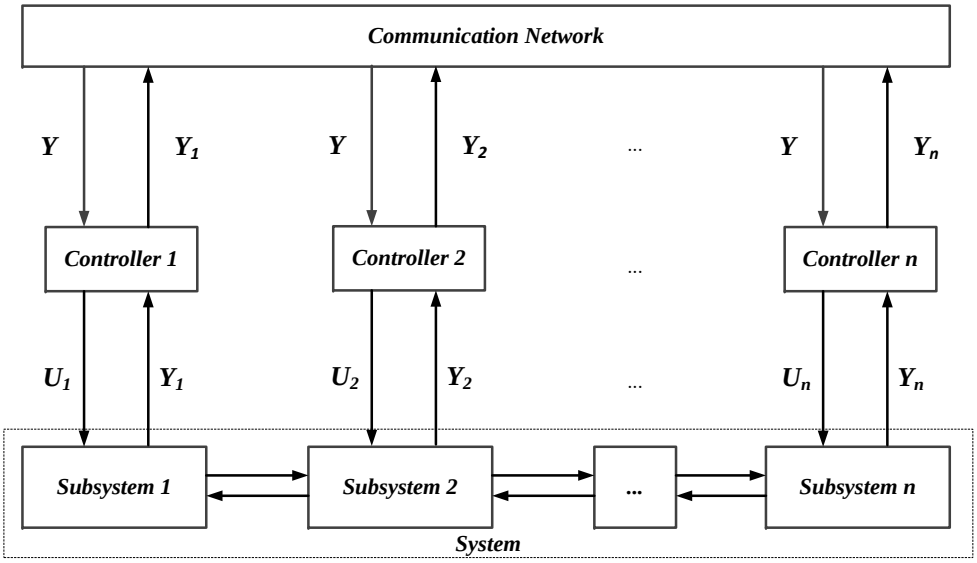

Figure 2.1: Network topology design for DNCSs with random communication delays.

at time t_{k-q}, then $d_{ij}(t_k) = q$. Further, the maximum and the minimum possible values of $d_{ij}(t)$ for $1 \leq i, j \leq n, i \neq j$ are predetermined, denoting as d_{max} and d_{min}, respectively. In each sampling period, all measurements of a subsystem are transmitted together as one package.

2.2.3 Controller structure

For many DNCSs, although systems are running distributedly, controllers can be centrally designed and then applied distributedly in the real-time functioning. In this case, the design of control law for each subsystem is done with common knowledge of the other subsystems. Thus, the design problem is more trackable and the global control performance is more reliable [15].

In this chapter, a distributed output feedback controller is designed in the centralized way for DNCSs shown in Figure 2.1. Without loss of generality, the controller for each subsystem is designed based on the available output information from all subsystems. The

whole controller can be expressed as $U_t = Q(t)Y_t$, where

$$Q(t) = \begin{bmatrix} q^{-d_{11}(t)}Q_{11}(t) & \cdots & q^{-d_{1n}(t)}Q_{1n}(t) \\ \vdots & \vdots & \vdots \\ q^{-d_{n1}(t)}Q_{n1}(t) & \cdots & q^{-d_{nn}(t)}Q_{nn}(t) \end{bmatrix} \tag{2.2}$$

is a controller of transfer function matrix in the backshift operator q^{-1} at time t. In equation (2.2), $Q_{ij}(t)$ is the $(i,j)^{th}$ sub block of $Q(t)$, and $d_{ij}(t)$ is the communication delay from subsystem j to i at time t. Normally, $d_{ij}(t) = 0$ when $i = j$. The controller of subsystem i is the i^{th} row of $Q(t)$ which can be expressed as

$$U_{it} = Q_{ii}(t)Y_{it} + \sum_{j=1}^{n,j\neq i} q^{-d_{ij}(t)}Q_{ij}(t)Y_{jt} \tag{2.3}$$

According to equation (2.3), in the controller of subsystem i, the output information of subsystem j is used up to time $t - d_{ij}(t)$, and all the information of subsystem j after time $t - d_{ij}(t)$ is unavailable to subsystem i due to communication delays.

The structure of $Q(t)$ is constrained by communication delays in the outputs at time t. Thus, the control structure considered in this chapter only depends on the output feedback. When a control structure also has input communication delays, further performance limitation will be expected. A time-varying controller is needed to achieve the theoretical lower bound of the output variance when there are random communication delays. Further, the controller shown in equation (2.2) can be reduced to a time-invariant controller if communication delays are time-invariant.

2.2.4 Main objective

The main objective of this chapter is to find the theoretically achievable lower bound of $tr[var(Y_t)]$ in DNCSs considering two types of communication delays; time-invariant communication delays and random communication delays, respectively. The achievable value of

$tr[var(Y_t)]$ is limited by system time delays when we can design multivariate controller with full degree of freedom. In DNCSs, such a value will further be limited by the controller structure constraints caused by communication delays. To distinguish the influence of different limitations, we denote the minimum output variance under distributed networked control as

$$\min_{Q(t)} tr[var(Y_t)] = J_{sysd} + J_{comd} \tag{2.4}$$

where $Q(t)$ is the controller with structure constraints shown in equation (2.2); J_{sysd} is equal to the multivariate minimum variance benchmark obtained in centralized control systems, which is the most fundamental limit of control performance caused by system time delays; J_{comd} is the additional term caused by communication delays in DNCSs, and can be served as the gap of the best achievable control performance between centralized control systems and DNCSs.

2.3 Limits of distributed minimum variance control performance considering time-invariant communication delays

In this section, we derive an explicit relationship between the minimum achievable output variance and the distributed controller which suffers from time-invariant communication delays. The best achievable control performance for DNCSs with time-invariant communication delays is obtained through optimization-based method. Because communication delays are time-invariant, the parameter t is dropped from $Q(t)$ and $d_{ij}(t)$ in this section.

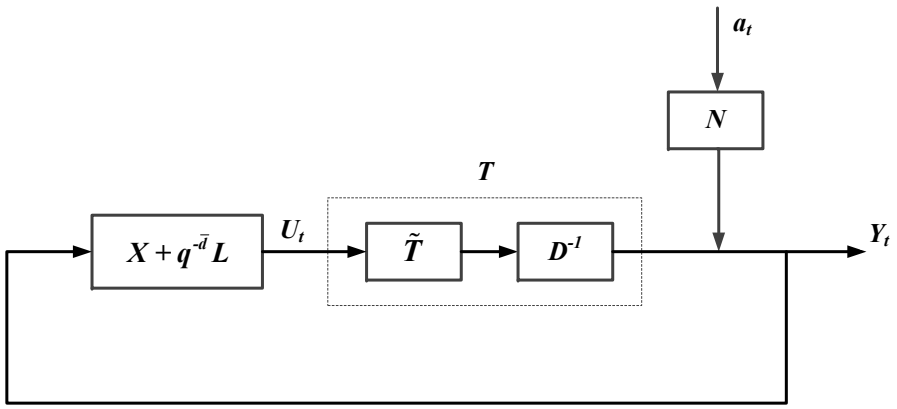

Figure 2.2: Closed-loop system with separation of the interactor matrix.

2.3.1 Problem formulation

Consider the system shown in Figure 2.2:

$$Y_t = D^{-1}\tilde{T}U_t + Na_t \tag{2.5}$$

where D is the unitary interactor matrix of transfer function matrix T. We assume that d_s is the order of D and $v_s = d_s - 1$ for the sake of convenience. For regulatory control $U_t = QY_t$, using the Diophantine identity [31]:

$$Q = X + q^{-\bar{d}}L \tag{2.6}$$

where $\bar{d} \geq 1$ is the maximum communication delay among d_{ij} for $1 \leq i, j \leq n$; X is a polynomial matrix of order $\bar{d}-1$, and L is the remaining transfer function matrix. According to equation (2.2), all the controller structure constraints caused by communication delays are contained in X, and L can be designed with full degree of freedom.

Multiplying both sides of equation (2.5) by $q^{-d_s}D$ yields

$$q^{-d_s}DY_t = q^{-d_s}\tilde{T}U_t + q^{-d_s}DNa_t \tag{2.7}$$

where using the Diophantine identity gives

$$q^{-d_s}DN = F + q^{-d_s}M + q^{-(d_s+\bar{d})}R \tag{2.8}$$

Here, F and M are polynomial matrices of order $d_s - 1$ and $\bar{d} - 1$, respectively; R is the remaining transfer function matrix. Substituting equations (2.6), (2.8) and $U_t = QY_t$ into equation (2.7), we obtain the following set of equation by rearranging (2.7):

$$q^{-d_s}DY_t|_{mvd} = Fa_t + Wa_{t-d_s} \tag{2.9}$$

$$\tilde{T}XY_{t-d_s}|_{mvd} = -(M - W)a_{t-d_s} + \theta a_{t-d_s-\bar{d}} \tag{2.10}$$

$$\tilde{T}LY_{t-d_s-\bar{d}}|_{mvd} = -(R + \theta)a_{t-d_s-\bar{d}} \tag{2.11}$$

where $Y_t|_{mvd}$ is the output with minimum achievable variance for DNCSs with time-invariant communication delays; Fa_t is the feedback controller-invariant term for centralized control systems; Wa_{t-d_s} is the additional term in minimum achievable output variance caused by communication delays; θ is a transfer function matrix. The equation set (2.9)-(2.11) is assumed to hold without loss of generality.

Proposition 1. *Term W is a polynomial matrix of order $\bar{d} - 1$ for all possible values of communication delays between different subsystems. $\sum_{i=0}^{\bar{d}-1} tr(W_i^T W_i)$ is served as the gap between the best achievable control performance under centralized control and distributed networked control, where W_i is the i^{th} coefficient matrix of W.*

Proof: When equation set (2.9)-(2.11) holds, equation (2.7) holds naturally. From

equation (2.9), $Y_t|_{mvd}$ can be solved as

$$\begin{aligned} Y_t|_{mvd} &= q^{d_s} D^{-1}(F + q^{-d_s} W)a_t \\ &= (q^{d_s} D^{-1} F + D^{-1} W)a_t \end{aligned} \tag{2.12}$$

For the unitary interactor matrix D, we have $D^{-1}(q) = D^T(q^{-1})$. Therefore,

$$\begin{aligned} E &= q^{d_s} D^{-1} F \\ &= (D_0^T + \cdots + D_{d_s-1}^T q^{d_s-1})(F_0 + \cdots + F_{d_s-1} q^{-d_s+1}) \end{aligned} \tag{2.13}$$

where F_i is the i^{th} coefficient matrix in F. Owing to causality, any term with a positive power of q in equation (2.13) must be zero. So, we have

$$E = E_0 + E_1 q^{-1} + \cdots + E_{d_s-1} q^{-d_s+1} \tag{2.14}$$

with $E_k = \sum_{i=0}^{d_s-1-k} D_i^T F_{i+k}$.

Substituting equation (2.12) into (2.10) yields

$$W = (I - \tilde{T} X D^{-1})^{-1}(M + \tilde{T} X E) - q^{-\bar{d}}(I - \tilde{T} X D^{-1})^{-1}\theta \tag{2.15}$$

where we define $P = (I - \tilde{T} X D^{-1})^{-1}(M + \tilde{T} X E)$. Using the Diophantine identity,

$$P = B + q^{-\bar{d}} C \tag{2.16}$$

where B is a polynomial matrix of order $\bar{d} - 1$, and C is the remaining transfer function matrix. Then, we have

$$var[Y_t|_{mvd}] = var[Fa_t] + var[Ba_{t-d_s}] + var[(C - (I - \tilde{T} X D^{-1})^{-1}\theta)a_{t-d_s-\bar{d}}] \tag{2.17}$$

where B only depends on X and generally cannot be zero when there are communication delays in DNCSs.

To minimize the output variance, we select

$$\theta = (I - \tilde{T}XD^{-1})C \tag{2.18}$$

to make the third term on left hand side of equation (2.17) equal to zero. Thus, the minimum achievable output variance is given by

$$var[Y_t|_{mvd}] = var[Fa_t] + var[Wa_{t-d_s}] \tag{2.19}$$

with $W = B$ a polynomial matrix of order $\bar{d} - 1$. Further, L is given by

$$L = -q^{d_s}\tilde{T}^{-1}(R + \theta)(F + q^{-d_s}W)^{-1}D \tag{2.20}$$

in order to satisfy the set of equations (2.9)-(2.11). ■

For any given X, W is required to be a polynomial matrix of order $\bar{d} - 1$ and this is ensured by selecting θ and L based on equations (2.18) and (2.20), respectively. According to equation (2.15), $W = B$ can be written in a compact matrix form as:

$$\begin{bmatrix} W_0 \\ W_1 \\ \vdots \\ W_{\bar{d}-1} \end{bmatrix} = \begin{bmatrix} H_0 \\ H_1 \\ \vdots \\ H_{\bar{d}-1} \end{bmatrix} + \begin{bmatrix} 0 & 0 & \cdots & 0 \\ K_0 & 0 & \cdots & 0 \\ \vdots & \vdots & \ddots & \vdots \\ K_{\bar{d}-2} & K_{\bar{d}-3} & \cdots & 0 \end{bmatrix} \begin{bmatrix} W_0 \\ W_1 \\ \vdots \\ W_{\bar{d}-1} \end{bmatrix} \tag{2.21}$$

$$\begin{bmatrix} H_0 \\ H_1 \\ \vdots \\ H_{\bar{d}-1} \end{bmatrix} = \begin{bmatrix} M_0 \\ M_1 \\ \vdots \\ M_{\bar{d}-1} \end{bmatrix} - \begin{bmatrix} \tilde{T}_0 & 0 & \cdots & 0 \\ \tilde{T}_1 & \tilde{T}_0 & \cdots & 0 \\ \vdots & \vdots & \ddots & \vdots \\ \tilde{T}_{\bar{d}-1} & \tilde{T}_{\bar{d}-2} & \cdots & \tilde{T}_0 \end{bmatrix} \begin{bmatrix} X_0 & 0 & \cdots & 0 \\ X_1 & X_0 & \cdots & 0 \\ \vdots & \vdots & \ddots & \vdots \\ X_{\bar{d}-1} & X_{\bar{d}-2} & \cdots & X_0 \end{bmatrix} \begin{bmatrix} E_0 \\ E_1 \\ \vdots \\ E_{\bar{d}-1} \end{bmatrix} \tag{2.22}$$

$$\begin{bmatrix} K_0 \\ K_1 \\ \vdots \\ K_{\bar{d}-2} \end{bmatrix} = \begin{bmatrix} \tilde{T}_0 & 0 & \cdots & 0 \\ \tilde{T}_1 & \tilde{T}_0 & \cdots & 0 \\ \vdots & \vdots & \ddots & \vdots \\ \tilde{T}_{\bar{d}-2} & \tilde{T}_{\bar{d}-3} & \cdots & \tilde{T}_0 \end{bmatrix} \begin{bmatrix} X_0 & 0 & \cdots & 0 \\ X_1 & X_0 & \cdots & 0 \\ \vdots & \vdots & \ddots & \vdots \\ X_{\bar{d}-2} & X_{\bar{d}-3} & \cdots & X_0 \end{bmatrix} \begin{bmatrix} D^T_{d_s-1} \\ D^T_{d_s-2} \\ \vdots \\ D^T_{d_s-\bar{d}+1} \end{bmatrix} \tag{2.23}$$

where W_i is the i^{th} coefficient matrix of W; H_i and K_i are coefficient matrices given in equations (2.22) and (2.23), respectively. In equations (2.22) and (2.23), $\tilde{T}_i$, M_i and X_i are the i^{th} coefficient matrices of T, M and X, respectively; E_i with $i > d_s - 1$ and D^T_i with $i < 0$ are 0.

Remark 1. *If a DNCS has perfect communication ($\bar{d} = 0$), in the equation set (2.9)-(2.11), term W, M, X and θ will be 0. Then, $Q = L = -q^{d_s}\tilde{T}^{-1}RF^{-1}D$ is just the minimum variance controller for centralized control systems [1]. Thus, the best achievable control performance of a system under distributed networked control and centralized control will be identical if there is no communication delay between all the subsystems.*

2.3.2 Best achievable control performance

According to Section 2.3.1, the distributed controller that provides the best achievable output variance is obtained by solving the following optimization problem

$$\begin{aligned} \min_{X} \quad & tr[var(Wa_{t-d_s})] \\ s.t. \quad & (2.21), (2.22), (2.23) \\ & X_k(i,j) = 0 \quad for \quad k \leq d_{ij} - 1 \end{aligned} \tag{2.24}$$

where $X_k(i,j)$ is the block in X_k with coordinate (i,j). The equality constraints in the optimization problem (2.24) accommodate the controller structure caused by communication delays, which is shown in equation (2.2). To deal with the proposed non-convex optimization problem with equality constraints, several global optimization methods can be used. Polynomial optimization algorithms are applied here.

Based on the assumption that a_t is white noise with zero mean and unit variance, we have

$$tr[var(Wa_{t-d_s})] = tr[W_0^T W_0 + \cdots + W_{\bar{d}-1}^T W_{\bar{d}-1}] \tag{2.25}$$

where each element in X_i for $i = 0, \cdots, \bar{d} - 1$ is defined as an individual variable, and the corresponding variables are assigned 0 according to the equality constraint in equation (2.24). Due to the quadratic form of W_i in equation (2.25), the cost function will be a strictly positive real-valued unconstrained polynomial with order $2\bar{d}$ which can be written in the sum of square form.

Global optimization of this kind of polynomials has been well established in literatures. It has been shown that the global unconstrained minimization of these polynomials can be approximated as closely as desired (and often can be obtained exactly) by solving a finite sequence of convex linear matrix inequality problems. For the theory on polynomial optimization, the interested reader is referred to [62, 63, 64, 65].

2.4 Limits of distributed minimum variance control performance considering random communication delays

If a DNCS suffers from random communication delays, based on the controller structure shown in equation (2.2), a time-varying controller is needed to achieve the theoretical minimum output variance. In order to deal with the plant-wide interaction using a time-varying distributed controller, each subsystem is required to transmit local information to all the other subsystems, including current output measurements, communication delays and control laws. We define

$$I_j(t_k) = \begin{bmatrix} V_j(t_k) \\ Q_j(t_k) \end{bmatrix} = \begin{bmatrix} d_{j1}(t_k) & \dots & d_{jn}(t_k) \\ Q_{j1}(t_k) & \dots & Q_{jn}(t_k) \end{bmatrix} \tag{2.26}$$

where $V_j(t_k)$ and $Q_j(t_k)$ are local communication delays and local control laws, respectively, in the subsystem j at time instant t_k. Because of communication delays, at time instant t_k, $I_j(t_k)$ is unavailable to subsystem i for all $j \in J$ with $J = \{j \in Z : d_{ij}(t_k) \geq 1, 1 \leq j \leq n\}$. Thus, there are two main challenges in designing such a distributed time-varying minimum variance controller:

1. The whole controller structure of $Q(t_k)$ is unavailable to subsystem i due to the absence of information $D_j(t_k)$ for $j \in J$, which makes it almost impossible to consider a global control objective in the time-varying local controller design of subsystem i. Although independent algorithms can be applied in which each local controller optimizes a local performance index, such a control strategy can be unstable and far from the solution when considering a global control objective [5].

2. For the system shown in equation (2.1) under output feedback control, the closed-loop response $T_{cl}(t_k)$ at time instant t_k is the relationship between output and disturbance.

In minimum variance control, the disturbance rejection is realized by compensating the influence of disturbance using output feedback. If there are random communication delays in DNCSs, $T_{cl}(t_k)$ is unavailable to subsystem i due to the absence of information $Q_j(t_k)$ for $j \in J$, which makes the local disturbance rejection control law hard to design.

With these concerns, limits of minimum variance control performance for DNCSs with random communication delays is relaxed from a specific value to a region by proposing the lower and upper bounds of the minimum output variance. By selecting $d_{ij}(t) = d_{min}$ for $1 \leq i, j \leq n, i \neq j$, the lower bound of the minimum output variance can be obtained by solving a distributed minimum variance control problem considering time-invariant communication delays. Correspondingly, the upper bound of the minimum output variance can be obtained by selecting $d_{ij}(t) = d_{max}$ for $1 \leq i, j \leq n, i \neq j$.

A two-step performance assessment strategy is proposed under this framework. The system that indicates good performance compared to the lower bound of the minimum output variance is guaranteed to be in a perfect condition; otherwise, the system needs to be re-evaluated based on the upper bound of the minimum output variance. The system that indicates poor performance compared to the upper bound of the minimum output variance needs controller tuning or redesign of the controller. Moreover, different approaches can be considered, e.g. the use of feedforward control.

The proposed performance assessment strategy has its advantages from an implementation perspective. When performance assessment is conducted for DNCSs with random communication delays, the lower and upper bounds of the minimum output variance can be calculated off-line in advance without considering random communication delays at each time instant which may lead to a high computational load in application.

Remark 2. *The use of bounds based on time-invariant delays may introduce conservativeness into the results. If we refer to the lower bound of the best achievable control performance, we get an overestimated result; on the other hand, if we refer to the upper bound, we may get a conservative performance. In practice, the lower and upper bounds of the best achievable*

performance provide a fundamental reference for controller tuning.

2.5 Simulations

2.5.1 Case of time-invariant communication delays

Consider the following 2×2 system adapted from [1]

$$\begin{bmatrix} Y_{1t} \\ Y_{2t} \end{bmatrix} = \begin{bmatrix} \frac{q^{-1}}{1-0.4q^{-1}} & \frac{k_{12}q^{-2}}{1-0.1q^{-1}} \\ \frac{0.3q^{-1}}{1-0.1q^{-1}} & \frac{q^{-2}}{1-0.8q^{-1}} \end{bmatrix} \begin{bmatrix} U_{1t} \\ U_{2t} \end{bmatrix} + \begin{bmatrix} \frac{1}{1-0.5q^{-1}} & \frac{-0.6}{1-0.5q^{-1}} \\ \frac{0.5}{1-0.5q^{-1}} & \frac{1}{1-0.5q^{-1}} \end{bmatrix} \begin{bmatrix} a_{1t} \\ a_{2t} \end{bmatrix} \tag{2.27}$$

where the system is divided into 2 univariate subsystems, (Y_{1t}, U_{1t}) and (Y_{2t}, U_{2t}), respectively; k_{12} controls the extent of interaction between the 2 subsystems. The unitary interactor matrix D can be factored out as

$$D = \begin{bmatrix} -0.9578q & -0.2873q \\ 0.2873q^2 & -0.9578q^2 \end{bmatrix} \tag{2.28}$$

The output with minimum variance under centralized control is $Y_t|_{mvc} = Fa_t$, where F is obtained by separating $q^{-d_s}DN$ in the form of equation (2.8) as

$$F = \begin{bmatrix} -1.1015q^{-1} & 0.2874q^{-1} \\ -0.1916 - 0.0958q^{-1} & -1.1302 - 0.5651q^{-1} \end{bmatrix} \tag{2.29}$$

Therefore, the minimum output variance under centralized control is $tr[var(Y_t|_{mvc})] = tr[var(Fa_t)] = 2.9383$, where disturbance is assumed to have unit variance.

By selecting the interaction index $k_{12} = 1$ and communication delays $d_{12} = 2, d_{21} = 1$, we obtain the part of the distributed minimum variance controller that contains structure

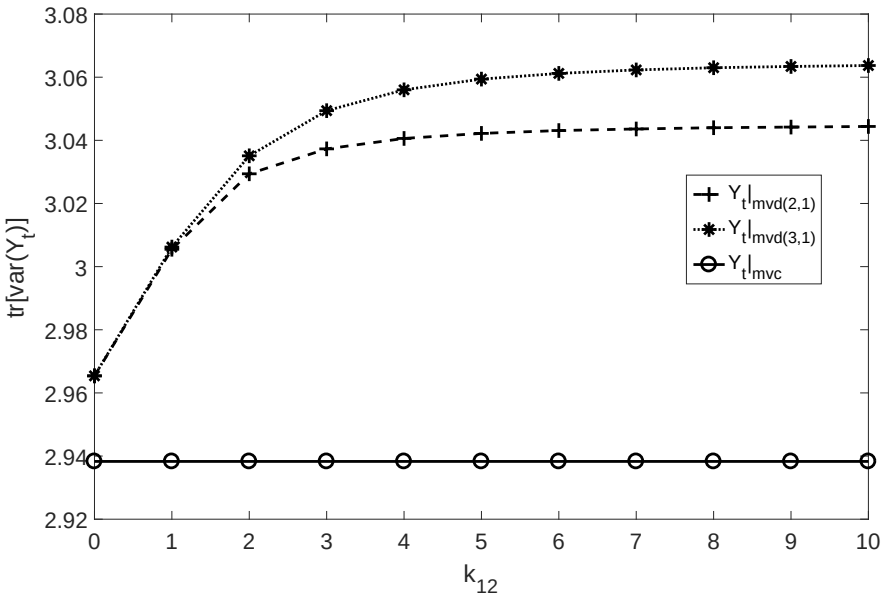

Figure 2.3: Comparison of minimum achievable output variance under centralized control and distributed networked control with time-invariant communication delays.

constraints caused by communication delays as follows

$$X = \begin{bmatrix} -0.4521 - 0.0441q^{-1} & 0 \\ -0.0011q^{-1} & -0.1262 + 0.0233q^{-1} \end{bmatrix} \tag{2.30}$$

where the off diagonal elements in X are zero or have time delay which indicate the limitations on interaction compensation caused by communication delays. The additional term in the output with minimum variance is

$$W = \begin{bmatrix} -0.0788 + 0.0490q^{-1} & -0.1395 + 0.0815q^{-1} \\ -0.0446 & -0.1746 \end{bmatrix} \tag{2.31}$$

According to equation (2.31), the order of the additional term in Y_{1t} is 1, which is consistent with the maximum value of $d_{1j}-1$ for $1 \leq j \leq 2$, and this conclusion also holds for subsystem 2.

By selecting $d_{12} = 2$, $d_{21} = 1$, and $d_{12} = 3$, $d_{21} = 1$, respectively, $tr[var(Y_t|_{mvd})]$ for

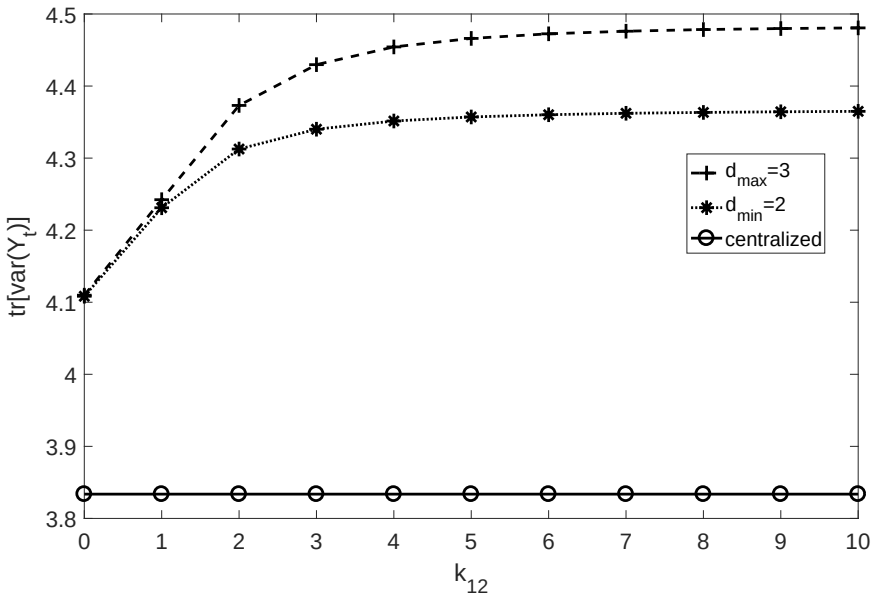

Figure 2.4: Comparison of minimum achievable output variance under centralized control and its lower and upper bounds under distributed networked control with random communication delays.

various k_{12} are compared to determine how the influence of communication delays on best achievable control performance changes with the extent of interaction between 2 subsystems. According to Figure 2.3, for each value of k_{12}, there exists a distributed controller that closely matches the performance of minimum variance controller in centralized case. The gaps between $Y_t|_{mvc}$, $Y_t|_{mvd(2,1)}$ and $Y_t|_{mvd(3,1)}$ are caused by communication delays, and larger communication delays will lead to a larger minimum achievable output variance. $Y_t|_{mvd(3,1)}$ is exactly equal to $Y_t|_{mvd(2,1)}$ when $k_{12} = 0$, which indicates that communication delay d_{12} will not affect system control performance if subsystem 1 is not influenced by subsystem 2. Further, the gap between $Y_t|_{mvd(2,1)}$ and $Y_t|_{mvd(3,1)}$ become larger when k_{12} increases, which implies that communication delay d_{12} has greater influence on system control performance if there is lager interaction from subsystem 2 to subsystem 1.

2.5.2 Case of random communication delays

Consider another 2×2 system adapted from [1]

$$\begin{bmatrix} Y_{1t} \\ Y_{2t} \end{bmatrix} = \begin{bmatrix} \frac{q^{-1}}{1-0.4q^{-1}} & \frac{k_{12}q^{-2}}{1-0.3q^{-1}} \\ \frac{0.7q^{-1}}{1-0.2q^{-1}} & \frac{q^{-2}}{1-0.9q^{-1}} \end{bmatrix} \begin{bmatrix} U_{1t} \\ U_{2t} \end{bmatrix} + \begin{bmatrix} \frac{1}{1-0.4q^{-1}} & \frac{-0.9}{1-0.3q^{-1}} \\ \frac{0.7}{1-0.5q^{-1}} & \frac{1}{1-0.7q^{-1}} \end{bmatrix} \begin{bmatrix} a_{1t} \\ a_{2t} \end{bmatrix} \tag{2.32}$$

where the system is divided into 2 univariate subsystems, (Y_{1t}, U_{1t}) and (Y_{2t}, U_{2t}), respectively; k_{12} controls the extent of interaction between 2 subsystems. We assume that the system shown in equation (2.32) is under distributed networked control and suffers from random communication delays, where $d_{max} = 3$ and $d_{min} = 2$, respectively. The proposed lower and upper bounds of the minimum output variance for various k_{12} are shown in Figure 2.4. The region between line $d_{max} = 3$ and line $d_{min} = 2$ can be treated as an alternative for the minimum variance benchmark value. The proposed two-step performance assessment strategy can be applied based on the obtained lower and upper bounds of the minimum output variance.

According to Figure 2.4, the system with performance lies between line $d_{min} = 2$ and line $d_{max} = 3$ is guaranteed to be in a perfect condition; the system with output variance larger but close to the value shown in line $d_{max} = 3$ has an acceptable performance, but there still is a potential for performance improvement; the system with output variance much larger than the value shown in line $d_{max} = 3$ indicates poor performance, then controller tuning or redesign of the controller is necessary. Comparing line *centralized* with line $d_{min} = 2$ and $d_{max} = 3$, there is a significant gap between the conventional minimum variance benchmark and the proposed limits of minimum variance control performance for DNCSs. Although controller for a DNCS with communication delays is well designed, it is highly likely to show a poor control performance if the conventional minimum variance benchmark is used as a criterion. Thus, the best achievable control performance is overly optimistic, and may lead engineers to search for non-existent distributed controllers. The proposed limits of minimum

variance control performance can give a more precise estimate on the best achievable control performance of DNCSs with communication delays.

2.6 Conclusions

In this chapter, we have discussed the limits of control performance for DNCSs, where the control objective is defined in terms of the output variance. Two scenarios are considered: DNCSs with time-invariant communication delays and random communication delays. For the case of time-invariant communication delays, communication delays are posed as the controller structure constraints and distributed minimum variance control is modeled as an optimization problem which is solved using sums of squares programming. For the case of random communication delays, the lower and upper bounds of the minimum output variance are proposed as an alternative for limits of minimum variance control performance by selecting communication delays between all subsystems as the minimum possible value and the maximum possible value, respectively. A simulated example is presented to show the results of the proposed work.

Chapter 3

Limits of LQG Control Performance for DNCSs with Random Communication Delays[2]

3.1 Introduction

Limits of minimum variance control performance for DNCSs provides useful information for control performance assessment, as no other distributed controller can achieve a lower output variance. However, tighter requirements on output variance result in stronger disturbance rejection, and typically requires more control effort [46]. Minimum variance control is usually not practical for real system operation due to its demand for excessive control effort and poor robustness. Then, one may be interested in knowing how far away the real system output variance is from the best achievable output variance with the same control effort. In this chapter, limits of LQG control performance for DNCSs with random communication delays is proposed as an alternative of the work in Chapter 2, where performance limitations of

[2]A shorter version of this chapter has been published in "Guoyang Yan, Jinfeng Liu, Yousef Alipouri, and Biao Huang. Performance assessment of distributed LQG control subject to communication delays. International Journal of Control. 2020 May 28: 1-23".

input communication delays and control effort penalty are further considered. Moreover, separation principle works on the fact that control actions will not influence state estimation error. But this condition is not hold in DNCSs with communication delays. In a DNCS, for each of the subsystems, some information of control actions of the other subsystems is missing due to the presence of communication delays. These missing information will lead to additional state estimation error in the local observer. Thus, to take into account the influence of control actions on state estimation error for DNCSs with communication delays, exploring algorithms for designing distributed controllers and distributed observers simultaneously is in need.

In this chapter, (i) the optimal structures of distributed state feedback controllers and distributed observers are proposed with considering both communication delays in inputs and communication delays in outputs; (ii) the best achievable control performance of DNCSs in the framework of LQG is presented where distributed controllers and distributed observers are designed simultaneously without using separation principle; (iii) the non-applicability of separation principle is illustrated in distributed networked control with communication delays; (iv) in order to handle random communication delays, the lower and upper LQG tradeoff curves are proposed to characterize the limits of LQG control performance for DNCSs; (v) implementation of the resulting control strategy is presented based on a numerical example.

3.2 Preliminaries

3.2.1 System description

In this chapter, we consider a class of discrete-time LTI systems described by the following state-space model

$$X_{k+1} = AX_k + BU_k + Ma_k \tag{3.1}$$
$$Z_k = CX_k + Na_k$$

where k indicates current time instant; X_k, U_k, Z_k and a_k are the state, input, output and disturbance vectors of dimensions n_x, n_u, n_z and n_a, respectively; A, B, C, M and N are matrices/vectors of appropriate dimensions. The entire system consists of n subsystems, with X_{ik}, U_{ik} and Z_{ik} being the state, input and output vectors of subsystem i, respectively. That is, $X_k = [X_{1k}, \ldots, X_{nk}]^T$, $U_k = [U_{1k}, \ldots, U_{nk}]^T$ and $Z_k = [Z_{1k}, \ldots, Z_{nk}]^T$.

It is assumed that each subsystem has its own observer and controller. The subsystem observers and controllers communicate and exchange information through a shared communication network and form a distributed networked control system. A schematic of the entire system is shown in Figure 3.1. Following assumptions are made without loss of generality:

1. pair (A, B) is controllable, and pair (A, C) is observable.

2. a_k consists of independent unit white noise which satisfies

$$E[a_k] = 0, E[a_k a_k^T] = I$$

where $E[\cdot]$ denotes the expectation of random variables. This assumption can always be satisfied by properly choosing matrices M and N.

3.2.2 Modeling of communication network

In this chapter, as shown in Figure 3.1, the designed network topology is fixed where each subsystem can communicate directly with all the other subsystems through a shared communication network. Although such kind of network design is not always applicable in real system operation, it can provide the theoretically best achievable control performance. Comparing with the control performance obtained in this case, one can further decide if improvement on network design is needed.

In the communication network, it is assumed that the measurements of the n subsystems are synchronously and periodically sampled at the beginning of each sampling period.

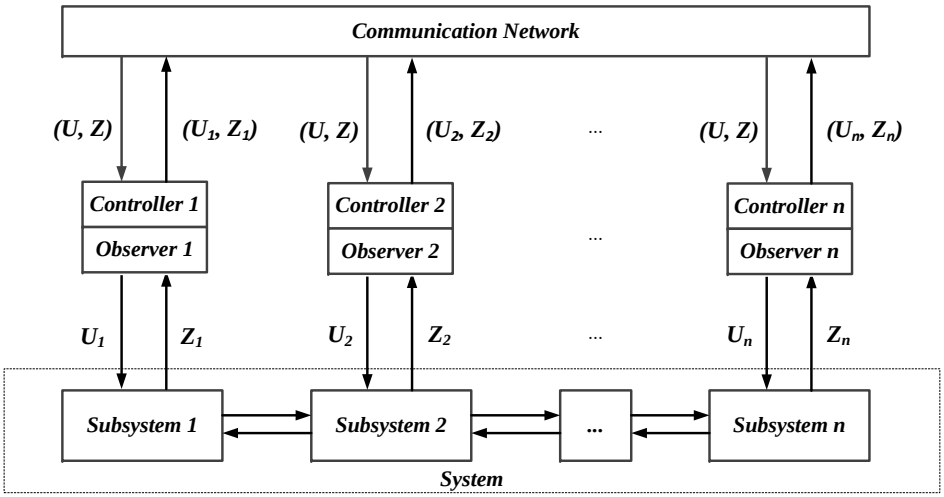

Figure 3.1: Network topology design for DNCSs with random communication delays.

The controller and observer of each subsystem have immediate access to its local measurements, and information of local measurements and control actions are transmitted to all the other subsystems through the shared communication network. The exchange of information between different subsystems is subject to communication delays. Further, information is assumed to be transmitted (and received) by subsystems once within each sampling period. Denote k as the starting time of the k^{th} sampling period and $d_{ij}(k)$ as the communication delay from subsystem j to subsystem i at time k. If at time k, controller i receives the latest information of controller j sent at time $k-q$, then $d_{ij}(k) = q$ with q a positive integer. Further, communication delays between different subsystems are assumed to be bounded within a predetermined region $[d_{min}, d_{max}]$. In each sampling period, all the information of a subsystem are transmitted together to the other subsystems as one package.

3.3 Objective and proposed approach

In this section, we first propose the optimal structure of distributed state feedback controllers considering communication delays in states, then we propose the optimal structure of dis-

tributed observers considering both communication delays in outputs and communication delays in inputs. Due to the fact that communication delays are typically time-varying and non-Gaussian, we propose to the lower and upper LQG tradeoff curves to characterize the best achievable LQG performance of a DNCS. The lower LQG tradeoff curve is obtained by assuming that the communication delays between all subsystems are equal to d_{min}. That is, at time k, only control actions and outputs of the other subsystems before time $k - d_{min}$ are available for each of the subsystem. Similarly, the upper LQG tradeoff curve is obtained by assuming that the communication delays between all subsystems are equal to d_{max}. At time k, for each of the subsystem, the distributed LQG problem is solved based on control actions and outputs of the other subsystems before time $k - d_{max}$ with regardless the available information after time $k - d_{max}$. Further, the best achievable performance of DNCSs in the framework of LQG is solved where distributed controllers and distributed observers are designed simultaneously without using separation principle.

3.3.1 Structure of subsystem controllers

It is well recognized that a state feedback control law $U_k = FX_k$ can achieve the optimal control performance for linear systems since the state vector X_k summarizes all the previous state information. However, when we consider DNCSs as shown in Figure 3.1, the entire state information of the current time instant is not available to each subsystem due to the presence of communication delays. Therefore, the following state feedback controller structure is proposed for subsystem i:

$$U_{ik} = F_{ii}^0 X_{ik} + F_{ii}^1 X_{ik-1} + \cdots + F_{ii}^{d-1} X_{ik-d+1} + \sum_{j=1}^{n} F_{ij}^d X_{jk-d} \tag{3.2}$$

where communication delays between all subsystems are assumed equal to d. That is, subsystem i only has access to the states of other subsystems at and before time $k - d$. Note that subsystem i has access to its own subsystem states at all times. d is chosen as d_{min} and

d_{max} for calculating the lower and upper LQG tradeoff curves, respectively. F_{ij}^q is the gain matrix for the states of subsystem j at time $k-q$. Based on the fact that the entire state information of the whole system at time $k-d$ is available, information before time $k-d$ is not used. In equation (3.2), states of subsystem i from time $k-d$ to time k and states of all the other subsystems at time $k-d$ are used to design the controller. Therefore, the proposed state feedback controller is designed based on all the useful state information.

Based on the proposed subsystem controller in equation (3.2), the entire system controller can be described as

$$U_k = F^0 X_k + F^1 X_{k-1} + \cdots + F^{d-1} X_{k-d+1} + F^d X_{k-d} \tag{3.3}$$

where $F^q = diag(F_{11}^q, \cdots, F_{nn}^q)$ for $q = 0, \cdots, d-1$ are controller gain matrices with block diagonal structure, and F^d is the gain matrix associated with the state X_{k-d}.

3.3.2 Structure of subsystem observers

According to equation (3.2), at time k, X_{k-d} and $X_{ik-d+1}, \cdots, X_{ik}$ are used in the local controller of subsystem i. A local state observer needs to be designed for subsystem i to estimate these states.

First, X_{k-d} is estimated. Communication delays between all subsystems are assumed equal to d ($d = d_{min}$ or $d = d_{\max}$). That is, all the control actions and outputs of the system at and before time $k-d$ are available to each subsystem. Thus, X_{k-d} can be estimated by subsystem i ($i = 1, \ldots, n$) as follows:

$$\hat{X}_{k-d}^c = A\hat{X}_{k-d-1}^c + BU_{k-d-1} + L^c[Z_{k-d} - C(A\hat{X}_{k-d-1}^c + BU_{k-d-1})] \tag{3.4}$$

where $\hat{X}_{k-d}^c$ is the estimate of X_{k-d}. $A\widehat{X}_{k-d-1}^c + BU_{k-d-1}$ is the state prediction term based on the system model, and $L^c[Z_{k-d} - C(A\hat{X}_{k-d-1}^c + BU_{k-d-1})]$ is the correction term based on output prediction error. L^c is the gain matrix for the correction term and can be directly

assigned as the steady state Kalman filter gain for the entire system shown in equation (3.1). Note that a copy of observer in equation (3.4) is implemented in each of the subsystems.

Then, X_{ik-d+1} is estimated. X_{ik-d+1} is only used in the local controller of subsystems i. Due to the presence of communication delays, at time k, only local control actions and outputs after time $k-d$ are available to subsystem i. So, only prediction error for local outputs at time $k-d+1$ is available to update the state prediction. For subsystem i, the observer for X_{ik-d+1} is designed as

$$\hat{X}^p_{ik-d+1} = A_i\hat{X}^c_{k-d} + B_iU_{k-d} + L^z_{i11}[Z_{ik-d+1} - C_i(A\hat{X}^c_{k-d} + BU_{k-d})] \tag{3.5}$$

where $\hat{X}^p_{ik-d+1}$ is the estimate of states of subsystem i at time $k-d+1$, A_i, B_i and C_i are sub matrices in A, B and C associate with subsystem i, respectively. In equation (3.5), $A_i\hat{X}^c_{k-d} + B_iU_{k-d}$ is the prediction of local states based on local subsystem model, and $L^z_{i11}[Z_{ik-d+1} - C_i(A\hat{X}^c_{k-d} + BU_{k-d})]$ is the correction term based on local output prediction error. L^z_{i11} is the gain matrix for the correction term. Based on the proposed subsystem observer in equation (3.5), the entire system observer for X_{k-d+1} can be described as

$$\hat{X}^p_{k-d+1} = A\hat{X}^c_{k-d} + BU_{k-d} + L^z_{11}[Z_{k-d+1} - C(A\hat{X}^c_{k-d} + BU_{k-d})]$$

where $L^z_{11} = diag(L^z_{i11}, \cdots, L^z_{n11})$ is observer gain matrix with block diagonal structure.

$\hat{X}^p_{k-d+1}$ is not available to subsystem i at time k. Thus, when designing the observer for X_{ik-d+2} in subsystem i, the state prediction term can only be calculated from $\widehat{X}^c_{k-d}$. Also, only prediction errors for local outputs at time $k-d+1$ and $k-d+2$ are available to update the predictions due to communication delays. For subsystem i, the observer for X_{ik-d+2} is

designed as

$$\begin{aligned}\hat{X}^p_{ik-d+2} &= A_i(A\hat{X}^c_{k-d} + BU_{k-d}) \\ &+ L^z_{i21}[Z_{ik-d+2} - C_i(A^2\hat{X}^c_{k-d} + ABU_{k-d}))] \\ &+ L^z_{i12}[Z_{ik-d+1} - C_i(A\hat{X}^c_{k-d} + BU_{k-d}))] \\ &+ L^u_{i11}U_{ik-d+1}\end{aligned} \tag{3.6}$$

where $\hat{X}^p_{ik-d+2}$ is the estimate of states of subsystem i at time $k-d+2$. $A_i(A\hat{X}^c_{k-d}+BU_{k-d})$ is the two step ahead prediction of local states. $L^z_{i21}[Z_{ik-d+2} - C_i(A^2\hat{X}^c_{k-d} - ABU_{k-d}))]$ and $L^z_{i12}[Z_{ik-d+1} - C_i(A\hat{X}^c_{k-d} - BU_{k-d}))]$ are the correction terms based on local output prediction errors at time $k-d+2$ and $k-d+1$, respectively. Further, $L^u_{i11}U_{ik-d+1}$ is designed to compensate for the unavailable control actions at time $k-d+1$ from the other subsystems. L^z_{i21}, L^z_{i12} and L^u_{i11} are the corresponding gain matrices need to be designed. Then, the entire system observer for X_{k-d+2} can be described as

$$\begin{aligned}\hat{X}^p_{k-d+2} &= A^2\hat{X}^c_{k-d} + ABU_{k-d} \\ &+ L^z_{21}[Z_{k-d+2} - CA^2\hat{X}^c_{k-d} - CABU_{k-d})] \\ &+ L^z_{12}[Z_{k-d+1} - CA\hat{X}^c_{k-d} - CBU_{k-d})] \\ &+ L^u_{11}U_{k-d+1}\end{aligned} \tag{3.7}$$

where $L^z_{21} = diag(L^z_{i21}, \cdots, L^z_{n21})$, $L^z_{12} = diag(L^z_{i12}, \cdots, L^z_{n12})$ and $L^u_{11} = diag(L^u_{i11}, \cdots, L^u_{n11})$ are the observer gain matrices with block diagonal structure.

Further, based on the same idea, the entire system observer for X_{k-d+i} can be expressed

as

$$\begin{aligned}\hat{X}^p_{k-d+i} &= A^i\hat{X}^c_{k-d} + A^{i-1}BU_{k-d} \\ &+ L^z_{i1}[Z_{k-d+i} - CA^i\hat{X}^c_{k-d} - CA^{i-1}BU_{k-d})] + \cdots \\ &+ L^z_{1i}[Z_{k-d+1} - CA\hat{X}^c_{k-d} - CBU_{k-d})] \\ &+ L^u_{(i-1)1}U_{k-d+i-1} + \cdots + L^u_{1(i-1)}U_{k-d+1}\end{aligned} \tag{3.8}$$

where gain matrices $L^z_{i1}, \cdots, L^z_{1i}$ and $L^u_{(i-1)1}, \cdots, L^u_{1(i-1)}$ are restricted to block diagonal structure.

Remark 3. *Note that one subsystem does not have access to the recent control actions of the rest of the subsystems due to communication delays. At time k, in the proposed observer design, missing information of control actions of the other subsystems will lead to additional errors in both state predictions and output predictions in the subsystem i ($i = 1, \ldots, n$). These missing information will influence the state estimation accuracy of $X_{ik-d+1}, \cdots, X_{ik}$. Separation principle works on the fact that control actions will not influence state estimation error. But this condition is not hold in DNCSs with communication delays. Thus, distributed controllers and distributed observers should be designed simultaneously to take into account the influence of control actions on state estimation error.*

3.3.3 Lower and upper LQG tradeoff curves

The best achievable LQG control performance of a DNCS is time-varying due to the fact that communication delays are typically time-varying and non-Gaussian. Online update of the best achievable LQG control performance is challenging and time consuming under distributed networked control. Thus, the time-varying best achievable LQG control performance is hard to be used as a practical solution for control performance assessment.

With the above consideration, the lower and upper LQG tradeoff curves are proposed to characterize the time-varying best achievable LQG control performance of a DNCS. The

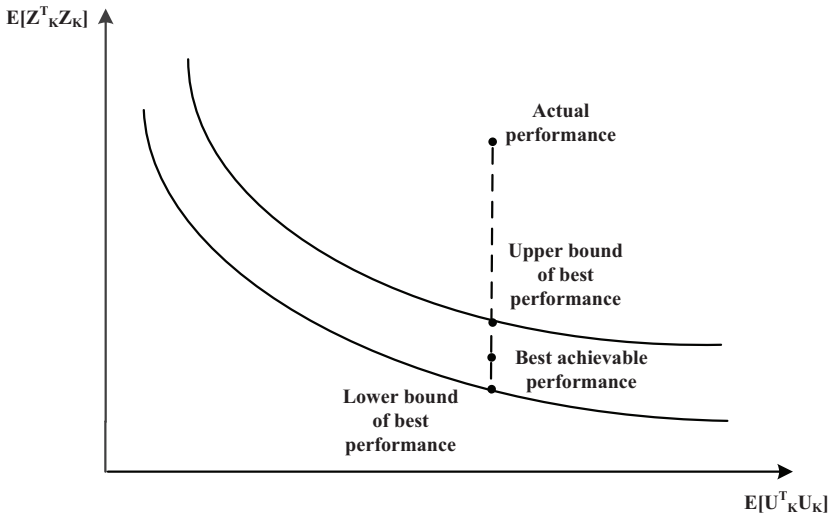

Figure 3.2: The lower and upper LQG tradeoff curves.

lower LQG tradeoff curve is obtained by assuming that communication delays between all subsystems are equal to d_{min}, and the upper LQG tradeoff curve is obtained by assuming that communication delays between all subsystems are equal to d_{max}. For example, the entire system is assumed to be divided into 2 subsystems with $d_{min} = 0$ and $d_{max} = 1$.

It is clear that the lower LQG tradeoff curve is the best case scenario where communication delays between the 2 subsystems are assumed to be equal to 0 at each time instant. Then, the controller and the observer for subsystem i ($i = 1, 2$) are given as follows based on the proposed structure:

$$U_{ik} = F_i^0 \hat{X}_k^c$$
$$\hat{X}_k^c = A\hat{X}_{k-1}^c + BU_{k-1} + L^c[Z_k - C(A\hat{X}_{k-1}^c + BU_{k-1})]$$

where F_i^0 is the sub matrices in F^0 associates with subsystem i. According to the above equation, calculation of U_{ik} needs Z_k and U_{k-1}. At time k, Z_k is not always available to

subsystem i in the real system due to the random communication delays. Thus, the achieved distributed LQG control in this case is actually not implementable, but this best case scenario measures the lower bound of the best achievable LQG control performance.

Similarly, the upper LQG tradeoff curve is the worst case scenario where communication delays between the 2 subsystems are assumed to be equal to 1 at each time instant. Then, the controller and the observer for subsystem i $(i = 1, 2)$ are given as follows:

$$
\begin{aligned}
U_{ik} &= F_{ii}^0 \hat{X}_{ik}^p + F_i^1 \hat{X}_{k-1}^c \\
\hat{X}_{k-1}^c &= A\hat{X}_{k-2}^c + BU_{k-2} + L^c[Z_{k-1} - C(A\hat{X}_{k-2}^c + BU_{k-2})] \\
\hat{X}_{ik}^p &= A_i\hat{X}_{k-1}^c + B_iU_{k-1} + L_{i11}^z[Z_{ik} - C_i(A\hat{X}_{k-1}^c + BU_{k-1})]
\end{aligned}
$$

where F_i^1 is the sub matrices in F^1 associates with subsystem i. According to the above equation, calculation of U_{ik} needs Z_{ik}, Z_{k-1}, U_{k-1} and U_{k-2}. At time k, these information is always available to subsystem i in the real system. The achieved distributed LQG control in this case is implementable, and this worst case scenario measures the upper bound of the best achievable LQG control performance.

As shown in Figure 3.2, the best achievable LQG control performance of a DNCS with random communication delays should lie between the proposed lower and upper LQG tradeoff curves. The difference between actual performance and lower bound of the best available performance provides at most how much can we further improve the control performance. While, the difference between actual performance and upper bound of the best available performance shows at least how much is the potential for control performance improvement. Although the use of bounds may introduce conservativeness into the results, the proposed lower and upper LQG tradeoff curves provide a fundamental reference for control performance assessment.

3.4 Limits of distributed LQG control performance

In this section, solution to the following LQG control problem is proposed by considering communication delays:

$$\begin{aligned} \min \quad & E[Z_k^T Z_k] + \lambda E[U_k^T U_k] \\ s.t. \quad & X_{k+1} = AX_k + BU_k + Ma_k \\ & Z_k = CX_k + Na_k \end{aligned} \tag{3.9}$$

where λ is the weighting factor of LQG objective function. Consider the following system with a new defined output $Z_k^{'}$:

$$\begin{aligned} X_{k+1} &= AX_k + BU_k + Ma_k \\ Z_k^{'} &= \begin{bmatrix} C \\ 0 \end{bmatrix} X_k + \begin{bmatrix} 0 \\ \sqrt{\lambda} \end{bmatrix} U_k + \begin{bmatrix} N \\ 0 \end{bmatrix} a_k \end{aligned} \tag{3.10}$$

The LQG control problem shown in equation (3.9) is equivalent to minimizing $E[(Z_k^{'})^T Z_k^{'}]$ which is the H_2 norm of system (3.10). The optimal distributed state feedback controllers considering communication delays are solved first. Then the results are extended to solve distributed state feedback controllers and distributed observers simultaneously without using separation principle. Here the solution of the optimal H_2 control problem is explicitly expressed in terms of the solutions of some matrix inequalities according to the well known result in [66]. Due to the non-applicability of separation principle, distributed controllers and distributed observers are designed simultaneously. Multiplication of the controller and the observer optimization parameters lead to complex non-linear conditions in the formulation. Further, block diagonal structures are imposed on the controller and the observer optimization parameters to satisfy the constraints caused by communication delays. Therefore, non-linear conditions is unable to reduce through non-linear transformation of variables,

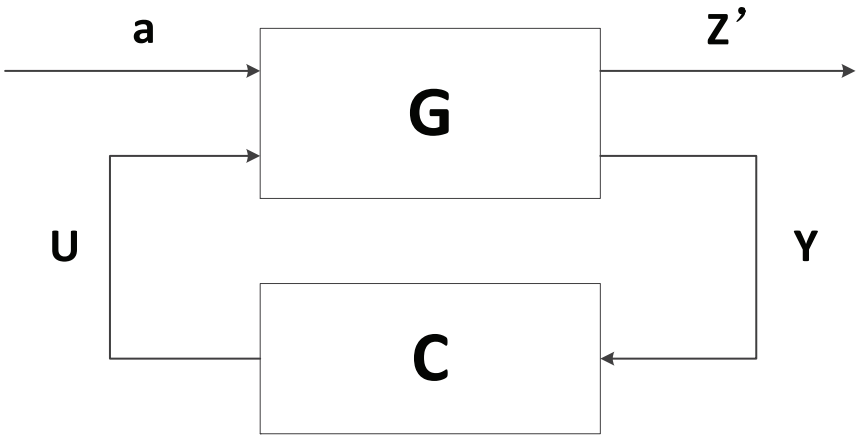

Figure 3.3: Schematic of the closed-loop system.

and the optimal H_2 control problem is formulated as bilinear matrix inequalities (BMIs).

The solution for this BMI problem is proposed by iteratively solving a sequence of linearized problems, which at each step parameters in distributed controllers and distributed observers are guaranteed to provide a better control performance than the previous ones. An algorithm is proposed to calculate the stabilizing initial values for controller and observer parameters used in the iterative algorithm. Finally, a procedure is introduced to calculated the lower and upper LQG tradeoff curves based on the solution of the LQG control problem.

3.4.1 Distributed state feedback control

Throughout this section it is assumed that the state information is available for feedback. Moreover, the state information is not corrupted by the disturbance a_k. Consider the closed-loop system shown in Figure 3.3. G is the system model defined in equation (3.10), measurement $Y_k = X_k$, and C is the integration of distributed state feedback controllers defined

in equation (3.2) with its state space realization given by

$$X_{k+1}^c = A_c X_k^c + B_c Y_k \tag{3.11}$$
$$U_k = C_c X_k^c + D_c Y_k$$

where $X_k^c = [X_{k-1}^T, X_{k-2}^T, \cdots, X_{k-d}^T]^T$ is the state of C. The system matrices in C are given by

$$A_c = \begin{bmatrix} 0 & 0 & \cdots & 0 & 0 \\ I & 0 & \cdots & 0 & 0 \\ \vdots & \vdots & & \vdots & \vdots \\ 0 & 0 & \cdots & I & 0 \end{bmatrix} \quad B_c = \begin{bmatrix} I \\ 0 \\ \vdots \\ 0 \end{bmatrix} \quad C_c = \begin{bmatrix} F^1 & F^2 & \cdots & F^d \end{bmatrix} \quad D_c = \begin{bmatrix} F^0 \end{bmatrix} \tag{3.12}$$

This feedback structure produces a closed-loop system from a_k to $Z_k^{'}$:

$$\overline{X}_{k+1} = A_{cl}\overline{X}_k + B_{cl} a_k \tag{3.13}$$
$$Z_k^{'} = C_{cl}\overline{X}_k + D_{cl} a_k$$

where $\overline{X}_k = [X_k^T, X_k^{cT}]^T$, and the closed-loop system matrices

$$A_{cl} = \begin{bmatrix} A + BD_c & BC_c \\ B_c & A_c \end{bmatrix} \quad B_{cl} = \begin{bmatrix} M \\ 0 \end{bmatrix} \quad C_{cl} = \begin{bmatrix} C & 0 \\ \sqrt{\lambda} D_c & \sqrt{\lambda} C_c \end{bmatrix} \quad D_{cl} = \begin{bmatrix} N \\ 0 \end{bmatrix} \tag{3.14}$$

The symbol $H_{az'}$ denotes the transfer function from the disturbance a_k to the output Z_k'. The following lemma is a well known result that completely characterizes the H_2 norm of a system [66].

Lemma 1. *The inequality* $\|H_{az'}\|_2^2 \leq \mu$ *holds if, and only if, there exists a matrix* Λ *and*

symmetric matrices P and W such that

$$
\begin{aligned}
& trace(W + D_{cl}D_{cl}^T) \leq \mu \\
s.t. \quad & \begin{bmatrix} W & C_{cl}\Lambda \\ \Lambda C_{cl}^T & \Lambda + \Lambda^T - P \end{bmatrix} > 0 \\
& \begin{bmatrix} P & A_{cl}\Lambda & B_{cl} \\ \Lambda A_{cl}^T & \Lambda + \Lambda^T - P & 0 \\ B_{cl}^T & 0 & I \end{bmatrix} > 0
\end{aligned}
\tag{3.15}
$$

is feasible.

Nonlinear conditions appear after replacing equation (3.14) and (3.12) into the inequalities of equation (3.15). Owing to the block diagonal structure constraints in the controller gain matrices caused by communication delays, these nonlinear conditions cannot be reduced through nonlinear transformation. To solve the BMI problem shown in (3.15), a path-following method is introduced [67].

Theorem 1. *The path-following method is proceeded as follows:*

1. *Set $i = 0$, compute a set of stabilizing initial values of $F^{0(i)}, \cdots, F^{d(i)}$ based on Theorem 2.*

2. *With $F^0 = F^{0(i)}, \cdots, F^d = F^{d(i)}$, compute the H_2 norm of the closed-loop system and corresponding matrices Λ^i, P^i and W^i based on equation (3.15).*

3. *Define $F^0 = F^{0(i)} + \Delta(F^{0(i)}), \cdots, F^d = F^{d(i)} + \Delta(F^{d(i)}), \Lambda = \Lambda^i + \Delta(\Lambda^i), P = P^i + \Delta(P^i)$ and $W = W^i + \Delta(W^i)$, where $\Delta(\cdot)$ denotes the perturbation of $(\cdot)$. The matrix inequalities in equation (3.15) are linearized by ignoring all the second order terms on*

$\Delta(\cdot)$. *The constraints*

$$\|\Delta(\cdot)\|_2 \leq \begin{cases} 0.02\|(\cdot)\|_2 & if \quad \|(\cdot)\|_2 \neq 0 \\ 0.2 & if \quad \|(\cdot)\|_2 = 0 \end{cases}$$

are added so that the perturbations are small and the linear approximation should be valid.

4. *Solve the linearized BMI problem around* $F^{0(i)}, \cdots, F^{d(i)}, \Lambda^i, P^i$ *and* W^i *using semidefinite program to get the perturbations.*

5. *Let* $F^{0(i+1)} = F^{0(i)} + \Delta(F^{0(i)}), \cdots, F^{d(i+1)} = F^{d(i)} + \Delta(F^{d(i)}), i = i+1$ *and go to step 2.*

6. *The iteration stops whenever the* H_2 *norm of the closed-loop system cannot be improved any further.*

Remark 4. *The LQG tradeoff curve consists of various optimal solutions of* $E[U_k^T U_k]$ *and* $E[Z_k^T Z_k]$ *with respect to different values of* λ. *For the LQG objective function with a given value of* λ, *a set of optimal controller parameters obtained based on Lemma 1 and Theorem 1 can be directly used as the initial values of controller parameters for the LQG objective function with a neighbouring* λ. *Thus, the whole LQG tradeoff curve can be achieved by solving each LQG control problem step by step.*

A stabilizing controller in the form of equation (3.3) should be designed first as the initial values used in Theorem 1. Due to the presence of structure constraints, $F^{0(0)}, \cdots, F^{d-1(0)}$ are selected to be 0 to simplify the problem. Thus, controller $U_k = F^{d(0)} X_{k-d}$ is designed to stabilize the system, where $F^{d(0)}$ can be designed with full degree of freedom. The following Theorem 2 is proposed to design $F^{d(0)}$, and Lemma 2 [68] is first presented which is then used in the proof.

Lemma 2. *The following statement is true:*

$$(K+J)^T H(K+J) \leq (1+\varepsilon)K^T HK + (1+\varepsilon^{-1})J^T HJ \tag{3.16}$$

where symmetric matrix $H > 0$, K and J are matrices with proper dimension and ε is a positive constant.

Theorem 2. *Based on Lyapunov method, the system shown in equation (3.10) with controller $U_k = F^{d(0)}X_{k-d}$ is asymptotically stable if there exists a real symmetric matrix $H > 0$ such that*

$$(1+\varepsilon_m)A^T HA + (\frac{1+\varepsilon_m}{\varepsilon_m})A_d^T HA_d - H < 0 \tag{3.17}$$

where $A_d = BF^{d(0)}$ and $\varepsilon_m = \|A_d\|_2\|A\|_2^{-1}$. The conclusion is in Riccati equation form, and the solvers for which are well designed.

Proof: Consider the following Lyapunov function

$$V(X_k) = X_k^T HX_k + \sum_{l=1}^{d} X_{k-l}^T SX_{k-l} \tag{3.18}$$

where symmetric matrix $S \geq 0$. Taking forward difference from equation (3.18) gives

$$\begin{aligned} \Delta V(X_k) &= V(X_{k+1}) - V(X_k) \\ &= [AX_k + A_dX_{k-d}]^T H[AX_k + A_dX_{k-d}] - X_k^T HX_k \\ &\quad + \sum_{l=1}^{d} X_{k-l+1}^T SX_{k-l+1} - \sum_{l=1}^{d} X_{k-l}^T SX_{k-l} \end{aligned} \tag{3.19}$$

Utilizing Lemma 2, inequality on equation (3.19), yields

$$\begin{aligned}\Delta V(X_k) &\leq (1+\varepsilon)X_k^T A^T H A X_k + (1+\varepsilon^{-1})X_{k-d}^T A_d^T H A_d X_{k-d} - X_k^T H X_k \\ &\quad + X_k^T S X_k - X_{k-d}^T S X_{k-d} \\ &= X_k^T[(1+\varepsilon)A^T H A + S - H]X_k + X_{k-d}^T[(1+\varepsilon^{-1})A_d^T H A_d - S]X_{k-d}\end{aligned} \tag{3.20}$$

Now, select $S = (1+\varepsilon^{-1})A_d^T H A_d$, then

$$\Delta V(X_k) \leq X_k^T[(1+\varepsilon)A^T H A + (1+\varepsilon^{-1})A_d^T H A_d - H]X_k = \varphi(X_k, \varepsilon) \tag{3.21}$$

Thus, the system is asymptotically stable if there exists a real symmetric matrix $H > 0$ such that

$$(1+\varepsilon)A^T H A + (1+\varepsilon^{-1})A_d^T H A_d - H < 0$$

where ε can be selected as any positive constant. A suggested value of ε can be selected based on the following derivation:

Since matrices $A^T H A$ and $A_d^T H A_d$ are symmetric and positive semidefinite then, we have

$$\begin{aligned}\varphi(X_k, \varepsilon) &\leq X_k^T[(1+\varepsilon)\lambda_{max}(A^T H A) + (1+\varepsilon^{-1})\lambda_{max}(A_d^T H A_d) - \lambda_{max}(H)]X_k \\ &= g(\varepsilon)\lambda_{max}(H)\|X_k\|_2^2\end{aligned} \tag{3.22}$$

where $g(\varepsilon) = (1+\varepsilon)\sigma_{max}^2(A) + (1+\varepsilon^{-1})\sigma_{max}^2(A_d) - 1$, $\lambda_{max}(\cdot)$ denotes the maximum eigenvalue value of $(\cdot)$, and $\sigma_{max}(\cdot)$ denotes the maximum singular value of $(\cdot)$. Maximum of the function $g(\varepsilon)$ can be found by taking derivative with respect to ε, which yields

$$\frac{dg(\varepsilon)}{d\varepsilon} = 0 \quad \Rightarrow \quad \sigma_{max}^2(A) - \frac{\sigma_{max}^2(A_d)}{\varepsilon^2} = 0 \tag{3.23}$$

The optimum value for ε is

$$\varepsilon_m = \sigma_{max}(A_d)\sigma^{-1}_{max}(A) \tag{3.24}$$

Therefore, we can conclude

$$\begin{aligned} \Delta V(X_k) &\leq \varphi(X_k, \varepsilon_m) \\ &= X_k^T[(1+\varepsilon_m)A^T H A + (\frac{1+\varepsilon_m}{\varepsilon_m})A_d^T H A_d - H]X_k \end{aligned} \tag{3.25}$$

Now, if the condition (3.17) is satisfied then system (3.10) is asymptotically stable. ■

3.4.2 Distributed state feedback control combined with distributed state estimation

Throughout this section it is assumed that only information of control actions and outputs is available for feedback. Consider the closed-loop system shown in Figure 3.4. G is the system model defined in equation (3.10), measurement $Y_k = [Z_k^T, U_k^T]^T$, and C is the integration of distributed state feedback controllers defined in equation (3.2). E and O constitute the distributed observers designed in the previous section. Owing to the presence of communication delays, C, E and O are designed simultaneously without using separation principle.

Structure of O can be expressed as

$$\begin{aligned} X^o_{k+1} &= A_o X^o_k + B_o Y_k \\ Y^o_k &= C_o X^o_k + D_o Y_k \end{aligned} \tag{3.26}$$

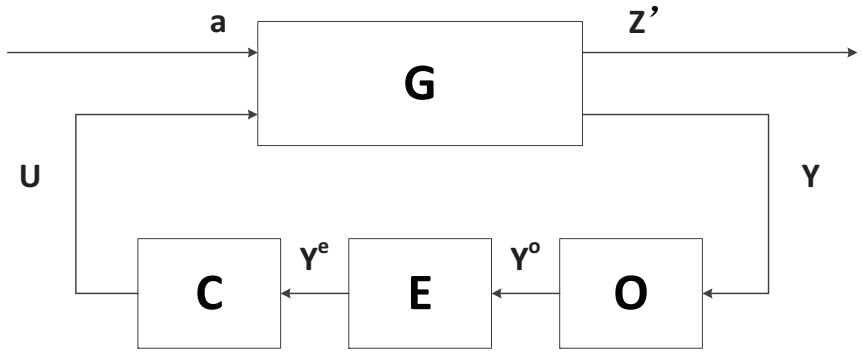

Figure 3.4: Schematic of the closed-loop system.

where the system matrices in O are given by

$$A_o = C_o = \begin{bmatrix} 0 & 0 & \cdots & 0 & 0 \\ I & 0 & \cdots & 0 & 0 \\ \vdots & \vdots & & \vdots & \vdots \\ 0 & 0 & \cdots & I & 0 \end{bmatrix} \quad B_o = D_o = \begin{bmatrix} I \\ 0 \\ \vdots \\ 0 \end{bmatrix} \tag{3.27}$$

Then $X_k^o = [Z_{k-1}^T, U_{k-1}^T, \cdots, Z_{k-d-2}^T, U_{k-d-2}^T]^T$ is the state of O, and $Y_k^o = [Z_k^T, U_k^T, \cdots, Z_{k-d-1}^T, U_{k-d-1}^T]^T$ is the output of O which provides all the information needed in the distributed observers.

Based on equation (3.8), the structure of observer E can be expressed as

$$\begin{aligned} X_{k+1}^e &= A_e X_k^e + B_e Y_k^o \\ Y_k^e &= C_e' X_{k+1}^e + D_e' Y_k^o \end{aligned} \tag{3.28}$$

where $X_{k+1}^e = \hat{X}_{k-d}^c$ and $Y_k^e = [\hat{X}_{k-d}^c, \hat{X}_{k-d+1}^p, \cdots, \hat{X}_k^p]^T$ are the state and the output of E,

respectively. The system matrices in E are given by

$$
\begin{aligned}
A_e &= A - L^c CA \\
B_e &= \begin{bmatrix} 0 & \cdots & 0 & L^c & 0 & 0 & B - L^c CB \end{bmatrix} \\
C'_e &= \begin{bmatrix} I \\ A - L^z_{11} CA \\ A^2 - L^z_{12} CA - L^z_{21} CA^2 \\ \vdots \\ A^d - L^z_{1d} CA - L^z_{2(d-1)} CA^2 - \cdots - L^z_{(d-1)2} CA^{d-1} - L^z_{d1} CA^d \end{bmatrix}
\end{aligned}
\tag{3.29}
$$

$$
D'_e = \begin{bmatrix}
 & & & & & & & \cdots & 0 \\
 & & & \cdots & 0 & L^z_{11} & 0 & 0 \; Q^1 & 0 & 0 \\
 & \cdots & 0 & L^z_{21} & 0 & L^z_{12} & L^u_{11} & 0 \; Q^2 & 0 & 0 \\
 & & & & & \vdots & & & & \\
L^z_{d1} & 0 & L^z_{(d-1)2} & L^u_{(d-1)1} & \cdots & L^z_{1(d)} & L^u_{1(d-1)} & 0 \; Q^d & 0 & 0
\end{bmatrix}
$$

where

$$
Q^i = A^{i-1}B - L^z_{i1} CA^{i-1}B - L^z_{(i-1)2} CA^{i-2}B - \cdots - L^z_{2(i-1)} CAB - L^z_{1i} CB \tag{3.30}
$$

Further, the standard state-space expression of E is

$$
\begin{aligned}
X^e_{k+1} &= A_e X^e_k + B_e Y^o_k \\
Y^e_k &= C'_e A_e X^e_k + (C'_e B_e + D'_e) Y^o_k
\end{aligned}
\tag{3.31}
$$

Based on equation (3.3), controller C can be expressed as $U_k = D_c Y^e_k$ with $D_c =$

$[F^d \quad F^{d-1} \quad \cdots \quad F^0]$. Combining C, E and O, the whole feedback part is defined as F with Y_k as input and U_k as output. Structure of F can be express as

$$X_{k+1}^f = A_f X_k^f + B_f Y_k \tag{3.32}$$

$$U_k = C_f X_k^f + D_f Y_k \tag{3.33}$$

where $X_k^f = [X_k^{oT}, X_k^{eT}]^T$ is the state of F. The system matrices in F are given by

$$A_f = \begin{bmatrix} A_o & 0 \\ B_e C_o & A_e \end{bmatrix} \quad B_f = \begin{bmatrix} B_o \\ B_e D_o \end{bmatrix} \quad D_f = D_c(D_e' + C_e' B_e) D_o \tag{3.34}$$

$$C_f = D_c \begin{bmatrix} (D_e' + C_e' B_e) C_0 & C_e' A_e \end{bmatrix}$$

Substituting equations (3.9), (3.34) and $Y_k = [Z_k^T, U_k^T]^T$ into equation (3.33), yields

$$(I - D_f \begin{bmatrix} 0 \\ I \end{bmatrix}) U_k = C_f X_k^f + D_f \begin{bmatrix} C \\ 0 \end{bmatrix} X_k + D_f \begin{bmatrix} N \\ 0 \end{bmatrix} a_k \tag{3.35}$$

where $D_f [0 \quad I]^T = 0$ can be proved based on simple matrix multiplication. Thus we have

$$U_k = C_f X_k^f + D_f \begin{bmatrix} C \\ 0 \end{bmatrix} X_k + D_f \begin{bmatrix} N \\ 0 \end{bmatrix} a_k$$

Then the feedback structure shown in Figure 3.3 produces a closed-loop system from a_k to $Z_k^{'}$:

$$\overline{X}_{k+1} = A_{cl} \overline{X}_k + B_{cl} a_k \tag{3.36}$$

$$Z_k^{'} = C_{cl} \overline{X}_k + D_{cl} a_k$$

where $\overline{X}_k = [X_k^T, X_k^{fT}]^T$ is the closed-loop system state. The system matrices in equation

(3.36) are given by

$$A_{cl} = \begin{bmatrix} A + BD_f \begin{bmatrix} C \\ 0 \end{bmatrix} & BC_f \\ B_f \begin{bmatrix} C \\ 0 \end{bmatrix} + B_f \begin{bmatrix} 0 \\ I \end{bmatrix} D_f \begin{bmatrix} C \\ 0 \end{bmatrix} & A_f + B_f \begin{bmatrix} 0 \\ I \end{bmatrix} C_f \end{bmatrix} \tag{3.37}$$

$$B_{cl} = \begin{bmatrix} BD_f \begin{bmatrix} N \\ 0 \end{bmatrix} + M \\ B_f \begin{bmatrix} 0 \\ I \end{bmatrix} D_f \begin{bmatrix} N \\ 0 \end{bmatrix} \end{bmatrix} \quad D_{cl} = \begin{bmatrix} \begin{bmatrix} 0 \\ \sqrt{\lambda} \end{bmatrix} D_f \begin{bmatrix} N \\ 0 \end{bmatrix} + \begin{bmatrix} N \\ 0 \end{bmatrix} \end{bmatrix}$$

$$C_{cl} = \begin{bmatrix} \begin{bmatrix} C \\ 0 \end{bmatrix} + \begin{bmatrix} 0 \\ \sqrt{\lambda} \end{bmatrix} D_f \begin{bmatrix} C \\ 0 \end{bmatrix} & \begin{bmatrix} 0 \\ \sqrt{\lambda} \end{bmatrix} C_f \end{bmatrix}$$

Remark 5. *The solution to distributed LQG problem considering state feedback control and state estimation simultaneously can be obtained by minimizing the H_2 norm of the system shown in equation (3.36) following Lemma 1 and Theorem 1. First, a set of stabilizing initial values of controller gain matrices are calculated based on Theorem 2 where only X_{k-d} is used for the initial distributed controllers design. Since information of the entire system at and before time $k-d$ is available to each subsystem, then initial distributed observer is designed in each subsystem to estimate $\hat{X}_{k-d}$ based on equation (3.4) with gain matrix L^c selected as the steady state gain of the Kalman filter designed for the entire system shown in equation (3.1). Further, the lower and upper LQG tradeoff curves can be obtained following Remark 4 by selecting $d_{ij}(k) = d_{min}$ and $d_{ij}(k) = d_{max}$ for all k and $1 \leq i, j \leq n, i \neq j$, respectively.*

According to the achieved lower and upper LQG tradeoff curves, the system with performance lies between the lower and upper LQG tradeoff curves is guaranteed to be in a perfect

condition; the system with performance above but close to the upper LQG tradeoff curve has an acceptable performance, but there still is a potential for performance improvement; the system with performance far above the upper LQG tradeoff curve indicates poor performance, then tuning of distributed controllers and distributed observers or improvement on communication network topology is necessary.

3.5 Simulations

Considering the following 2×2 system:

$$\begin{aligned}
\begin{bmatrix} X_{1k+1} \\ X_{2k+1} \end{bmatrix} &= \begin{bmatrix} 0.914 & 0.08 \\ -0.126 & 0.917 \end{bmatrix} \begin{bmatrix} X_{1k} \\ X_{2k} \end{bmatrix} + \begin{bmatrix} 2.091 & -0.0744 \\ -0.211 & -0.0156 \end{bmatrix} \begin{bmatrix} U_{1k} \\ U_{2k} \end{bmatrix} \\
&+ \begin{bmatrix} 0.914 & 0.08 \\ -0.126 & 1.632 \end{bmatrix} \begin{bmatrix} a_{1k} \\ a_{2k} \end{bmatrix} \\
\begin{bmatrix} Z_{1k} \\ Z_{2k} \end{bmatrix} &= \begin{bmatrix} 1 & 0 \\ 0 & 1 \end{bmatrix} \begin{bmatrix} X_{1k} \\ X_{2k} \end{bmatrix} + \begin{bmatrix} 1 & 0 \\ 0 & 1 \end{bmatrix} \begin{bmatrix} a_{1k} \\ a_{2k} \end{bmatrix}
\end{aligned} \tag{3.38}$$

where the system is divided into 2 univariate subsystems, (X_{1k}, Z_{1k}, U_{1k}) and (X_{2k}, Z_{2k}, U_{2k}), respectively. We assume that the system shown in equation (3.38) is under distributed networked control and suffers from random communication delays, where $d_{min} = 1$ and $d_{max} = 2$, respectively. In the following, different solutions of the LQG problem

$$J(\lambda) = E[Z_k^T Z_k] + \lambda E[U_k^T U_k] \tag{3.39}$$

is discussed to illustrate the proposed work.

First, the applicability of separation principle in distributed networked control is tested.

Considering the case with $d = 2$, optimal controller is in the form of

$$U_k = F^0 X_k + F^1 X_{k-1} + F^2 X_{k-2} \tag{3.40}$$

where X_k, X_{k-1} and X_{k-2} need to be estimated with the proposed observer. For the LQG problem in equation (3.39) with $\lambda = 2$ and $\lambda = 2^{-4}$, distributed LQG control are designed without using separation principle based on the proposed algorithm. When $\lambda = 2$, the optimal controller parameters are

$$F^0 = \begin{bmatrix} -0.1600 & 0 \\ 0 & 0.0735 \end{bmatrix} F^1 = \begin{bmatrix} -0.2001 & 0 \\ 0 & 0.0090 \end{bmatrix} F^2 = \begin{bmatrix} -0.0134 & 0.1307 \\ 0.0080 & -0.0264 \end{bmatrix} \tag{3.41}$$

while, the optimal controller parameters for $\lambda = 2^{-4}$ are

$$F^0 = \begin{bmatrix} -0.2259 & 0 \\ 0 & 1.1123 \end{bmatrix} F^1 = \begin{bmatrix} -0.2504 & 0 \\ 0 & 0.5087 \end{bmatrix} F^2 = \begin{bmatrix} -0.0248 & 0.1875 \\ -0.0171 & 0.2103 \end{bmatrix} \tag{3.42}$$

To test the influence of communication delays in control actions on separation principle, the optimal observer parameters design for $\lambda = 2$ is applied to both the cases of $\lambda = 2$ and $\lambda = 2^{-4}$, where the observer parameters are given as

$$L^c = \begin{bmatrix} 0.5694 & 0.0007 \\ 0.0007 & 0.7693 \end{bmatrix} \quad L^z_{11} = \begin{bmatrix} 0.1222 & 0 \\ 0 & -0.0611 \end{bmatrix} L^z_{12} = \begin{bmatrix} 0.1747 & 0 \\ 0 & -0.0687 \end{bmatrix} \tag{3.43}$$
$$L^z_{21} = \begin{bmatrix} 1.9154 & 0 \\ 0 & 0.5170 \end{bmatrix} \quad L^u_{11} = \begin{bmatrix} 0.1715 & 0 \\ 0 & -0.7995 \end{bmatrix}$$

Control actions and state estimation errors for these two cases are shown in Figure 3.5, where the blue curve represent the case of controller designed for $\lambda = 2$ combined with observer designed for $\lambda = 2$ and the red curve represent the case of controller designed for $\lambda = 2^{-4}$

combined with observer designed for $\lambda = 2$. X_{ik}, X_{ik-1} and X_{k-2} are estimated in subsystem i $(i = 1, 2)$ based on the local observer design in equations (3.6). Theoretically, when there is no communication delay between different subsystems, the optimal estimation of X_{ik-1} and X_{k-2} can be achieved in subsystem i with Y_{k-1}, U_{k-2} and Y_{k-2}, U_{k-3} respectively. Thus, when $d = 2$, separation principle holds for the estimation of X_{ik-1} and X_{k-2} due to U_{k-2} and U_{k-3} are available to subsystem i at time k. As shown in Figure 3.5, $e_{X_{ik-1}}$ and $e_{X_{ik-2}}$, the state estimation errors of X_{ik-1} and X_{ik-2}, respectively, are the same in blue and red curves. However, in subsystem i, the optimal estimation of X_{ik} is related to U_{k-1} which is not available due to $d = 2$. Then, missing information of control actions will lead to additional state estimation error. Due to the smaller weighting coefficient in LQG cost function, control actions with larger control effort are applied to the system when $\lambda = 2^{-4}$ comparing with the case $\lambda = 2$. With the same observer, larger control effort in red curve leads to larger state estimation error of X_{2k}, which proves that separation principle does not hold when there is communication delays in control actions.

Then, to test performance of the proposed LQG design, the optimal controller parameters design for $\lambda = 2^{-4}$ is combined with the optimal observer parameters design for both the cases of $\lambda = 2^{-4}$ and $\lambda = 2$. The optimal observer parameters for $\lambda = 2^{-4}$ are given as

$$L^c = \begin{bmatrix} 0.5694 & 0.0007 \\ 0.0007 & 0.7693 \end{bmatrix} \quad L^z_{11} = \begin{bmatrix} 0.0615 & 0 \\ 0 & -0.0573 \end{bmatrix} L^z_{12} = \begin{bmatrix} 0.0878 & 0 \\ 0 & -0.0628 \end{bmatrix} \tag{3.44}$$
$$L^z_{21} = \begin{bmatrix} 1.9925 & 0 \\ 0 & 1.3360 \end{bmatrix} \quad L^u_{11} = \begin{bmatrix} -0.0352 & 0 \\ 0 & -0.3918 \end{bmatrix}$$

Outputs and designed control actions for these two cases are shown in Figure 3.6, where the blue curve represent the case of controller designed for $\lambda = 2^{-4}$ combined with observer designed for $\lambda = 2^{-4}$ and the red curve represent the case of controller designed for $\lambda = 2^{-4}$ combined with observer designed for $\lambda = 2$. For the blue curve, $E[Z_k^T Z_k] = 13.3715$ and $E[U_k^T U_k] = 17.0140$, then the LQG cost function $J(\lambda = 2^{-4})|_{blue} = 14.4348$. For the red curve,

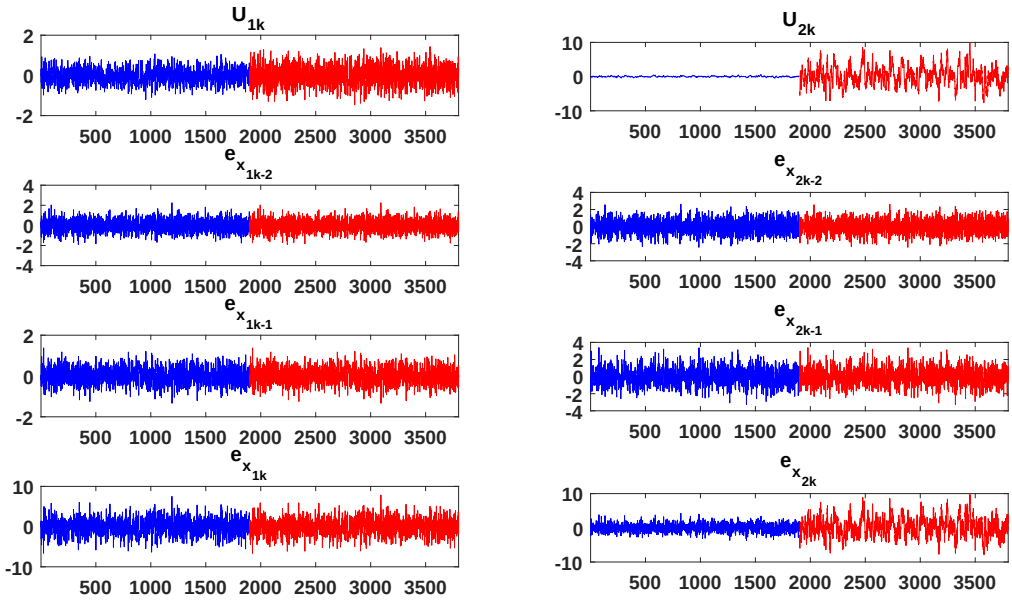

Figure 3.5: Control actions and state estimation errors for two cases: 1) controller designed for $\lambda = 2$ combined with observer designed for $\lambda = 2$; 2) controller designed for $\lambda = 2^{-4}$ combined with observer designed for $\lambda = 2$.

$E[Z_k^T Z_k] = 14.1906$ and $E[U_k^T U_k] = 7.7791$, then the LQG cost function $J(\lambda = 2^{-4})|_{red}$= 14.6768. There are larger control effort and better LQG performance in the blue curve. These results show that control actions are designed more appropriately when designing controllers and observers simultaneously in DNCSs.

Further, the tradeoff curve of the best achievable LQG control performance is formed based on the solutions of the LQG problem in equation (4.39) by varying $\lambda = 2^i$ from $i = -7.5$ to $i = 2$ with a step size of 0.5 in i. The proposed lower and upper LQG tradeoff curves are shown as the curve $d = 1$ and $d = 2$ in Figure 3.6, respectively. The region between curve $d = 1$ and $d = 2$ can be treated as an alternative for the centralized LQG benchmark. The system with performance lying between curve $d = 1$ and curve $d = 2$ may be considered as a good performance; the system with performance above but close to the curve $d = 2$ has an acceptable performance, but there still is a potential for performance improvement; the system with performance far above the curve $d = 2$ indicates poor performance, then

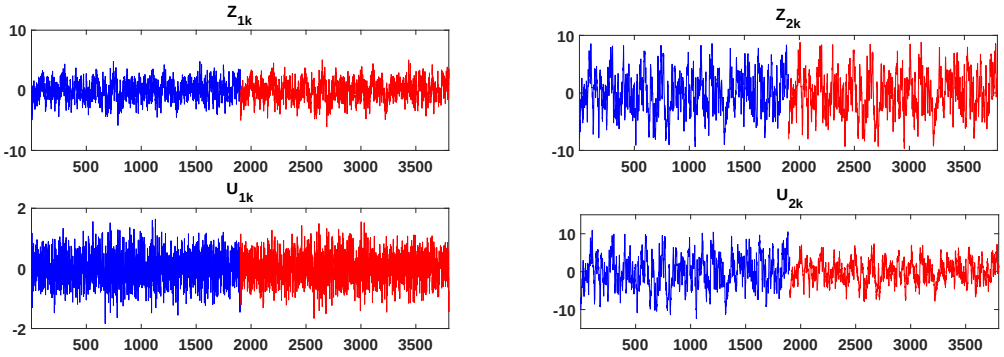

Figure 3.6: LQG control performance for two cases: 1) controller designed for $\lambda = 2^{-4}$ combined with observer designed for $\lambda = 2^{-4}$; 2) controller designed for $\lambda = 2^{-4}$ combined with observer designed for $\lambda = 2$.

controller tuning or improvement on communication network topology is helpful. As shown in Figure 3.7, there is a significant gap between curve *centralized* and curve $d = 1, d = 2$ which indicates that the best control performance in the centralized case is non-achievable for a DNCS with communication delays. Thus, if centralized LQG tradeoff curve is used as the criterion for performance assessment, although controller for a DNCS is well designed, it is highly likely to show a poor control performance and may lead engineers to search for the non-existent distributed controllers. The proposed lower and upper LQG tradeoff curves can give a more practical estimate on the best achievable control performance when the system has random communication delays. It is therefore more suitable for control performance assessment of DNCSs.

For the case of state feedback combined with state estimation, optimal control efforts for the LQG cost functions with different weighting factors are shown in Figure 3.8. When $\lambda \geq 2^{-4.5}$, control efforts for the case of $d = 1$ are small, and loss of information of control actions caused by communication delays does not have a big influence on state estimation error. Thus, with a goal towards good control performance, control efforts for the case of $d = 1$ are larger than the control efforts for the case of centralized control due to the structure constraints in the controller. When $\lambda \leq 2^{-4.5}$, control efforts for the case of $d = 1$ are large, and loss of information of control actions caused by communication delays has a

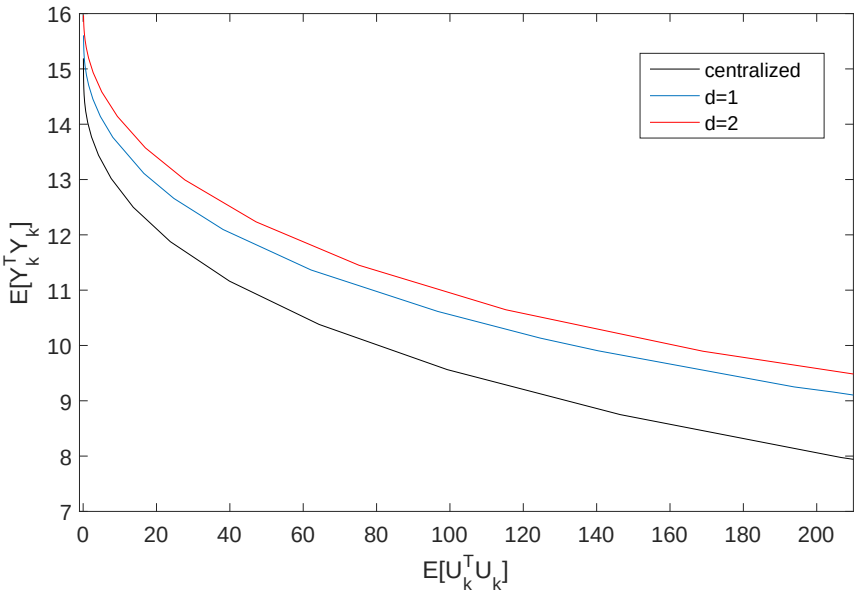

Figure 3.7: Comparison of best achievable LQG control performance under state feedback control combine with state estimation in case of centralized control and distributed networked control.

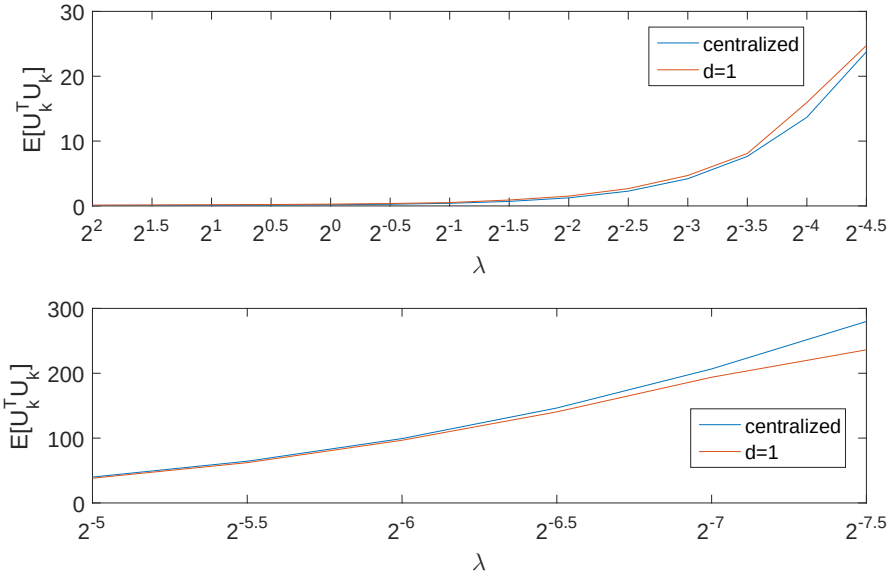

Figure 3.8: Optimal control efforts for the LQG cost function with different weights.

big influence on state estimation error which will decrease the control performance. Thus, there is a tradeoff between state feedback control performance and state estimation error which makes control efforts for the case of $d = 1$ smaller than the control efforts for the case of centralized control. It also proves that separation principle is not applicable on the system with communication delays in control actions.

3.6 Conclusions

This chapter investigates the lower and upper LQG tradeoff curves designed for DNCSs with random communication delays. By designing the optimal distributed controllers and distributed observers simultaneously without using separation principle, the best achievable control performance of a DNCS is presented in the form of the lower and upper LQG tradeoff curves. The obtained tradeoff curves can be used to evaluate the potential performance improvement of an existing DNCS that indicates the potential needs on tuning of distributed controllers and distributed observers or improvement on communication network topology. Further, separation principle is found non-applicable on DNCSs with communication delays, and this conclusion is tested through a numerical example.

Chapter 4

Practical Solutions to LTV Minimum Variance Benchmark for NCSs with Random Communication Delays[3]

4.1 Introduction

The research of NCS has been one of the most attractive areas in both industry and academia due to continuously expanding physical setups and functionality in modern industrial systems [2, 3]. A typical NCS consists of the spatially distributed controller and system (physical plants, actuators, sensors, etc.). In a NCS, control loops are closed through information exchange between system components over a shared network. The elimination of unnecessary wiring in NCSs reduces overall cost for the installation of control systems and provides ease in maintenance. In addition, by connecting cyber to physical space through communication network, NCSs are able to fuse global information and operate systems over long distance [6, 7]. However, in a NCS, network-induced communication delays are inevitable and normally

[3]A shorter version of this chapter has been published in "Guoyang Yan, Jinfeng Liu, and Biao Huang. MV benchmark for networked control systems with random communication delays. IFAC-PapersOnLine, 52(1): 970 C 975, 2019. 12th IFAC Symposium on Dynamics and Control of Process Systems, including Biosystems DYCOPS 2019".

random. Random communication delays will degrade the system control performance and lead to a non-stationary behavior of the closed-loop system [10, 11].

On the other hand, control performance assessment is a widely used process monitoring technique aiming at optimal control performance and cost effectiveness. Among the various control performance assessment approaches, minimum variance benchmark is the most widely used one [69]. One of the reasons for the successes in the research and the application of the univariate minimum variance benchmark is that this benchmark can be calculated from routine operating data and only the *a priori* knowledge of time delay between a pair of input and output is required. However, the convenience is lost for multivariate case where time delay between a set of inputs and outputs is termed as the interactor matrix. Due to the presence of random communication delays within the closed-loop system, the NCSs are naturally multivariate and non-stationary. The interactor matrices estimated from closed-loop data are generally not accurate enough in practice, especially when there are non-stationary characteristics in closed-loop data. Hence, the elimination of using the interactor matrix in obtaining the control performance assessment benchmark for NCSs would simplify the calculation and reduce the uncertainty associated with the estimation of multivariate performance index from routine operating data.

Motivated by the above discussions, this chapter considers the LTV minimum variance benchmark designed for NCSs with random communication delays. Sensor-to-controller communication delay and controller-to-actuator communication delay are considered simultaneously. These two communication delays are both modeled as random variables with a given bounded region. Complete knowledge of the interactor matrix is not needed in this work. Only OIM and RIM are assumed to be known as the *a priori* knowledge. These two variables can be more easily estimated from closed-loop data. Thus, instead of estimating the true LTV minimum variance benchmark, the best we can do is deriving a bound on the benchmark control in this case.

The main contributions of this chapter are listed as follows. Firstly, explicit solutions

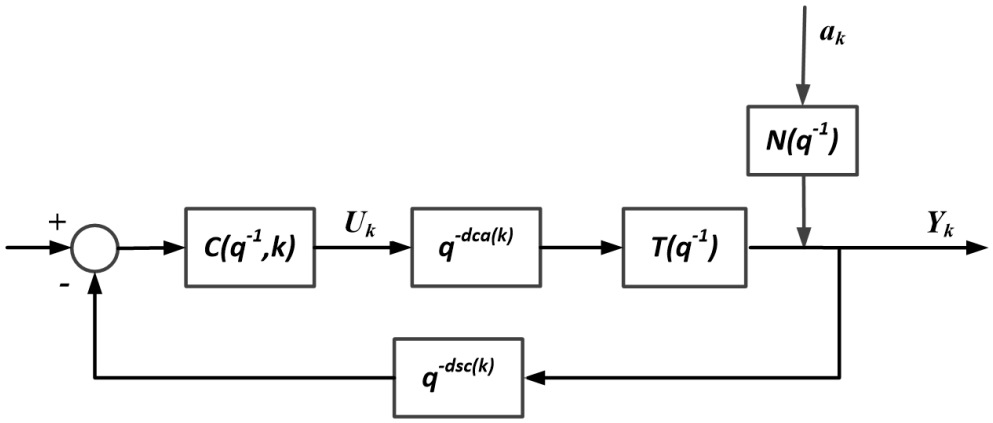

Figure 4.1: Schematic of NCSs with random communication delays.

to the true LTV minimum variance benchmark and corresponding LTV minimum variance control law are derived for NCSs with use of the simple interactor matix (all the control loops in the multivariate system have same time delay). Secondly, the lower and upper bounds of the LTV minimum variance benchmark region is proposed as a relaxation of the true LTV minimum variance benchmark for NCSs with general interactor matix (time delay can be different among control loops in the multivariate system). Explicit solutions to the lower and upper bounds of LTV minimum variance control performance are derived. It is shown that the lower and upper bounds can be calculated from the first few terms in the impulse response form of the closed-loop model. The upper bound of the proposed benchmark is proven to be achievable by a practical controller. Further, an explicit and direct method to estimate closed-loop output under LTV minimum variance control from routine operating data is proposed.

4.2 Preliminaries

4.2.1 System description

This chapter mainly concerns with the multivariate NCSs shown in Figure 4.1:

$$Y_k = Tq^{-d_{ca}(k)}U_k + Na_k \tag{4.1}$$
$$U_k = -C(k)q^{-d_{sc}(k)}Y_k$$

where k indicates current time instant; T and N are proper rational transfer function matrices in the backshift operator q^{-1}; Y_k, U_k and a_k are output, input and white-noise vectors of appropriate dimensions; $C(k)$ is the LTV output feedback control law to be designed; $d_{ca}(k)$ and $d_{sc}(k)$ are the random controller-to-actuator and sensor-to-controller communication delays, respectively. Further, $d_{ca}(k)$ and $d_{sc}(k)$ are assumed to be bounded and independent with each other:

$$0 \leq d_{ca}(k) \leq \bar{d}_{ca} \quad \text{and} \quad 0 \leq d_{sc}(k) \leq \bar{d}_{sc}$$

where $\bar{d}_{ca}$ and $\bar{d}_{sc}$ are the upper bounds of $d_{ca}(k)$ and $d_{sc}(k)$, respectively.

4.2.2 Illustrative example

To show the drawbacks of applying the conventional minimum variance benchmark on NCSs with random communication delays, an illustrative example adopt from [1] is presented in this section. Control performance assessment is conducted on a two interacting-tank process shown in Figure 4.2. The levels $(h_1; h_2)$ of the two tanks are the controlled variables, and the corresponding inlet flow rates $(u_1; u_2)$ are the manipulated variables.

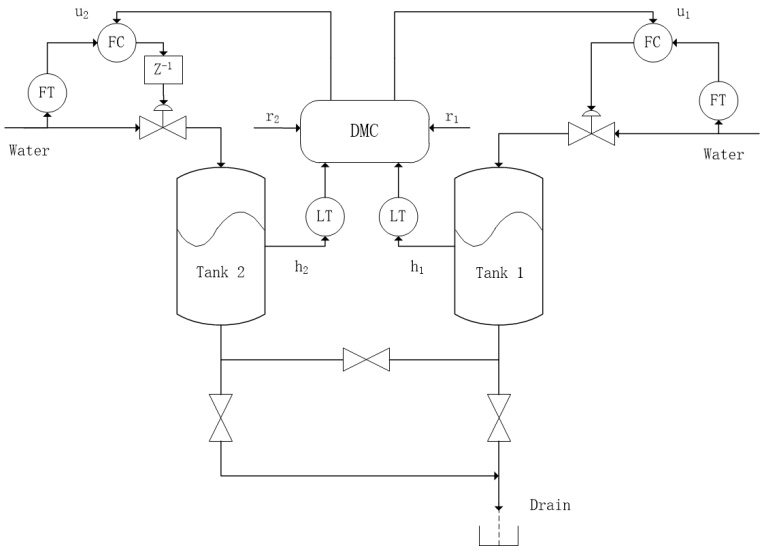

Figure 4.2: Schematic diagram of the pilot-scale process.

The open-loop model is given as

$$T = \begin{bmatrix} \frac{0.1963q^{-1}-0.1737q^{-2}-0.0112q^{-3}}{1-1.7208q^{-1}+0.7272q^{-2}} & \frac{0.0406q^{-7}-0.0113q^{-8}+0.0009q^{-9}}{1-0.6495q^{-1}+0.0482q^{-2}} \\ \frac{0.0147q^{-1}-0.0127q^{-2}+0.02q^{-3}}{1-1.3537q^{-1}+0.3707q^{-2}} & \frac{0.0406q^{-2}-0.0299q^{-3}-0.0047q^{-4}}{1-1.7849q^{-1}+0.7902q^{-2}} \end{bmatrix} \tag{4.2}$$

The hypothetical disturbance dynamics are taken as

$$N = \begin{bmatrix} \frac{1}{1-q^{-1}} & 0 \\ 0 & \frac{1}{1-q^{-1}} \end{bmatrix} \tag{4.3}$$

An internal model control (IMC) controller is implemented on this process. The optimal IMC controller is the inverse of the delay-free model $\tilde{T} = DT$, where D can be factored out from T as

$$D = \begin{bmatrix} -0.9972q & -0.0748q \\ 0.0748q^2 & -0.9972q^2 \end{bmatrix} \tag{4.4}$$

To make the IMC controller implementable, a filter

$$f = \begin{bmatrix} \frac{0.1}{1-0.9q^{-1}} & 0 \\ 0 & \frac{0.1}{1-0.9q^{-1}} \end{bmatrix} \tag{4.5}$$

is cascaded to the optimal IMC controller. The final IMC controller is $Q^* = \tilde{T}^{-1} f$ where Q^* is the controller in the IMC framework [70].

Control performance of this IMC controller under both centralized control and networked control are tested with the conventional minimum variance benchmark. Sensor-to-controller communication delay $d_{sc}(k)$ and controller-to-actuator communication delay $d_{ca}(k)$ are considered simultaneously in the networked control. The series of $d_{sc}(k)$ and $d_{ca}(k)$ are generated by values randomly taken from the set $\{0, \cdots, \bar{d}_c\}$ with equal probability. The step-type setpoint tracking performance is of interest in this example. The setpoint levels of the two tanks are $h_{1s} = 3$ and $h_{2s} = 4$, and a random binary dither signal with amplitude of 0.25 is inserted in the two setpoints. When $\bar{d}_c = 4$, the generated communication delay sequences are shown in Figure 4.3, and the closed-loop test of the designed IMC controller under centralized control and networked control is shown in Figure 4.4 where blue curve and red curve are centralized control result and networked control result, respectively. According to the closed-loop test, we can find that the designed IMC controller can achieve setpoint tracking when there are random communication delays, although its performance is degraded.

Then, control performance assessment results of the designed IMC controller with $\bar{d}_c = \{1, \cdots, 5\}$ is summarized in Table 4.1. It is easy to find that larger communication delays will lead to poorer control performance. However, the degradation of control performance is not only because of that we do not consider communication delays in the design of IMC controller, but also because of that the presence of communication delays further limits the best achievable control performance. The conventional minimum variance benchmark mainly considers the performance limitations caused by the process itself. When applying it to NCSs with random communication delays, the best achievable control performance can

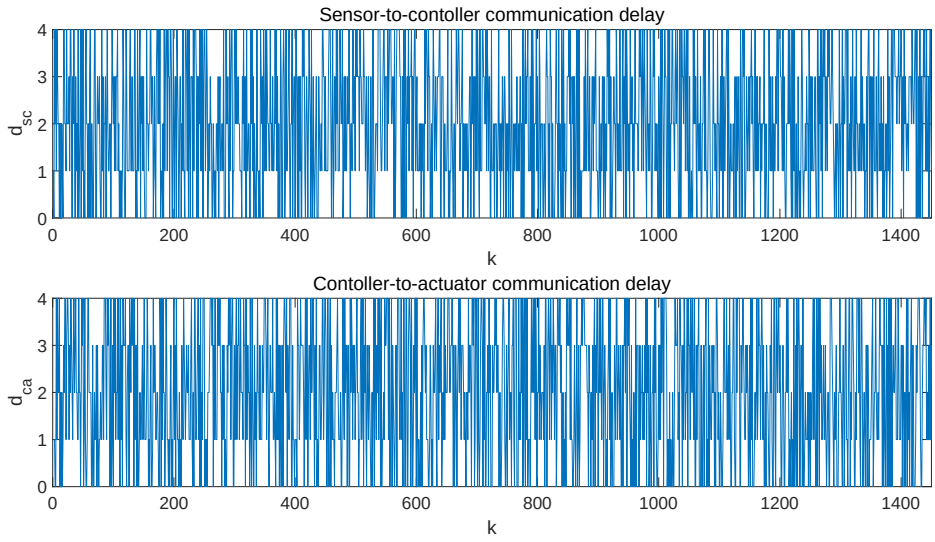

Figure 4.3: Sequences of communication delays.

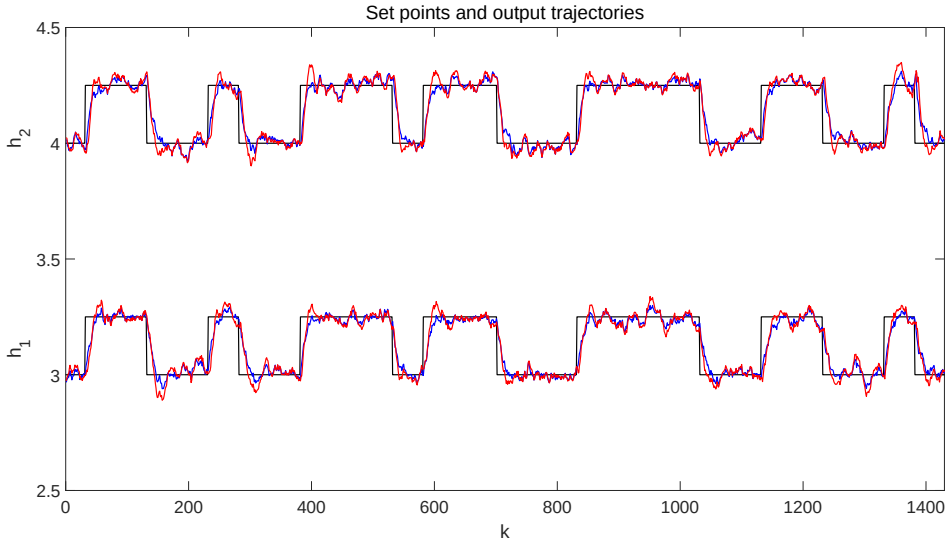

Figure 4.4: Closed-loop test of the IMC controller.

be overly optimistic because the performance limitations caused by communication delays are not considered. Thus, testing performance of networked control using the conventional minimum variance control as a benchmark is not appropriate, and may lead engineers to search for a controller with a better performance that may not exist.

Table 4.1: Control performance assessment results of the pilot-scale process

	centralized control	$\bar{d}_c = 1$	$\bar{d}_c = 2$	$\bar{d}_c = 3$	$\bar{d}_c = 4$	$\bar{d}_c = 5$
η_c	0.3008	0.2599	0.2250	0.1897	0.1587	0.0953

Further, there are two important assumptions for using conventional minimum variance control as the benchmark. The first is that the closed-loop data is stationary. Under stationary condition, the process output variance can be directly calculated with routine operating data, and filtering the process output with the interactor matrix will not change its variance. The second is that the interactor matrix is known as the *a priori* knowledge.

In a NCS, the closed-loop system is non-stationary due to the presence of random communication delays, and obtaining the interactor matrix is even harder under non-stationary condition. On the other hand, d_s can be interpreted as the time used for the control actions having influence on all the outputs; while $d_s - v_s$ can be interpreted as the time used for the control actions having influence on at least one of the outputs. Thus, system time delay of the multivariate process T can be treated as lower bounded by $d_s - v_s$ and upper bounded by d_s, respectively. Therefore, OIM and RIM are useful in control performance assessment. Further, comparing with the *a priori* knowledge of the interactor matrix, OIM and RIM can be obtained more easily. Based on these considerations, in the following sections, design of a practical LTV control performance benchmark with OIM and RIM is proposed for NCSs with random communication delays.

4.3 Control performance assessment of NCSs with random communication delay

In this section, first, preliminary knowledge on the calculation of LTV transfer function matrices is introduced. Then, we derive a LTV minimum variance control law $U_k = -C(k)q^{-d_{sc}(k)}Y_k$ for NCSs with the simple interactor matrix, such that the control objective function $J_k = E[Y_k^T Y_k]$ is minimized at each time instant. Further, based on this result, solutions of the upper and lower bounds of the LTV minimum variance benchmark for NCSs with the general interactor matrix are proposed with the requirement on the *a priori* knowledge of OIM and RIM. It is shown that the obtained upper and lower bounds of the LTV minimum variance benchmark consist of the first few terms in the impulse response form of the closed-loop transfer function matrix and can be estimated from routine operating data.

4.3.1 Calculation of LTV transfer function matrices

Before proceeding, we need to introduce some basic properties of the calculation of LTV transfer function matrices. These properties will be used throughout this chapter. The most fundamental property is that for any LTV transfer function matrix $A(k)$ we have the following identity [43]:

$$q^{-d}A(k) = A(k-d)q^{-d} \tag{4.6}$$

Then, based on this property, the multiplication of LTV transfer function matrices is introduced below. Let $V(k)$, $W(k)$ and $X(k)$ be three LTV polynomial matrices in q^{-1} with

order n, m and l, respectively:

$$V(k) = v_0(k) + v_1(k)q^{-1} + \cdots + v_n(k)q^{-n} \tag{4.7}$$
$$W(k) = w_0(k) + w_1(k)q^{-1} + \cdots + w_m(k)q^{-m}$$
$$X(k) = x_0(k) + x_1(k)q^{-1} + \cdots + x_l(k)q^{-l}$$

According to equation (4.6), the multiplication of two LTV polynomial matrices $V(k)$ and $W(k)$ can be conducted as:

$$\begin{aligned} V(k)W(k) &= \sum_{i=0}^{n}\sum_{j=0}^{m} v_i(k)q^{-i}w_j(k)q^{-j} \\ &= \sum_{i=0}^{m}\sum_{j=0}^{n} v_i(k)w_j(k-i)q^{-(i+j)} \end{aligned} \tag{4.8}$$

and some properties in the multiplication of LTV transfer function matrices can be extended from equation (4.8) as follows:

- Commutativity law: $V(k)W(k) \neq W(k)V(k)$
- Associativity law: $[V(k)W(k)]X(k) = V(k)[W(k)X(k)]$
- Distributive law: $[V(k) + W(k)]X(k) = V(k)X(k) + W(k)X(k)$,

Further, the inverse of an LTV transfer function matrix is elaborated as follows. Define $WL(k)$ as the left inverse of $W(k)$ and $WR(k)$ as the right inverse of $W(k)$. $WL(k)$ and $WR(k)$ are both LTV transfer function matrices of q^{-1} with

$$WL(k) = wl_0(k) + wl_1(k)q^{-1} + \cdots + wl_n(k)q^{-n} + \cdots$$
$$WR(k) = wr_0(k) + wr_1(k)q^{-1} + \cdots + wr_n(k)q^{-n} + \cdots$$

According to the definition of inversion, we have

$$WL(k)W(k) = I \tag{4.9}$$

$$W(k)WR(k) = I \tag{4.10}$$

$WL(k)$ and $WR(k)$ can be calculated by equating coefficients of both sides of equations (4.9) and (4.10), respectively. Then, we can obtain $WL(k) = WR(k)$, that is, the left inverse of an LTV transfer function matrix is equal to its right inverse. Proofs of the results shown in this section are provided in Appendix A.1.

4.3.2 LTV minimum variance benchmark for NCSs with the simple interactor matrix

The interactor matrix D can be one of the three forms discussed in Section 1.2.2. Although processes with the simple interactor matrices are the simplest ones and are not common in practice, the results presented in this section are the foundation of solutions to processes with the general interactor matrices that follow later.

Consider NCSs with random communication delays shown in Figure 4.1. The process model is assumed to have the simple interactor matrix $D = q^{d_s}I$. Thus, $T = q^{-d_s}\tilde{T}$, where the time used for each of the control actions having influence on each of the outputs is d_s. Output sensor measurements are sent from the sensors to the controller subject to random communication delay $d_{sc}(k)$, while designed control actions are sent from the controller to the actuators subject to random communication delay $d_{ca}(k)$. Then, in the closed-loop system, the total time used for the designed control actions having influence on the outputs is

$$d_{co}(k) = d_s + d_{ca}(k - d_s) \tag{4.11}$$

and the total time used for the output sensor measurements having influence on the outputs

through the feedback and forward channels is

$$d_{so}(k) = d_s + d_{ca}(k - d_s) + d_{sc}(k - d_s - d_{ca}(k - d_s)) \tag{4.12}$$

The following results present the design of LTV minimum variance control for NCSs with the simple interactor matrix, and the corresponding performance assessment using the LTV minimum variance control as the benchmark. For a NCS with random communication delays shown in Figure 4.1, solutions of the LTV minimum variance benchmark are given by the following steps:

1. The LTV minimum variance control law is given by

$$C(k) = \tilde{T}^{-1} R(k + d_{ca}(k'') + d_s) F^{-1}(k - d_{sc}(k)) \tag{4.13}$$

   where $F(k)$ and $R(k)$ are solved from a Diophantine identity [1]:

$$N = F(k) + R(k) q^{-d_{so}(k)} \tag{4.14}$$

   where $F(k)$ is the LTV polynomial matrix that consists of the first $d_{so}(k)$ terms in the impulse response form of N, and $R(k)q^{-d_{so}(k)}$ is the remaining LTV transfer function matrix in N. In equation (4.14), coefficient matrices in $F(k)$ and $R(k)$ are consistent with those in N, and only the order of $F(k)$ varies with time.

2. The closed-loop output under the LTV minimum variance control is given by a finite-order moving average process

$$Y_k|_{mv} = F(k)a_k = (F_0(k) + F_1(k)q^{-1} + \cdots + F_{d_{so}(k)-1}(k)q^{-d_{so}(k)+1})a_k \tag{4.15}$$

   where $F_i(k)$ (for $i = 0, \cdots, d_{so}(k) - 1$) is the i_{th} coefficient matrix in $F(k)$. The LTV

minimum variance benchmark $\Phi_{mv}(k)$ can be calculated as

$$\Phi_{mv}(k) = E[Y_k|_{mv}^T Y_k|_{mv}] = \sum_{i=0}^{d_{so}(k)-1} tr(F_i^T(k)F_i(k)) \tag{4.16}$$

3. The closed-loop output $Y_k|_{actual}$ for the actual process can be modeled by an infinite-order moving average process

$$\begin{aligned} Y_k|_{actual} &= G_{cl}(k)a_k \\ &= F(k)a_k + L(k)a_k \\ &= (F_0(k) + F_1(k)q^{-1} + \cdots + F_{d_{so}(k)-1}(k)q^{-d_{so}(k)+1} + L_0(k)q^{-d_{so}(k)} + \cdots)a_k \end{aligned} \tag{4.17}$$

where $G_{cl}(k)$ is the LTV closed-loop transfer function matrix, and $L(k)$ is a LTV transfer function matrix with the i_{th} coefficient matrix given by $L_i(k)$ (for $i = 0, \cdots$). The first $d_{so}(k)$ terms of $G_{cl}(k)a_k$ constitute the process output under the LTV minimum variance control as shown in equation (4.15), while the appearance of term $L(k)a_k$ is caused by the implemented non-optimal control law in the real process. The actual output variance $\Phi_{actual}(k)$ can be calculated as

$$\Phi_{actual}(k) = E[Y_k^T Y_k] = ||G_{cl}(k)||_2^2 \tag{4.18}$$

4. Then, the time-varying performance index is given by

$$\eta_n(k) = \frac{\Phi_{mv}(k)}{\Phi_{actual}(k)} \tag{4.19}$$

Derivations for the results shown in this section are provided in Appendix A.2.

4.3.3 Solutions to LTV minimum variance benchmark for NCSs with the general interactor matrix

In the practical application, as discussed in the previous sections, the general interactor matrix is often not available or not easy to interpret even if available due to its complexity. These are the major difficulties for the application of multivariate control performance assessment algorithms. Extending the proposed LTV minimum variance benchmark to the NCSs with the general interactor matrix will face the same problem.

Further, the explicit solutions of minimum variance control for the stationary systems can be obtained based on filtering the systems with the general interactor matrices [1]. While this good property only holds in the stationary case, NCSs with random communication delays are naturally multivariate and non-stationary. Explicit solution of control performance assessment algorithm is desired, as it yields a considerably simple computation procedure in practical application. Hence, in order to explore an explicit solution of the LTV minimum variance benchmark for NCSs with the general interactor matrix, a bound on minimum variance control benchmark is proposed as follows based on OIM and RIM.

Consider NCSs with random communication delays shown in Figure 4.1. The process model is assumed to have the general interactor matrix

$$D = D_0 q^{d_s} + D_1 q^{d_s-1} + \cdots + D_{v_s} q^{d_s-v_s} \tag{4.20}$$

Thus, $T = D^{-1}\tilde{T}$, and d_s can be interpreted as the time used for the control actions having influence on all the outputs, while $d_s - v_s$ can be interpreted as the time used for the control actions having influence on at least one of the outputs. The system time delay of process T can be treated as lower bounded by $d_s - v_s$ and upper bounded by d_s, respectively.

Thus, in the closed-loop system, the total time used for the designed control actions having influence on the outputs $d_{co}(k)$ can be treated as lower bounded by $d_{co}(k)|_{lower}$ and

upper bounded by $d_{co}(k)|_{upper}$, respectively, with

$$\begin{aligned} d_{co}(k)|_{lower} &= d_s - v_s + d_{co}(k - d_s + v_s) \\ d_{co}(k)|_{upper} &= d_s + d_{co}(k - d_s) \end{aligned} \tag{4.21}$$

while the total time used for the output sensor measurements having influence on the outputs through the feedback and forward channels $d_{so}(k)$ can be treated as lower bounded by $d_{so}(k)|_{lower}$ and upper bounded by $d_{so}(k)|_{upper}$, respectively, with

$$\begin{aligned} d_{so}(k)|_{lower} &= d_s - v_s + d_{ca}(k - d_s + v_s) + d_{sc}(k - d_s + v_s - d_{ca}(k - d_s + v_s)) \\ d_{so}(k)|_{upper} &= d_s + d_{ca}(k - d_s) + d_{sc}(k - d_s - d_{ca}(k - d_s)) \end{aligned} \tag{4.22}$$

Then, it is natural to extend the conclusion in equation (4.17) to NCSs with the general interactor matrices. That is, the lower bound of the LTV minimum variance benchmark consists of the first $d_{so}(k)|_{lower}$ terms in the impulse response form of $G_{cl}(k)$

$$Y_k|_{mv,lower} = \tilde{F}(k)|_{lower} a_k = (\tilde{F}_0(k) + \cdots + \tilde{F}_{d_{so}(k)|_{lower}-1}(k) q^{-d_{so}(k)|_{lower}+1}) a_k \tag{4.23}$$

where $\tilde{F}(k)|_{lower}$ is solved from a Diophantine identity:

$$G_{cl}(k) = \tilde{F}(k)|_{lower} + \tilde{R}(k)|_{lower} q^{-d_{so}(k)|_{lower}} \tag{4.24}$$

where $\tilde{F}(k)|_{lower}$ is the LTV polynomial matrix that consists of the first $d_{so}(k)|_{lower}$ terms in the impulse response form of $G_{cl}(k)$, and $\tilde{R}(k) q^{-d_{so}(k)|_{lower}}$ is the remaining LTV transfer function matrix in $G_{cl}(k)$. While the upper bound of the LTV minimum variance benchmark consists of the first $d_{so}(k)|_{upper}$ terms in the impulse response form of $G_{cl}(k)$

$$Y_k|_{mv,upper} = \tilde{F}(k)|_{upper} a_k = (\tilde{F}_0(k) + \cdots + \tilde{F}_{d_{so}(k)|_{upper}-1}(k) q^{-d_{so}(k)|_{upper}+1}) a_k \tag{4.25}$$

where $\tilde{F}(k)|_{upper}$ is solved from a Diophantine identity:

$$G_{cl}(k) = \tilde{F}(k)|_{upper} + \tilde{R}(k)|_{upper} q^{-d_{so}(k)|_{upper}} \tag{4.26}$$

If this obvious extension of the results proposed in Section 4.3.2 can be served as a meaningful benchmark, this bound on minimum variance control benchmark should satisfy two conditions: 1) it should contain the theoretical best achievable control performance; 2) it should be achievable by a physically implementable control. In the following, the use of this LTV minimum variance benchmark region is analytically justified.

First, we prove that the LTV minimum variance benchmark is lower bounded by $Y_k|_{mv,lower} = \tilde{F}(k)|_{lower} a_k$. For the system shown in equation (4.1), the closed-loop output under the LTV control law $U_k = -C(k)q^{-d_{sc}(k)}Y_k$ can be written as

$$Y_k = -D^{-1}\tilde{T}q^{-d_{ca}(k)}C(k)q^{-d_{sc}(k)}Y_k + Na_k \tag{4.27}$$

According to equation (4.20), define $D^{-1} = q^{-d_s+v_s}D_l^{-1}$ with

$$D_l^{-1} = D_{v_s}^T q^0 + \cdots + D_1^T q^{-v_s+1} + D_0^T q^{-v_s} \tag{4.28}$$

where D_l^{-1} consists of terms with the power of q less than or equal to 0. Thus, D_l^{-1} is a proper polynomial matrix. Substituting $D^{-1} = q^{-d_s+v_s}D_l^{-1}$ into equation (4.27), we have

$$Y_k = -q^{-d_s+v_s}D_l^{-1}\tilde{T}q^{-d_{ca}(k)}C(k)q^{-d_{sc}(k)}Y_k + Na_k \tag{4.29}$$

Further, N is divided to two parts based on the Diophantine equation:

$$N = F(k)|_{lower} + R(k)|_{lower} q^{-d_{so}(k)|_{lower}} \tag{4.30}$$

where $F(k)|_{lower}$ is the LTV polynomial matrix that consists of the first $d_{so}(k)|_{lower}$ terms

in the impulse response form of N, and $R(k)|_{lower}q^{-d_{so}(k)|_{lower}}$ is the remaining LTV transfer function matrix in N. From equations (4.6), (4.24) and (4.30), it follows that

$$\begin{aligned}&\tilde{F}(k)|_{lower}a_k + \tilde{R}(k)|_{lower}a_{k-d_{so}(k)|_{lower}} \\ =&F(k)|_{lower}a_k + R(k)|_{lower}a_{k-d_{so}(k)|_{lower}} \\ &- D_l^{-1}\tilde{T}C(k-d_{co}(k)|_{lower})G_{cl}(k-d_{so}(k)|_{lower})a_{k-d_{so}(k)|_{lower}}\end{aligned} \tag{4.31}$$

It is clear that $\tilde{F}(k)|_{lower}= F(k)|_{lower}a_k$ and $F(k)|_{lower}a_k$ is related to the white noise from time $k-d_{so}(k)|_{lower}+1$ to time k which is future noise to the second and third terms on the right hand side of equation (4.31). Thus,

$$\min E[Y_k^T Y_k] \geq E[(\tilde{F}(k)|_{lower}a_k)^T(\tilde{F}(k)|_{lower}a_k)] \tag{4.32}$$

The theoretical best achievable control performance is lower bounded by

$$Y_k|_{mv,lower}= \tilde{F}(k)|_{lower}a_k = (\tilde{F}_0(k) + \tilde{F}_1(k)q^{-1} + \cdots + \tilde{F}_{d_{so}(k)|_{lower}-1}(k)q^{-d_{so}(k)|_{lower}+1})a_k \tag{4.33}$$

and the lower bound of the LTV minimum variance benchmark $\Phi_{mv}^{lower}(k)$ can be calculated as

$$\Phi_{mv}^{lower}(k) = \sum_{i=0}^{d_{so}(k)|_{lower}-1} tr(\tilde{F}_i^T(k)\tilde{F}_i(k)) \tag{4.34}$$

Second, we prove that for any LTV controller $U_k = -C(k)q^{-d_{sc}(k)}Y_k$ with its closed-loop model given as equation (4.26), the closed-loop response $Y_k|_{mv,upper}= \tilde{F}(k)|_{upper}a_k$ is achievable by a physically realizable controller $U_k = -C^*(k)q^{-d_{sc}(k)}Y_k$. Thus, $Y_k|_{mv,upper}= \tilde{F}(k)|_{upper}a_k$ can provide the measure of the upper bound of the LTV minimum variance benchmark. For the system shown in equation (4.1), the closed-loop output under the LTV

control law $U_k = -C(k)q^{-d_{sc}(k)}Y_k$ can be written as

$$Y_k = (1 + D^{-1}\tilde{T}q^{-d_{ca}(k)}C(k)q^{-d_{sc}(k)})^{-1}Na_k \tag{4.35}$$

where D^{-1} is equivalent to $q^{-d_s}(q^{d_s}D^{-1})$. Then we have

$$Y_k = (1 + q^{-d_s}(q^{d_s}D^{-1})\tilde{T}q^{-d_{ca}(k)}C(k)q^{-d_{sc}(k)})^{-1}Na_k \tag{4.36}$$

where the term $(q^{d_s}D^{-1})\tilde{T}$ is denoted as $\hat{T}$. $\hat{T}$ is invertible, and its inverse is given by

$$\hat{T}^{-1} = \tilde{T}^{-1}(q^{-d_s}D) \tag{4.37}$$

where $\tilde{T}$ is invertible according to the assumptions made in Section 1.2.2. Since the highest power of q in D is d_s, $q^{-d_s}D$ is a proper polynomial matrix. Therefore, $T = q^{-d_s}(q^{d_s}D^{-1})\tilde{T} = q^{-d_s}\hat{T}$ which has the same form as the process model with the simple interactor matrix. Then, for the LTV controllers $c(k)$ and $c^*(k)$ we have

$$\tilde{F}(k)|_{upper} + \tilde{R}(k)|_{upper}q^{-d_{so}(k)|_{upper}} = (1 + q^{-d}\hat{T}q^{-d_{ca}(k)}C(k)q^{-d_{sc}(k)})^{-1}Na_k \tag{4.38}$$

$$\tilde{F}(k)|_{upper} = (1 + q^{-d}\hat{T}q^{-d_{ca}(k)}C^*(k)q^{-d_{sc}(k)})^{-1}Na_k \tag{4.39}$$

From equation (4.6), the difference between equations (4.38) and (4.39) provides

$$\begin{aligned}&\hat{T}[C^*(k - d_{co}(k)|_{upper}) - C(k - d_{co}(k)|_{upper})]\tilde{F}(k - d_{so}(k)|_{upper})|_{upper}q^{-d_{so}(k)|_{upper}} \\ =&(1 + \hat{T}C(k - d_{co}(k)|_{upper})q^{-d_{so}(k)|_{upper}})\tilde{R}(k)|_{upper}q^{-d_{so}(k)|_{upper}}\end{aligned} \tag{4.40}$$

Solving equation (4.40), we will get

$$\begin{aligned}C^*(k - d_{co}(k)|_{upper}) &= C(k - d_{co}(k)|_{upper}) \\ &+ \hat{T}^{-1}(1 + \hat{T}C(k - d_{co}(k)|_{upper})q^{-d_{so}(k)|_{upper}})\tilde{R}(k)|_{upper}\tilde{F}^{-1}(k - d_{so}(k)|_{upper})|_{upper}\end{aligned} \tag{4.41}$$

According to the derivations in equations (A.11-A.14), equation (4.41) can be rewritten as

$$C^*(k) = C(k) + \hat{T}^{-1}(1 + \hat{T}C(k)q^{-d_{sc}(k)})\tilde{R}(k + d_{ca}(k^{''}) + d_s)|_{upper}\tilde{F}^{-1}(k - d_{sc}(k))|_{upper} \tag{4.42}$$

where $k = k^{''} - d_{ca}(k^{''})$. The closed-loop response $Y_k = G_{cl}(k)$ is stable, so $R(k)|_{upper}$ is stable too. $\tilde{F}^{-1}(k - d_{sc}(k))|_{upper}$ is stable and proper by the assumption of N. Finally, $\hat{T}$ is proved to be invertible. Therefore, $C^*(k)$ as solved from equation (4.42) is a physically achievable control, and the theoretical best achievable control performance is upper bounded by $Y_k|_{mv,upper} = \tilde{F}(k)|_{upper}a_k$.

$$\min E[Y_k^T Y_k] \leq E[(\tilde{F}(k)|_{upper}a_k)^T(\tilde{F}(k)|_{upper}a_k)] \tag{4.43}$$

and the upper bound of the LTV minimum variance benchmark $\Phi_{mv}^{upper}(k)$ can be calculated as

$$\Phi_{mv}^{upper}(k) = \sum_{i=0}^{d_{so}(k)|_{upper}-1} tr(\tilde{F}_i^T(k)\tilde{F}_i(k)) \tag{4.44}$$

4.3.4 Practical considerations

In control performance assessment, it is important that the designed benchmark is achievable by a physically implementable control and can be estimated from routine operating data without artificially perturbing the operation of system. But the existence of controller-to-actuator communication delay challenges the satisfaction of these two conditions.

In equation (4.42), sensor-to-controller communication delay $d_{sc}(k)$ and controller-to-actuator communication delay $d_{ca}(k'')$ are compensated in the designed LTV minimum variance control law by the term $\tilde{F}^{-1}(k - d_{sc}(k))|_{upper}$ and the term $\tilde{R}(k + d_{ca}(k'') + d_s)|_{upper}$, respectively. At time k, the term $\tilde{F}^{-1}(k-d_{sc}(k))|_{upper}$ is determined by its order $d_{so}(k-d_{sc}(k))$

with

$$d_{so}(k-d_{sc}(k)) = d_s + d_{ca}(k-d_{sc}(k)-d_s) + d_{sc}(k-d_{sc}(k)-d_s-d_{ca}(k-d_{sc}(k)-d_s)) \tag{4.45}$$

where $d_{sc}(k)$ is the communication delay from the sensors to the controller, and is known by the controller at time k. Thus, $d_{so}(k-d_{sc}(k))$ is known by the controller at time k since it is only related to current and past information. While the term $\tilde{R}(k+d_{ca}(k'')+d_s)|_{upper}$ is determined by the order of $\tilde{F}(k+d_{ca}(k'')+d_s)|_{upper}$, which is

$$\begin{aligned} & d_{so}(k+d_{ca}(k'')+d_s) \\ =& d_s + d_{ca}(k+d_{ca}(k'')) + d_{sc}(k+d_{ca}(k'')-d_{ca}(k+d_{ca}(k''))) \\ =& d_s + d_{ca}(k'') + d_{sc}(k) \end{aligned} \tag{4.46}$$

where $d_{ca}(k'') = k''-k$ requires that k'' should be known which is the time that the actuators receive the information sent by the controller at time k. If $d_{ca}(k'')$ is known by the controller at time k, the designed benchmark control in equation (4.42) is implementable. Then, the proposed LTV minimum variance benchmark in equation (4.44) can be used in control performance assessment of the NCSs. If $d_{ca}(k'')$ is not known by the controller at time k, the proposed LTV minimum variance benchmark in equation (4.42) is not achievable, and the best achievable control performance is further degraded.

In this case, the order of the minimum variance term $\tilde{F}(k)|_{upper}$ cannot be directly chosen as $d_{so}(k)|_{upper}$ due to the unknown controller-to-actuator communication delay. The lower and upper bounds of the LTV minimum variance benchmark are proposed as follows to solve this problem.

1. The lower bound of the LTV minimum variance benchmark can be calculated from equations (4.33) and (4.34) by assuming $d_{ca}(k)$ is known to the controller at time k, which is the best case for the control of the NCSs with random communication delays.

The obtained LTV minimum variance control is actually not implementable, but the lower bound of the LTV minimum variance benchmark provides the maximum that we can further improve the control performance.

2. The upper bound of the LTV minimum variance benchmark is calculated from equations (4.42) and (4.44) by assuming $d_{ca}(k) = \bar{d}_{ca}$, which is the worst case of the control. The obtained LTV minimum variance control in this case is implementable. At time k, the control law is designed with $d_{ca}(k'') = \bar{d}_{ca}$ by the controller. Then, the control actions are sent to the actuators from the controller at time k, and can be implemented by the actuators at time $k + \bar{d}_{ca}$, although the control actions may be received by the actuators before time $k + \bar{d}_{ca}$. Further, the upper bound of the LTV minimum variance benchmark provides the minimum improvement that the controller can achieve.

To calculate the lower and upper bounds of LTV performance index in practice, firstly, recursive time series analysis algorithm can be used to estimate the LTV ARMA model from routine operating data [71, 72, 73]. If the closed-loop system is considered not to be rapidly varying under random communication delays, then moving window based identification of the LTI ARMA model can be used to approximate the LTV closed-loop model. Consider the identified LTV ARMA model with order (n, m) as

$$A(k)Y_k = C(k)a_k \tag{4.47}$$

where

$$\begin{aligned} A(k) &= a_0(k) + a_1(k)q^{-1} + \cdots + a_n(k)q^{-n} \\ C(k) &= c_0(k) + c_1(k)q^{-1} + \cdots + c_m(k)q^{-m} \end{aligned} \tag{4.48}$$

Then, the LTV closed-loop model $G_{cl}(k)$ can be calculated recursively by substituting equa-

tion (4.48) into equation (4.47)

$$G_{cl}(k) = a_0^{-1}(k)[C(k) - a_1(k)G_{cl}(k-1)q^{-1} - \cdots - a_n(k)G_{cl}(k-n)q^{-n}] \tag{4.49}$$

Then, one can determine how well the current controller is operating using the following indices

$$\begin{aligned} \eta_n(k)|_{lower} &= \frac{\Phi_{mv}^{lower}(k)}{\Phi_{actual}(k)} = \frac{\sum_{i=0}^{d_{so}(k)|_{lower}-1} tr(F_i^T(k)F_i(k))}{\|G_{cl}(k)\|_2^2} \\ \eta_n(k)|_{upper} &= \frac{\Phi_{mv}^{upper}(k)|_{d_{ca}(k)=\bar{d}_{ca}}}{\Phi_{actual}(k)} = \frac{\sum_{i=0}^{d_{so}(k)|_{upper}-1} tr(F_i^T(k)F_i(k))|_{d_{ca}(k)=\bar{d}_{ca}}}{\|G_{cl}(k)\|_2^2} \end{aligned} \tag{4.50}$$

where $\eta_n(k)|_{lower}$ and $\eta_n(k)|_{upper}$ are the performance indices calculated based on the lower and upper bounds of the LTV minimum variance benchmark, respectively. According to the obtained performance indices, the NCSs with performance lying between $\eta_n(k)|_{lower}$ and $\eta_n(k)|_{upper}$ is considered to be in a good condition; the NCSs with performance larger than and close to $\eta_n(k)|_{upper}$ is considered an acceptable performance, but there still is a potential for performance improvement; the NCSs with performance larger than and far from $\eta_n(k)|_{upper}$ indicates poor performance, and as a result controller tuning or redesign of the controller will be considered to be necessary.

4.4 Application to a reactor-separator example

In this section, a reactor-separator process as shown in Figure 4.5 is used to illustrate the proposed method. The process consists of two stirred tank reactors and one separator. Streams of pure reactant A are added to the two reactors. Reactant A is converted to product B and side product C by a first-order reaction and a parallel first-order reaction, respectively. Then, distillate of the separator is partially redirected to the first reactor. A

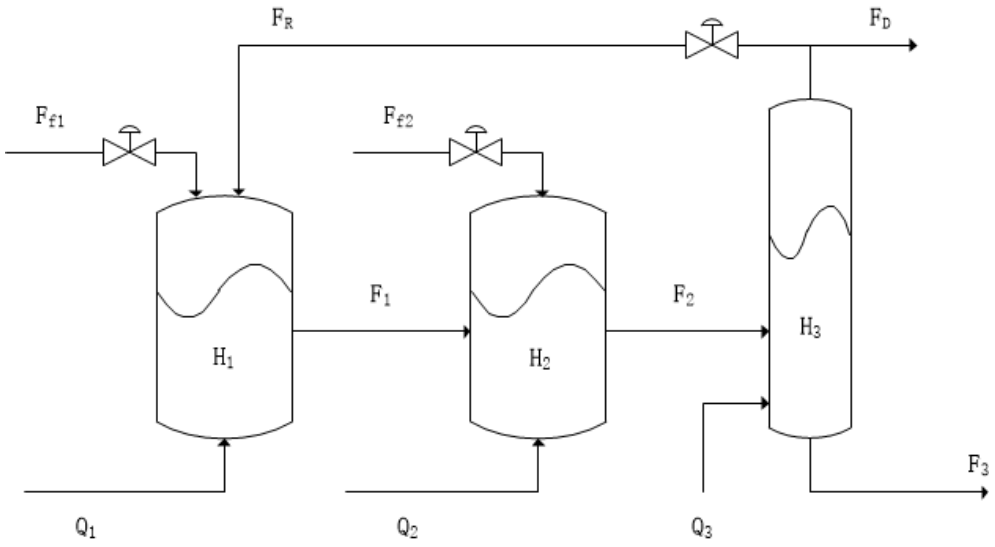

Figure 4.5: Schematic of the reactor-separator process.

dynamic model of this process has been established as following [74, 13]

$$
\begin{aligned}
\frac{dx_{A1}}{dt} &= \frac{1}{\rho A_1 H_1}(F_{f1}x_{A0} + F_R x_{AR} - F_1 x_{A1}) - k_{A1}x_{A1} \\
\frac{dx_{B1}}{dt} &= \frac{1}{\rho A_1 H_1}(F_R x_{BR} - F_1 x_{B1}) + k_{A1}x_{A1} - k_{B1}x_{B1} \\
\frac{dT_1}{dt} &= \frac{1}{\rho A_1 H_1}[F_{f1}(T_{10} + a_{T_{10}}) + F_R(T_3 + a_{T_3}) - F_1 T_1] \\
&\quad - \frac{1}{C_p}(k_{A1}x_{A1}\Delta H_A + k_{B1}x_{B1}\Delta H_B) + \frac{Q_1}{\rho A_1 C_p H_1} \\
\frac{dx_{A2}}{dt} &= \frac{1}{\rho A_2 H_2}(F_{f2}x_{A0} + F_1 x_{A1} - F_2 x_{A2}) - k_{A2}x_{A2} \\
\frac{dx_{B2}}{dt} &= \frac{1}{\rho A_2 H_2}(F_1 x_{B1} - F_2 x_{B2}) + k_{A2}x_{A2} - k_{B2}x_{B2} \\
\frac{dT_2}{dt} &= \frac{1}{\rho A_2 H_2}[F_{f2}(T_{20} + a_{T_{20}}) + F_1 T_1 - F_2 T_2] \\
&\quad - \frac{1}{C_p}(k_{A2}x_{A2}\Delta H_A + k_{B2}x_{B2}\Delta H_B) + \frac{Q_2}{\rho A_2 C_p H_2} \\
\frac{dx_{A3}}{dt} &= \frac{1}{\rho A_3 H_3}[F_{f2}x_{A2} - (F_R + F_D)x_{AR} - F_3 x_{A3}) \\
\frac{dx_{B3}}{dt} &= \frac{1}{\rho A_3 H_3}(F_2 x_{B2} - (F_R + F_D)x_{BR} - F_3 x_{B3}) \\
\frac{dT_3}{dt} &= \frac{1}{\rho A_3 H_3}[F_2 T_2 - (F_R + F_D)T_3 - F_3 T_3] + \frac{Q_3}{\rho A_3 C_p H_3}
\end{aligned}
$$

in which for $i = 1, 2, 3$

$$k_{Ai} = k_A exp(-\frac{E_A}{RT_i}) \quad k_{Bi} = k_B exp(-\frac{E_B}{RT_i})$$

The recycle flow and weight percentages satisfy

$$F_D = 0.01F_R \qquad x_{AR} = \frac{\alpha_A x_{A3}}{\bar{x}_3} \qquad x_{BR} = \frac{\alpha_B x_{B3}}{\bar{x}_3}$$
$$\bar{x}_3 = \alpha_A x_{A3} + \alpha_B x_{B3} + \alpha_C x_{C3} \quad x_{C3} = (1 - x_{A3} - x_{B3})$$

This process has 9 variables where x_{Ai} is the mass fraction of reactant A in the i_{th} vessel, x_{Bi} is the mass fraction of product B in the i_{th} vessel, and T_i is the temperature in the i_{th} vessel, for $i = 1, 2, 3$. We consider that the levels (H_1, H_2, H_3), the flow rates of the feed streams to the first and the second vessels (F_{f1}, F_{f2}), the flow rates of the effluent streams of the three vessels (F_1, F_2, F_3), and the recycle flow rate (F_R) are maintained at constant values. The manipulated inputs are chosen as the heating inputs (Q_1, Q_2, Q_3) provided by the jackets to the three vessels, while the controlled outputs are chosen as the product mass fractions (x_{B1}, x_{B2}, x_{B3}) in the three vessels. (T_{10}, T_{20}, T_3) are the temperatures of (F_{f1}, F_{f2}, F_R), respectively. $(a_{T_{10}}, a_{T_{20}}, a_{T_3})$ are considered as Guassian disturbances with mean 0 and variance 10 that affect (T_{10}, T_{20}, T_3), respectively. Three proportional-integral-derivative (PID) controllers are designed for Q_1, Q_2, Q_3 to control T_1, T_2, T_3, respectively, with the controller given in the form of

$$P_i + I_i T_s \frac{1}{q-1} + D_i \frac{N_i}{1 + N_i T_s \frac{1}{q-1}} \tag{4.51}$$

where P_i is the proportional gain, I_i is the integral gain, D_i is the derivative gain and N_i is the filter coefficient in the i_{th} PID controller, respectively. Further, actuator delays of $0.5s$, $1s$ and $1.5s$ are added to the control of Q_1, Q_2 and Q_3, respectively. The process model is linearized around the steady state and then discretized with sampling time $T_s = 0.5s$.

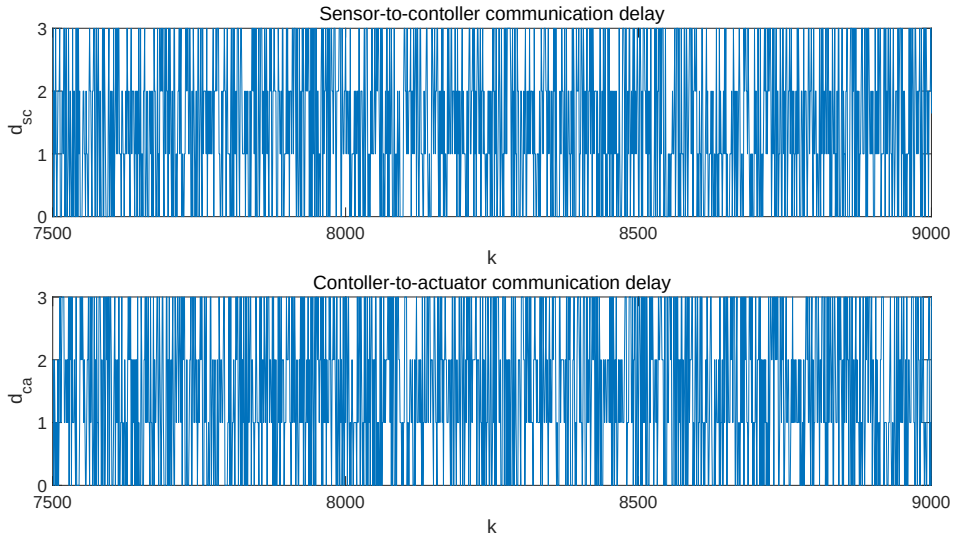

Figure 4.6: Sequences of communication delays.

The detailed steady state values, system parameters and controller parameters are given in Appendix A.3.

Control performance of this PID controller under both centralized control and networked control is tested using the conventional minimum variance and the proposed LTV minimum variance as the benchmarks, respectively. In networked control, $d_{sc}(k)$ and $d_{ca}(k)$ are assumed to be independent of each other and are assumed to be bounded with $0 \leq d_{sc}(k), d_{ca}(k) \leq 3$. Then, the series of $d_{sc}(k)$ and $d_{ca}(k)$ are generated by randomly taken values in the set $\{0, \cdots, 3\}$ with equal probability. The simulation is run for 20000 samples, and the results from samples 7500 to 9000 are presented as follows.

The generated communication delay sequences are shown in Figure 4.6, and the closed-loop test of the designed PID controller under centralized control and networked control is shown in Figure 4.7 where blue curve and red curve are centralized control result and networked control result, respectively. According to the closed-loop test, we can find that the designed PID controller is applicable to the case when there are random communication delays, although its performance is degraded.

Based on the simulated closed-loop data under networked control, moving window based

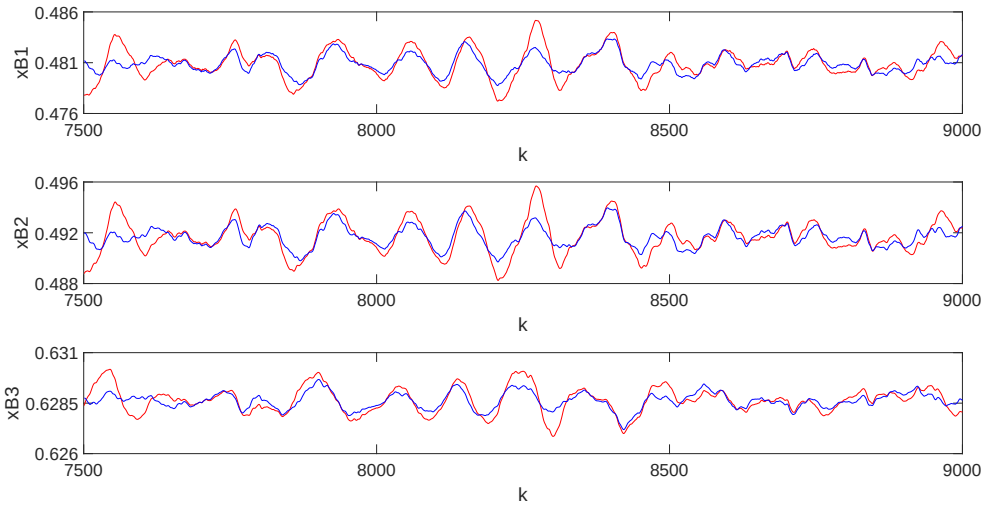

Figure 4.7: Closed-loop test of the PID controller

identification of LTI ARMA models is conducted to approximate the LTV closed-loop model. The window size is chosen as 2000 samples, and the window moves forward with a step size of every 50 samples. In this case, the closed-loop model is considered not to change very significantly within 50 samples. Then the lower bound and upper bound of the LTV minimum variance benchmark are calculated from the closed-loop model, and are shown as the blue curve and red curve in Figure 4.8, respectively. According to equation (4.50), for the performance of the PID controller under the networked control, the indexes with respect to the lower bound and upper bounds of the proposed LTV minimum variance benchmark are shown as the blue curve and red curve in Figure 4.9, respectively. Finally, for the performance of the PID controller under centralized control, the index with respect to the conventional minimum variance benchmark is shown as the black curve at the bottom Figure 4.9 [30].

By comparing Figure 4.7 and Figure 4.9, we can find that the obtained LTV minimum variance indexes can indicate the closed-loop performance effectively. In Figure 4.9, it shows poorer performance around the 8300_{th} sample and better performance for the rest. These results are consistent with the closed-loop test shown in Figure 4.7. Further, although the control performance is degraded under the networked control due to the presence of com-

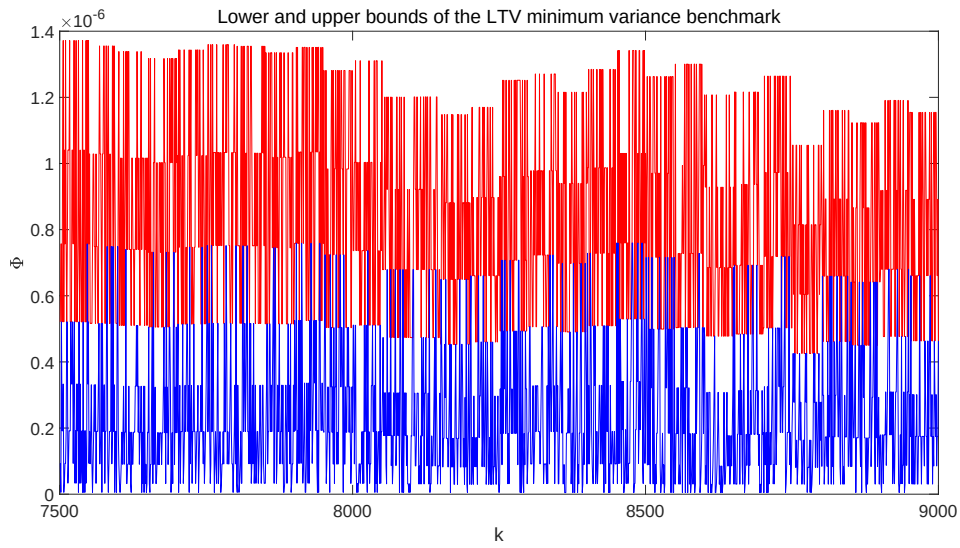

Figure 4.8: Lower and upper bounds of the LTV minimum variance benchmark.

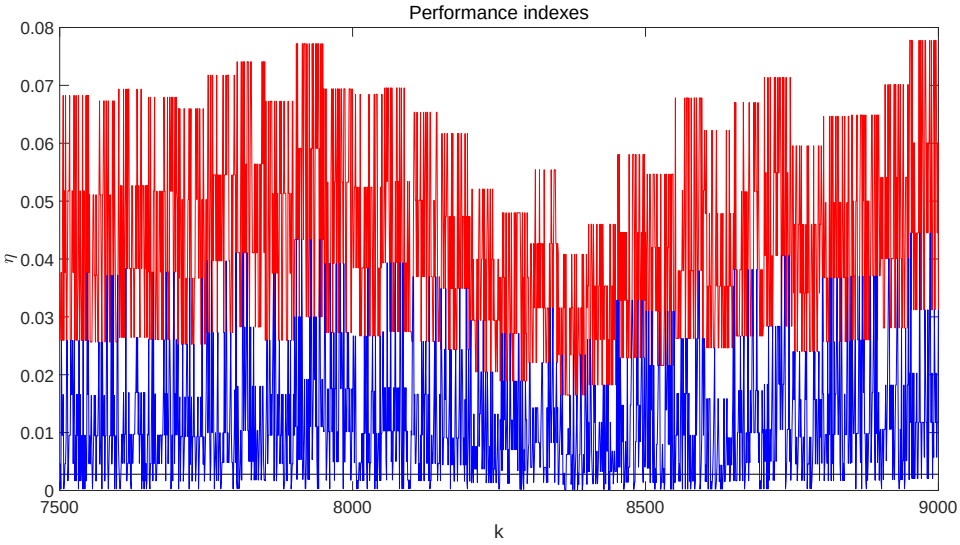

Figure 4.9: Performance indexes of the PID controller.

munication delays, the obtained LTV minimum variance performance indexes of this PID controller still show a competitive and even better result comparing with the performance indexes obtained in the centralized case. Thus, the proposed LTV minimum variance benchmark can efficiently take into account the influence of communication delays, and is more suitable to the control performance assessment of the NCSs.

4.5 Conclusions

In this chapter, practical solutions for the control performance assessment of NCSs with random communication delays are developed. Analytical expressions for the lower and upper bounds of the LTV minimum variance benchmark are derived, and the corresponding LTV minimum variance control laws are provided. It is shown that the proposed benchmark is achievable by a practical control. The estimation of the proposed benchmark from routine operating data is illustrated with the *a priori* knowledge of OIM and RIM. Although it does not provide a point estimation of the exact minimum variance benchmark, the proposed benchmark provides an answer on how much potential in terms of minimum and maximum improvement a controller has by tuning or redesigning. Finally, a reactor-separator process is introduced to demonstrate the effectiveness of the proposed work.

Chapter 5

Limits of Control Performance for Networked Model Predictive Control Systems with Random Communication Delays

5.1 Introduction

A number of works on the control of NCSs have been proposed to deal with random communication delays, among which MPC is of great concern [75]. The essence of MPC is as follows: at each sampling time, an optimal control problem over a fixed length of prediction horizon is solved and only the first optimal control move is implemented as the current control law; at the next sampling time, measurements are used to update the state estimate and the same procedure is repeated. This feature allows MPC to incorporate inequality constraints and compensate communication delays, which increases the possibility of its application in the synthesis and analysis of NCSs [18, 21, 76]. For stationary systems, the LQG solution can be achieved with the infinite MPC approach, or can be approximated by the MPC solution with

a finite prediction horizon in practice. Thus, the conventional LQG benchmark can be used for control performance assessment of model predictive control systems in centralized case, if performance limitations, such as hard constraints, model mismatch, etc., are not considered. However, this conclusion does not hold for networked model predictive control systems with random communication delays, where closed-loop systems are naturally non-stationary.

Motivated by the above discussions, following the idea of conventional LQG tradeoff curve, this chapter proposes the limits of control performance for networked model predictive control systems with random communication delays as an alternative of the work in Chapter 4, where performance limitation of control effort penalty is further considered. Sensor-to-controller communication delay and controller-to-actuator communication delay are considered simultaneously. These two kinds of communication delays are both modeled as first order Markov chains with known transition probabilities.

The main contributions of this chapter are listed as follows. Firstly, an explicit solution to time-varying MPC of NCSs with random communication delays is derived by minimizing the expectation of a quadratic cost function over all possible future communication delays in the prediction horizon. Based on this control design, the time-varying MPC performance tradeoff curve is presented to characterize the limits of control performance for networked model predictive control systems. Further, a strategy is provided for obtaining the time-varying MPC performance tradeoff curve from process model. The obtained MPC performance tradeoff curve can be used to evaluate how much potential of performance improvement an existing model predictive controller has by tuning or redesigning it. The effectiveness of the proposed control design and the use of the time-varying MPC performance tradeoff curve in control performance assessment are illustrated via a simulation study.

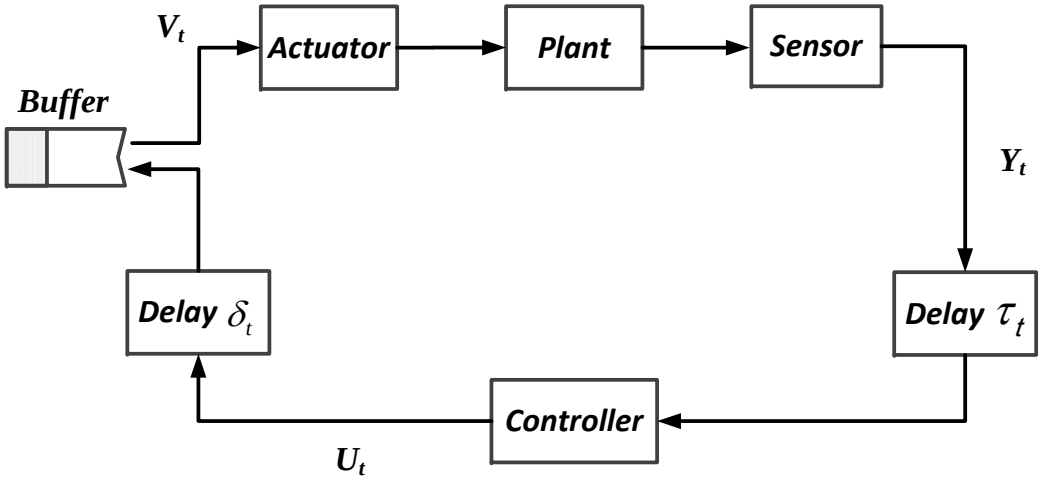

Figure 5.1: Schematic of NCSs with random communication delays.

5.2 Preliminaries

This chapter is mainly concerned with the NCSs shown in Figure 5.1, in which control loops are closed through information exchange between different system components over a shared network. We consider a class of discrete-time LTI process described by a state space model in the innovation form [77]:

$$X_{t+1} = AX_t + BV_t + Ka_t \tag{5.1}$$

$$Y_t = CX_t + a_t \tag{5.2}$$

where A, B, C are system matrices, and K is the Kalman filter gain; X_t, V_t and Y_t are the state, input and output vectors of dimensions n_x, n_v and n_y, respectively; a_t is white noise of dimension n_a with zero mean and unit variance. τ_t is random communication delay from the sensor to the controller, and δ_t is random communication delay from the controller to the actuator. τ_t and δ_t are modeled as two independent first order Markov chains with known

transition probability matrices $\Lambda_\tau = [\lambda_{ij}^\tau]$ and $\Lambda_\delta = [\lambda_{ij}^\delta]$, respectively [78]. In the first order Markov chain, the probabilistic description of current state is only related to its predecessor, i.e.,

$$\lambda_{ij}^\tau = P(\tau_t = j|\tau_{t-1} = i), \quad \lambda_{ij}^\delta = P(\delta_t = j|\delta_{t-1} = i) \tag{5.3}$$

where $\lambda_{ij}^\tau, \lambda_{ij}^\delta \geq 0$, $0 \leq \tau_t \leq \bar{\tau}$ and $0 \leq \delta_t \leq \bar{\delta}$.

The buffer is used to receive and store the control signals sent from the controller. The most recently received control signal will be used by the actuator with the rule of the buffer, namely, first-in-last-out. Thus, the control input of the plant $V_t = U_{t-\delta_t}$. We assume that δ_t is measurable at the plant and τ_t is measurable at the controller. Further, output Y_t, input V_t and delay information δ_t are together sent from the sensor to the controller through the communication network.

5.3 Time-varying MPC performance tradeoff curve for networked model predictive control systems

In this section, first, formulation of subspace matrices considering random communication delays is introduced. Then we derive an explicit solution of time-varying MPC for networked model predictive control systems with random communication delays based on the introduced subspace formulation. Further, according to the proposed control design, a strategy for obtaining MPC performance tradeoff curve from process model is provided.

5.3.1 Subspace matrices

Consider the networked control setup shown in Figure 5.1. Output Y_t, input V_t and delay information δ_t are measured at the remote system and sent from the sensor to the controller together through the communication network, while delay information τ_t is measured at the

controller. Then, due to the presence of communication delays, the available information to the controller at time t is $\{Y_{t-\tau_t}, \cdots, Y_0\}$, $\{V_{t-\tau_t}, \cdots, V_0\}$, $\{\delta_{t-\tau_t}, \cdots, \delta_0\}$, $\{\tau_t, \cdots, \tau_0\}$ and its local information $\{U_{t-1}, \cdots, U_0\}$.

From equations (5.1) and (5.2), by replacing the time subscript t with $t - \tau_t$

$$X_{t-\tau_t+1} = AX_{t-\tau_t} + BV_{t-\tau_t} + Ka_{t-\tau_t} \tag{5.4}$$

$$Y_{t-\tau_t} = CX_{t-\tau_t} + a_{t-\tau_t} \tag{5.5}$$

Combining equations (5.4) and (5.5) yields

$$X_{t-\tau_t+1} = (A - KC)X_{t-\tau_t} + KY_{t-\tau_t} + BV_{t-\tau_t} \tag{5.6}$$

Based on the regression analysis approach introduced in [79], recursively substituting equation (5.6) results in

$$\begin{aligned} X_{t-\tau_t+1} =& (A - KC)^L X_{t-\tau_t+1-L} + (A - KC)^{L-1}(KY_{t-\tau_t+1-L} + BV_{t-\tau_t+1-L}) \\ &+ \cdots + (A - KC)(KY_{t-\tau_t-1} + BV_{t-\tau_t-1}) \\ &+ KY_{t-\tau_t} + BV_{t-\tau_t} \end{aligned} \tag{5.7}$$

Then equation (5.7) can be rewritten in matrix equation form

$$\begin{aligned} X_{t-\tau_t+1} =& (A - KC)^L X_{t-\tau_t+1-L} \\ &+ \begin{bmatrix} (A - KC)^{L-1}K & \cdots & K \end{bmatrix} \begin{bmatrix} Y^T_{t-\tau_t+1-L} & \cdots & Y^T_{t-\tau_t} \end{bmatrix}^T \\ &+ \begin{bmatrix} (A - KC)^{L-1}B & \cdots & B \end{bmatrix} \begin{bmatrix} V^T_{t-\tau_t+1-L} & \cdots & V^T_{t-\tau_t} \end{bmatrix}^T \end{aligned} \tag{5.8}$$

The short-hand version of equation (5.8) is

$$X_{t-\tau_t+1} = \phi_x X_{t-\tau_t+1-L} + \phi_y Y_p + \phi_v V_p \tag{5.9}$$

where $\phi_x = (A - KC)^{L-1}$ represents error dynamics of a Kalman filter. Due to the stability of a Kalman filter, $\phi_x \to 0$ for $L \to \infty$. Then, for sufficient large L, the estimator equation for $X_{t-\tau_t+1}$ converges to

$$X_{t-\tau_t+1} = \begin{bmatrix} \phi_y & \phi_v \end{bmatrix} \begin{bmatrix} Y_p \\ V_p \end{bmatrix} = L_p W_p \tag{5.10}$$

where p denotes the past and stands for the time $t' \leq t - \tau_t$. W_p is a vector that consists of past outputs and inputs, in which

$$V_p = \begin{bmatrix} V_{t-\tau_t+1-L} \\ \cdots \\ V_{t-\tau_t} \end{bmatrix} = \begin{bmatrix} U_{t-\tau_t+1-L-\delta_{t-\tau_t+1-L}} \\ \cdots \\ U_{t-\tau_t-\delta_{t-\tau_t}} \end{bmatrix} = U_p \tag{5.11}$$

Then, according to equation (5.10), $X_{t-\tau_t+1}$ can be estimated in the controller at time t since all the information contained in W_p is available.

For equation (5.2), we can derive, for time $t - \tau_t + 1$

$$Y_{t-\tau_t+1} = CX_{t-\tau_t+1} + a_{t-\tau_t+1} \tag{5.12}$$

For time $t - \tau_t + 2$

$$Y_{t-\tau_t+2} = CX_{t-\tau_t+2} + a_{t-\tau_t+2} \tag{5.13}$$

Substituting the equation (5.1) for time $t - \tau_t + 1$ into equation (5.13) yields

$$Y_{t-\tau_t+2} = CAX_{t-\tau_t+1} + CBV_{t-\tau_t+1} + CKa_{t-\tau_t+1} + a_{t-\tau_t+2} \tag{5.14}$$

Similarly for time $t-\tau_t+3$, using equations (5.1) and (5.2), we can derive

$$Y_{t-\tau_t+3} = CA^2X_{t-\tau_t+1} + CABV_{t-\tau_t+1} + CBV_{t-\tau_t+2} + CAKa_{t-\tau_t+1} + CKa_{t-\tau_t+2} + a_{t-\tau_t+3} \tag{5.15}$$

Repeating this procedure until time $t+N$ and then assembling the results for time $\{t-\tau_t+1, t-\tau_t+2, \cdots, t+N\}$, we can obtain a matrix equation

$$\begin{bmatrix} Y_{t-\tau_t+1} \\ \cdots \\ Y_t \\ Y_{t+1} \\ \cdots \\ Y_{t+N} \end{bmatrix} = \begin{bmatrix} C \\ \cdots \\ CA^{\tau_t-1} \\ CA^{\tau_t} \\ \cdots \\ CA^{\tau_t+N-1} \end{bmatrix} X_{t-\tau_t+1} + \begin{bmatrix} 0 & \cdots & 0 & 0 & \cdots & 0 \\ \cdots & \cdots & \cdots & \cdots & \cdots & \cdots \\ CA^{\tau_t-2}B & \cdots & 0 & 0 & \cdots & 0 \\ CA^{\tau_t-1}B & \cdots & CB & 0 & \cdots & 0 \\ \cdots & \cdots & \cdots & \cdots & \cdots & \cdots \\ CA^{\tau_t+N-2}B & \cdots & CA^{N-2}B & CA^{N-3}B & \cdots & 0 \end{bmatrix} \begin{bmatrix} V_{t-\tau_t+1} \\ \cdots \\ V_t \\ V_{t+1} \\ \cdots \\ V_{t+N} \end{bmatrix} \tag{5.16}$$

$$+\begin{bmatrix} I & \cdots & 0 & 0 & \cdots & 0 \\ \cdots & \cdots & \cdots & \cdots & \cdots & \cdots \\ CA^{\tau_t-2}K & \cdots & I & 0 & \cdots & 0 \\ CA^{\tau_t-1}K & \cdots & CK & I & \cdots & 0 \\ \cdots & \cdots & \cdots & \cdots & \cdots & \cdots \\ CA^{\tau_t+N-2}K & \cdots & CA^{N-2}K & CA^{N-3}K & \cdots & I \end{bmatrix} \begin{bmatrix} a_{t-\tau_t+1} \\ \cdots \\ a_t \\ a_{t+1} \\ \cdots \\ a_{t+N} \end{bmatrix}$$

Decomposing the matrices in equation (5.16) to two parts with respect to $Y_{pre} = [Y_{t-\tau_t+1}^T, \cdots, Y_t^T]^T$ and $Y_f = [Y_{t+1}^T, \cdots, Y_{t+N}^T]^T$, the short-hand version of equation (5.16) can be written as

$$\begin{bmatrix} Y_{pre} \\ Y_f \end{bmatrix} = \begin{bmatrix} \Gamma_{pre}^N|_{\tau_t} \\ \Gamma_f^N|_{\tau_t} \end{bmatrix} X_{t-\tau_t+1} + \begin{bmatrix} H_{pre}^N|_{\tau_t} \\ H_f^N|_{\tau_t} \end{bmatrix} \begin{bmatrix} V_{pre} \\ V_f \end{bmatrix} + \begin{bmatrix} Z_{pre}^N|_{\tau_t} \\ Z_f^N|_{\tau_t} \end{bmatrix} \begin{bmatrix} A_{pre} \\ A_f \end{bmatrix} \tag{5.17}$$

where f denotes the future and stands for the time $t' \geq t+1$, while pre stands for the time interval $t' \in [t-\tau_t+1, t]$. Then $A_{pre} = [a_{t-\tau_t+1}^T, \cdots, a_t^T]^T$, $A_f = [a_{t+1}^T, \cdots, a_{t+N}^T]^T$ and

$$V_{pre} = \begin{bmatrix} V_{t-\tau_t+1} \\ \cdots \\ V_t \end{bmatrix} = \begin{bmatrix} U_{t-\tau_t+1-\delta_{t-\tau_t+1}} \\ \cdots \\ U_{t-\delta_t} \end{bmatrix}, \quad V_f = \begin{bmatrix} V_{t+1} \\ \cdots \\ V_{t+N} \end{bmatrix} = \begin{bmatrix} U_{t+1-\delta_{t+1}} \\ \cdots \\ U_{t+N-\delta_{t+N}} \end{bmatrix} \tag{5.18}$$

Defining $V_{pref} = [V_{pre}^T, V_f^T]^T$, we further separate V_{pref} to two parts as

$$V_{pref} = \begin{bmatrix} U_{pre} \\ U_f \end{bmatrix}, \quad U_{pre} = \begin{bmatrix} U_{t-\tau_t+1-\delta_{t-\tau_t+1}} \\ \cdots \\ U_{t-1} \end{bmatrix}, \quad U_f = \begin{bmatrix} U_t \\ \cdots \\ U_{t+N-\delta_{t+N}} \end{bmatrix} \tag{5.19}$$

where U_{pre} consists of the control signals that are generated from the controller in the past, and U_f consists of the future control signals over the prediction horizon. The dimensions of U_{pre} and U_f are related to the unknown delay sequence $\Delta = \{\delta_{t-\tau_t+1}, \cdots, \delta_{t+N}\}$. U_{pre} is not

completely available in control design since Δ is unknown, and a strategy on making use of U_{pre} is proposed in the following section. Then by omitting white noise sequences A_{pre} and A_f , the predictor equation is given by

$$\hat{Y}_f = \Gamma_f^N|_{\tau_t} X_{t-\tau_t+1} + H_f^N|_{\tau_t} V_{pref} \tag{5.20}$$

Substituting equation (5.10) into equation (5.20), one can obtain

$$\begin{aligned} \hat{Y}_f &= \Gamma_f^N|_{\tau_t} L_p W_p + H_f^N|_{\tau_t} V_{pref} \\ &= L_w^N|_{\tau_t} W_p + H_f^N|_{\tau_t} V_{pref} \end{aligned} \tag{5.21}$$

where $L_w^N|_{\tau_t}$ and $H_f^N|_{\tau_t}$ vary with τ_t at each time instant

- $L_w^N|_{\tau_t}$ is subspace matrix corresponding to the past inputs and outputs W_p with prediction length N and communication delay τ_t
- $H_f^N|_{\tau_t}$ is subspace matrix corresponding to the deterministic inputs V_{pref} with prediction length N and communication delay τ_t

5.3.2 Time-varying MPC design

Sensor-to-controller communication delay τ_t is measurable by the controller, and its influence on the predicted outputs $\hat{Y}_f$ is completely considered in the formulation of subspace matrices $L_w^N|_{\tau_t}$ and $H_f^N|_{\tau_t}$. The influence of controller-to-actuator communication delay δ_t on the predicted outputs $\hat{Y}_f$ is reflected in the past inputs V_p and the future inputs V_{pref}. The past delay information $\{\delta_{t-\tau_t}, \cdots, \delta_{t-\tau_t+1-L}\}$ in V_p is known by the controller, while the future delay sequence Δ in V_{pref} is unavailable.

To deal with the unknown delay sequence Δ, a time-varying MPC is designed to minimize

the expectation of the following quadratic cost function over all possible Δ

$$\begin{aligned} J(\omega) &= \underset{\Delta}{E}\{\hat{Y}_f^T\hat{Y}_f + U_f^T(\omega I)U_f\} \\ &= \sum_{\delta_{t-\tau_t+1}=0}^{\bar{\delta}} \cdots \sum_{\delta_{t+N}=0}^{\bar{\delta}} \prod_{i=t-\tau_t}^{t+N-1} \lambda_{\delta_i\delta_{i+1}}^{\delta} \{\hat{Y}_f^T\hat{Y}_f + U_f^T(\omega I)U_f\} \end{aligned} \tag{5.22}$$

where reference trajectory is assumed to be zero, E is the expectation operator and $\omega > 0$ is the user defined input weighting parameter. $\sum_{\delta_{t-\tau_t+1}=0}^{\bar{\delta}} \cdots \sum_{\delta_{t+N}=0}^{\bar{\delta}}$ is the sum of all possible combinations of future delay sequence Δ and $\prod_{i=t-\tau_t}^{t+N-1} \lambda_{\delta_i\delta_{i+1}}^{\delta}$ is the probability of each possible Δ. Substituting equation (5.21) into equation (5.22) yields

$$\begin{aligned} J(\omega) =& W_p^T L_w^N|_{\tau_t}^T L_w^N|_{\tau_t} W_p + (L_w^N|_{\tau_t} W_p)^T \Big(\sum_{\delta_{t-\tau_t+1}=0}^{\bar{\delta}} \cdots \sum_{\delta_{t+N}=0}^{\bar{\delta}} \prod_{i=t-\tau_t}^{t+N-1} \lambda_{\delta_i\delta_{i+1}}^{\delta} H_f^N|_{\tau_t} V_{pref} \Big) \\ &+ \Big(\sum_{\delta_{t-\tau_t+1}=0}^{\bar{\delta}} \cdots \sum_{\delta_{t+N}=0}^{\bar{\delta}} \prod_{i=t-\tau_t}^{t+N-1} \lambda_{\delta_i\delta_{i+1}}^{\delta} H_f^N|_{\tau_t} V_{pref} \Big)^T L_w^N|_{\tau_t} W_p \\ &+ \sum_{\delta_{t-\tau_t+1}=0}^{\bar{\delta}} \cdots \sum_{\delta_{t+N}=0}^{\bar{\delta}} \prod_{i=t-\tau_t}^{t+N-1} \lambda_{\delta_i\delta_{i+1}}^{\delta} V_{pref}^T H_f^N|_{\tau_t}^T H_f^N|_{\tau_t} V_{pref} \\ &+ \sum_{\delta_{t-\tau_t+1}=0}^{\bar{\delta}} \cdots \sum_{\delta_{t+N}=0}^{\bar{\delta}} \prod_{i=t-\tau_t}^{t+N-1} \lambda_{\delta_i\delta_{i+1}}^{\delta} U_f^T(\omega I)U_f \end{aligned} \tag{5.23}$$

where $L_w^N|_{\tau_t} W_p$ is constant term, $H_f^N|_{\tau_t}$ is a coefficient matrix, while V_{pref} and U_f are related to Δ.

First, defining $H_f^N|_{\tau_t}(:, j)$ as the j^{th} block column of $H_f^N|_{\tau_t}$ and $V_{pref}(j)$ as the j^{th} vector element of V_{pref}, we can get

$$H_f^N|_{\tau_t} V_{pref} = \Big[H_f^N|_{\tau_t}(:, 1), \cdots, H_f^N|_{\tau_t}(:, N+\tau_t) \Big] \Big[V_{pref}^T(1), \cdots, V_{pref}^T(N+\tau_t) \Big]^T \tag{5.24}$$

Since all possible Δ is considered, in equation (5.23), $\sum_{\delta_{t-\tau_t+1}=0}^{\bar{\delta}} \cdots \sum_{\delta_{t+N}=0}^{\bar{\delta}} V_{pref}$ contains all the control signals in the set of $\{U_{t-\tau_t+1-\bar{\delta}}, \cdots, U_{t+N}\}$. Analogous to equation (5.24), we

can rewrite part of the second term on the right hand side of equation (5.23) as

$$\begin{aligned}
&\sum_{\delta_{t-\tau_t+1}=0}^{\bar{\delta}} \cdots \sum_{\delta_{t+N}=0}^{\bar{\delta}} \prod_{i=t-\tau_t}^{t+N-1} \lambda^{\delta}_{\delta_i\delta_{i+1}} H_f^N|_{\tau_t} V_{pref} \qquad (5.25)\\
=&\left[\theta_1^N|_{\tau_t}, \cdots, \theta^N_{N+\tau_t+\bar{\delta}}|_{\tau_t}\right]\left[U^T_{t-\tau_t+1-\bar{\delta}}, \cdots, U^T_{t+N}\right]^T\\
=&\Theta^N|\tau_t U^J_{pref}
\end{aligned}$$

where $U^J_{pref} = [U^T_{t-\tau_t+1-\bar{\delta}}, \cdots, U^T_{t+N}]^T$ consists of all the control signals used in cost function $J(\omega)$. $\Theta^N|\tau_t$ is the coefficient matrix corresponding to U^J_{pref} with

$$\theta_i^N|_{\tau_t} = \sum_{j=1}^{N+\tau_t} [P(V_{pref}(j) = U_{t+i-\bar{\delta}-\tau_t}|\delta_{t-\tau_t}) H_f^N|_{\tau_t}(:, j)] \qquad (5.26)$$

for $i = 1, \cdots, N + \tau_t + \bar{\delta}$. In equation (5.26),

$$P(V_{pref}(j) = U_{t+i-\bar{\delta}-\tau_t}|\delta_{t-\tau_t}) = P(\delta_{t-\tau_t+j} = j + \bar{\delta} - i|\delta_{t-\tau_t}) \qquad (5.27)$$

is the probability for $U_{t+i-\bar{\delta}-\tau_t}$ being the j^{th} vector element in V_{pref} with the initial delay state $\delta_{t-\tau_t}$. This probability is calculable off-line with given $\delta_{t-\tau_t} \in [0, \cdots, \bar{\delta}]$ and $\{\lambda^{\delta}_{ij} \mid i, j \in [0, \cdots, \bar{\delta}]\}$ [78]. Then, decomposing equation (5.25) to two parts gives

$$\Theta^N|\tau_t U^J_{pref} = \begin{bmatrix}\Theta^N_{pre}|\tau_t & \Theta^N_f|\tau_t\end{bmatrix}\begin{bmatrix}U^J_{pre}\\ U^J_f\end{bmatrix} \qquad (5.28)$$

where

$$U^J_{pre} = \begin{bmatrix}U_{t-\tau_t+1-\bar{\delta}}\\ \cdots\\ U_{t-1}\end{bmatrix}, \quad U^J_f = \begin{bmatrix}U_t\\ \cdots\\ U_{t+N}\end{bmatrix} \qquad (5.29)$$

U_{pre}^J consists of all the previously designed control signals that are contained in the cost function $J(\omega)$, while U_f^J consists of all the future control signals that are contained in the cost function $J(\omega)$. $\Theta_{pre}^N|\tau_t$ and $\Theta_f^N|\tau_t$ are coefficient matrices with respect to U_{pre} and U_f, respectively.

Second, defining $\Psi^N|_{\tau_t} = H_f^N|_{\tau_t}^T H_f^N|_{\tau_t}$ and $\Psi^N|_{\tau_t}(i,j)$ as the $(i,j)^{th}$ block element of $\Psi^N|_{\tau_t}$, we can get

$$V_{pref}^T H_f^N|_{\tau_t}^T H_f^N|_{\tau_t} V_{pref} = \sum_{i=1}^{N+\tau_t} \sum_{j=1}^{N+\tau_t} V_{pref}^T(i) \Psi^N|_{\tau_t}(i,j) V_{pref}(j) \tag{5.30}$$

Similarly, analogous to equation (5.30), we can rewrite the fourth term on the right hand side of equation (5.23) as

$$\begin{aligned} &\sum_{\delta_{t-\tau_t+1}=0}^{\bar{\delta}} \cdots \sum_{\delta_{t+N}=0}^{\bar{\delta}} \prod_{i=t-\tau_t}^{t+N-1} \lambda_{\delta_i \delta_{i+1}}^{\delta} V_{pref}^T H_f^N|_{\tau_t}^T H_f^N|_{\tau_t} V_{pref} \\ = &\sum_{i=1}^{N+\tau_t+\bar{\delta}} \sum_{j=1}^{N+\tau_t+\bar{\delta}} U_{t+i-\tau_t-\bar{\delta}}^T \Upsilon_{(i,j)}^N|\tau_t \; U_{t+j-\tau_t-\bar{\delta}} \end{aligned} \tag{5.31}$$

where

$$\Upsilon_{(i,j)}^N|\tau_t = \sum_{p=1}^{N+\tau_t} \sum_{q=1}^{N+\tau_t} [P(V_{pref}(p) = U_{t+i-\bar{\delta}-\tau_t}, V_{pref}(q) = U_{t+j-\bar{\delta}-\tau_t}|\delta_{t-\tau_t}) \Psi^N|_{\tau_t}(p,q)] \tag{5.32}$$

for $i, j = 1, \cdots, N + \tau_t + \bar{\delta}$. In equation (5.32)

$$\begin{aligned} &P(V_{pref}(p) = U_{t+i-\bar{\delta}-\tau_t}, V_{pref}(q) = U_{t+j-\bar{\delta}-\tau_t}|\delta_{t-\tau_t}) \\ =&P(\delta_{t-\tau_t+p} = p + \bar{\delta} - i, \delta_{t-\tau_t+q} = q + \bar{\delta} - j|\delta_{t-\tau_t}) \end{aligned} \tag{5.33}$$

is the probability for $U_{t+i-\bar{\delta}-\tau_t}$ and $U_{t+j-\bar{\delta}-\tau_t}$ being the p^{th} and the q^{th} vector elements in V_{pref}, respectively, with the initial delay state $\delta_{t-\tau_t}$. The calculation of this probability can also be referred to [78]. Then, rewriting equation (5.31) in matrix equation form and further

decomposing it to two parts, we can obtain

$$\begin{aligned}
&\sum_{\delta_{t-\tau_t+1}=0}^{\bar{\delta}} \cdots \sum_{\delta_{t+N}=0}^{\bar{\delta}} \prod_{i=t-\tau_t}^{t+N-1} \lambda^{\delta}_{\delta_i\delta_{i+1}} V_{pref}^T H_f^N|_{\tau_t}^T H_f^N|_{\tau_t} V_{pref} \qquad (5.34)\\
=&(U_{pref}^J)^T \Upsilon^N|_{\tau_t}\, U_{pref}^J\\
=&\begin{bmatrix}(U_{pre}^J)^T & (U_f^J)^T\end{bmatrix}\begin{bmatrix}\Upsilon_{11}^N|_{\tau_t} & \Upsilon_{12}^N|_{\tau_t}\\ \Upsilon_{21}^N|_{\tau_t} & \Upsilon_{22}^N|_{\tau_t}\end{bmatrix}\begin{bmatrix}U_{pre}^J\\ U_f^J\end{bmatrix}
\end{aligned}$$

where $\Upsilon^N|_{\tau_t}$ is a coefficient matrix with $\Upsilon^N_{(i,j)}|_{\tau_t}$ as its $(i,j)^{th}$ block element. $\Upsilon^N|_{\tau_t}$ is proven to be a positive semi-definite matrix in the Appendix B.1. Subsequently, $\Upsilon^N_{22}|_{\tau_t}$ is a positive semi-definite matrix and $\Upsilon^N_{12}|_{\tau_t}^T = \Upsilon^N_{21}|_{\tau_t}$.

Finally, following the same idea, the fifth term on the right hand side of the equation (5.23) can be rewritten as

$$\begin{aligned}
&\sum_{\delta_{t-\tau_t+1}=0}^{\bar{\delta}} \cdots \sum_{\delta_{t+N}=0}^{\bar{\delta}} \prod_{i=t-\tau_t}^{t+N-1} \lambda^{\delta}_{\delta_i\delta_{i+1}} U_f^T(\omega I) U_f \qquad (5.35)\\
=&\sum_{\delta_{t-\tau_t+1}=0}^{\bar{\delta}} \cdots \sum_{\delta_{t+N}=0}^{\bar{\delta}} \prod_{i=t-\tau_t}^{t+N-1} \lambda^{\delta}_{\delta_i\delta_{i+1}} [\sum_{j=1}^{N-\delta_{t+N}+1} U_{t+j-1}^T(\omega I) U_{t+j-1}]\\
=&\sum_{i=1}^{N+1} U_{t+i-1}^T(\Omega_i^N|_{\tau_t} I) U_{t+i-1}
\end{aligned}$$

where

$$\Omega_i^N|_{\tau_t} = \omega \sum_{j=1}^{N+\tau_t} [P(V_{pref}(j) = U_{t+i-1}|\delta_{t-\tau_t})] \qquad (5.36)$$

for $i = 1, \cdots, N+1$. In equation (5.36),

$$P(V_{pref}(j) = U_{t+i-1}|\delta_{t-\tau_t}) = P(\delta_{t-\tau_t+j} = j - \tau_t - i + 1|\delta_{t-\tau_t}) \qquad (5.37)$$

is the probability for U_{t+i-1} being the j^{th} vector element in V_{pref} with the initial delay $\delta_{t-\tau_t}$. Then, the matrix equation form of equation (5.35) is given by

$$\begin{aligned}&\sum_{\delta_{t-\tau_t+1}=0}^{\bar{\delta}} \cdots \sum_{\delta_{t+N}=0}^{\bar{\delta}} \prod_{i=t-\tau_t}^{t+N-1} \lambda^{\delta}_{\delta_i\delta_{i+1}} U_f^T(\omega I) U_f \\ =&(U_f^J)^T \Omega^N|_{\tau_t} U_f^J\end{aligned} \tag{5.38}$$

where $\Omega^N|_{\tau_t}$ is a block diagonal matrix with $\Omega_i^N|_{\tau_t}$ as its i^{th} diagonal element. Due to $\omega > 0$, $\Omega^N|_{\tau_t}$ is a positive definite matrix.

Substituting equations (5.28), (5.34) and (5.38) into equation (5.23), we can get

$$\begin{aligned}J(\omega) =&W_p^T L_w^N|_{\tau_t}^T L_w^N|_{\tau_t} W_p + (L_w^N|_{\tau_t} W_p)^T(\Theta_{pre}^N|\tau_t U_{pre}^J + \Theta_f^N|\tau_t U_f^J) \\ &+ (\Theta_{pre}^N|\tau_t U_{pre}^J + \Theta_f^N|\tau_t U_f^J)^T L_w^N|_{\tau_t} W_p \\ &+ (U_{pre}^J)^T \Upsilon_{11}^N|\tau_t U_{pre}^J + (U_{pre}^J)^T \Upsilon_{12}^N|\tau_t U_f^J + (U_f^J)^T \Upsilon_{21}^N|\tau_t U_{pre}^J + (U_f^J)^T \Upsilon_{22}^N|\tau_t U_f^J \\ &+ (U_f^J)^T \Omega^N|_{\tau_t} U_f^J\end{aligned} \tag{5.39}$$

where U_f^J is a vector of future control signals to be designed, while all the other matrices and vectors are constant and known values, respectively. Taking partial differentiation of $J(\omega)$ with respect to U_f^J and setting it to zero yields the optimal control law as

$$U_f^J = -(\Upsilon_{22}^N|\tau_t + \Omega^N|_{\tau_t})^{-1} \begin{bmatrix}\Theta_f^N|\tau_t^T L_w^N|_{\tau_t} & \Upsilon_{21}^N|\tau_t\end{bmatrix} \begin{bmatrix}W_p \\ U_{pre}^J\end{bmatrix} \tag{5.40}$$

where $(\Upsilon_{22}^N|\tau_t + \Omega^N|_{\tau_t})^{-1}$ always exists, since $\Upsilon_{22}^N|\tau_t \geq 0$ and $\Omega^N|_{\tau_t} > 0$.

In the controller, at each sampling time t, the controller design scheme can be stated as follows:

1. Receive $\delta_{t-\tau_t}$ from the remote system, measure τ_t and generate vectors W_p and U_{pre}^J;

2. Calculate the subspace matrices $L_w^N|_{\tau_t}$ and $H_f^N|_{\tau_t}$, as well as the coefficient matrices

$\Omega^N|_{\tau_t}$, $\Upsilon^N|\tau_t$ and $\Theta^N\tau_t$;

3. Calculate U_f^J in equation (5.40) such that $J(\omega)$ is minimized;

4. Implement U_t which is the first element in U_f^J.

5.3.3 Time-varying MPC performance tradeoff curve

For centralized model predictive control systems, the conventional LQG tradeoff curve can be used for its control performance assessment, since an infinite horizon MPC objective function converges to a LQG objective function in centralized case [80]. However, this conclusion does not hold for networked model predictive control systems with random communication delays. In order to find the limits of control performance and to further develop the control performance assessment technology for networked model predictive control systems, in this section, the time-varying MPC performance tradeoff curve is proposed following the idea of conventional LQG tradeoff curve.

The time-varying MPC performance tradeoff curve is obtained from solving the MPC objective function defined in equation (5.22). By varying ω, various solutions of $E[U_t^T U_t]$ and $E[Y_t^T Y_t]$ for the system controlled by benchmark MPC is calculated at each time instant. Then, the time-varying MPC performance tradeoff curve can be determined from these solutions with $E[U_t^T U_t]$ as the x-axis and $E[Y_t^T Y_t]$ as the y-axis, respectively. This time-varying MPC performance tradeoff curve shows the limits of control performance for networked model predictive control systems. To assess performance of networked model predictive control systems with the proposed time-varying MPC performance tradeoff curve, we compare performance of the current controller with the benchmark controller in terms of both $E[Y_t^T Y_t]$ and $E[U_t^T U_t]$. This gives rise to two problems: 1) design benchmark MPC; 2) obtain $E[Y_t^T Y_t]$ and $E[U_t^T U_t]$ of the system under current controller and benchmark controller, respectively. The first problem has been solved in the previous sections. In the conventional LQG benchmark, solution to the second problem can be found in [50] where an

algorithm for extracting $E[Y_t^T Y_t]$ and $E[U_t^T U_t]$ of the benchmark control system from routine operating data has been proposed, while $E[Y_t^T Y_t]$ and $E[U_t^T U_t]$ of the current control system can be calculated from routine operating data directly.

When it comes to NCSs with random communication delays, the second problem becomes more challenging. The benchmark MPC designed in equation (5.40) is time-varying. Extracting $E[Y_t^T Y_t]$ and $E[U_t^T U_t]$ for such a benchmark control system from routine operating data is very difficult. Further, random communication delays will lead to a non-stationary behavior of the closed-loop system. $E[Y_t^T Y_t]$ and $E[U_t^T U_t]$ for the current control system also change over time, and cannot be calculated from routine operating data directly. In this chapter, we choose to calculate $E[Y_t^T Y_t]$ and $E[U_t^T U_t]$ of the benchmark control system based on process model instead of from routine operating data. Although it imposes a higher requirement on the *a priori* knowledge of process model, it provides us a tractable solution to the problem.

In spite of the presence of random communication delays, the relationship between time series Y_t and V_t still follows the process model shown in equations (5.1) and (5.2). Then system matrices A, B, C and the Kalman filter gain K can be identified according to the work [77]. To obtain $E[Y_t^T Y_t]$ and $E[U_t^T U_t]$ of the benchmark control system, we need to calculate the closed-loop expressions for input and output of the system at time t in terms of the disturbance. By assuming zero initial state of the system, from equations (5.8), (5.16) and (5.40), we can calculate the closed-loop expressions for Y_t and U_t of the benchmark control system for different time instants in terms of a_t recursively. Without giving a detailed mathematical derivation, for the benchmark control system, we can express its output and input as

$$\begin{aligned} Y_{t,opt} &= G_{Y_{opt}}(t) a_t \\ U_{t,opt} &= G_{U_{opt}}(t) a_t \end{aligned} \tag{5.41}$$

where $Y_{t,opt}$ and $U_{t,opt}$ are the output and the input of the benchmark control system at time t , respectively. $G_{Y_{opt}}(t)$ and $G_{U_{opt}}(t)$ are the LTV closed-loop transfer function matrices in backshift operator q^{-1} accordingly. Then, we can get

$$E[Y_{t,opt}^T Y_{t,opt}] = \|G_{Y_{opt}}(t)\|_2^2 \tag{5.42}$$
$$E[U_{t,opt}^T U_{t,opt}] = \|G_{U_{opt}}(t)\|_2^2$$

To obtain $E[Y_t^T Y_t]$ and $E[U_t^T U_t]$ of the current control system, firstly, recursive time series analysis algorithm can be used to identify the LTV ARMA models for output and input of the current control system [71, 72, 73]. Consider the identified LTV ARMA model of Y_t with order (n, m) as

$$L(t)Y_t = Q(t)a_t \tag{5.43}$$

where

$$L(t) = l_0(t) + l_1(t)q^{-1} + \cdots + l_n(t)q^{-n} \tag{5.44}$$
$$Q(t) = q_0(t) + q_1(t)q^{-1} + \cdots + q_m(t)q^{-m}$$

Then, the LTV closed-loop model $G_Y(t)$ can be calculated recursively by substituting equation (5.44) into equation (5.43)

$$G_Y(t) = l_0^{-1}(t)[Q(t) - l_1(t)G_Y(t-1)q^{-1} - \cdots - l_n(t)G_Y(t-n)q^{-n}] \tag{5.45}$$

Similarly, we can obtain the LTV closed-loop model $G_U(t)$ of U_t following the same procedure.

Then, we have

$$E[Y_t^T Y_t] = \|G_Y(t)\|_2^2 \tag{5.46}$$
$$E[U_t^T U_t] = \|G_U(t)\|_2^2$$

Further, in the cost function $J(\omega)$, we optimize a quadratic term $\hat{Y}_f^T \hat{Y}_f + U_f^T(\omega I)U_f$ over the prediction horizon instead of exactly optimizing $E[Y_t^T Y_t] + E[U_t^T(\omega I)U_t]$. The obtained $E[Y_{t,opt}^T Y_{t,opt}]$ and $E[U_{t,opt}^T U_{t,opt}]$ may have large differences among the neighbouring time instants due to this issue. To avoid the potential rapidly change of the time-varying MPC performance tradeoff curve and reduce the computation burden in online application, we recommend to use the average values $\frac{1}{r}\sum_{i=1}^{r} E[Y_{t+i,opt}^T Y_{t+i,opt}]$ and $\frac{1}{r}\sum_{i=1}^{r} E[U_{t+i,opt}^T U_{t+i,opt}]$ to determine the curve where r is an user defined parameter.

Then, for time interval $t' \in [t, t+r]$, various solutions of $E[U_{t',opt}^T U_{t',opt}]$ and $E[Y_{t',opt}^T Y_{t',opt}]$ can be calculated by varying ω. Afterward, the time-varying MPC performance tradeoff curve for time interval $t' \in [t, t+r]$ can be determined from these solutions with $\frac{1}{r}\sum_{i=1}^{r} E[U_{t+i,opt}^T U_{t+i,opt}]$ as the x-axis and $\frac{1}{r}\sum_{i=1}^{r} E[Y_{t+i,opt}^T Y_{t+i,opt}]$ as the y-axis, respectively. The distance from the current operating point $(\frac{1}{r}\sum_{i=1}^{r} E[U_{t+i}^T U_{t+i}], \frac{1}{r}\sum_{i=1}^{r} E[Y_{t+i}^T Y_{t+i}])$ to the obtained MPC performance tradeoff curve can be used for control performance assessment.

5.4 Simulations

Consider the following state space model which is modified from the example in [77]:

$$X_{t+1} = \begin{bmatrix} 0.6 & 0.6 & 0 \\ -0.6 & 0.6 & 0 \\ 0 & 0 & 0.7 \end{bmatrix} X_t + \begin{bmatrix} 0.808 \\ -0.1741 \\ 1.3159 \end{bmatrix} U_t + \begin{bmatrix} -1.1472 \\ -1.5204 \\ -3.1993 \end{bmatrix} a_t \tag{5.47}$$
$$Y_t = \begin{bmatrix} -0.4373 & -0.5046 & 0.0936 \end{bmatrix} X_t + a_t$$

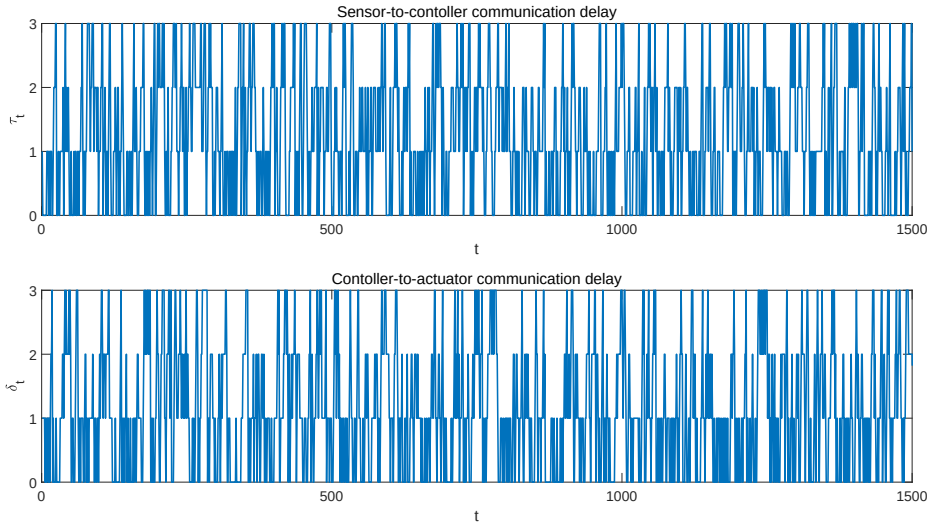

Figure 5.2: Sequences of communication delays.

We assume that the process shown in equation (5.45) is under the networked control setup shown in Figure 5.1. τ_t and δ_t are modeled as two independent first order Markov chains with known transition probability matrices Λ_τ and Λ_δ, respectively. In this simulation, τ_t and δ_t are bounded within the set $\{0, 1, 2, 3\}$. The transition probability matrices are given as $\Lambda_\tau = \Lambda_\delta = P$, with

$$P = \begin{bmatrix} 0.5 & 0.5 & 0 & 0 \\ 0.3 & 0.4 & 0.3 & 0 \\ 0.1 & 0.2 & 0.4 & 0.3 \\ 0.1 & 0.2 & 0.3 & 0.4 \end{bmatrix} \tag{5.48}$$

where a practical constraint of communication delays is considered as $\delta_{t+1} \leq \delta_t + 1$ ($\tau_{t+1} \leq \tau_t + 1$). The communication delay sequences are generated for 1500 samples and the results are shown in Figure 5.2. The top and the bottom figures are the sequences for sensor-to-controller and the controller-to-actuator communication delays, respectively.

First, the proposed time-varying MPC is tested for two cases: 1) the transition probability matrices are known accurately; 2) the *a priori* knowledge of the transition probability

matrices is not available. In the first case, the transition probability matrix P shown in equation (5.46) is used in the controller design; while, in the second case, the following transition probability matrix P_1 is used

$$P_1 = \begin{bmatrix} 1/2 & 1/2 & 0 & 0 \\ 1/3 & 1/3 & 1/3 & 0 \\ 1/4 & 1/4 & 1/4 & 1/4 \\ 1/4 & 1/4 & 1/4 & 1/4 \end{bmatrix} \tag{5.49}$$

where equal probability is assigned to elements in each raw of the matrix. Here, we choose $\omega = 1$ and $L = N = 30$ for the control design proposed in Section 5.3. Then the output trajectories of these two control cases are shown in Figure 5.3. The top and the middle figures are the output trajectories for the first case and the second case, respectively. The bottom figure is the difference of the two output trajectories. Our proposed control design can restrict the variation of the output in a small region according to the control results. Also, the proposed control design has a very good robustness to the selection of the transition probability matrices. As shown in the bottom figure, the outputs with the transition probability matrices being selected as P and P_1, respectively, are close to each other. This is because that the proposed control design is conservative. All possible combinations of the future delay sequences are considered in the cost function, which reduce the requirement on the accuracy of the *a priori* knowledge of the transition probability matrices.

Further, by choosing $L = N = 30$, $r = 10$, $\omega = 2^i$ and varying i from -15 to 9 with a step size of 1, various optimal control solutions for equation (5.22) are calculated to generate the time-varying MPC performance tradeoff curves following the procedure introduced in Section 5.3.3. The following transition probability matrix P_2 is used to design the current

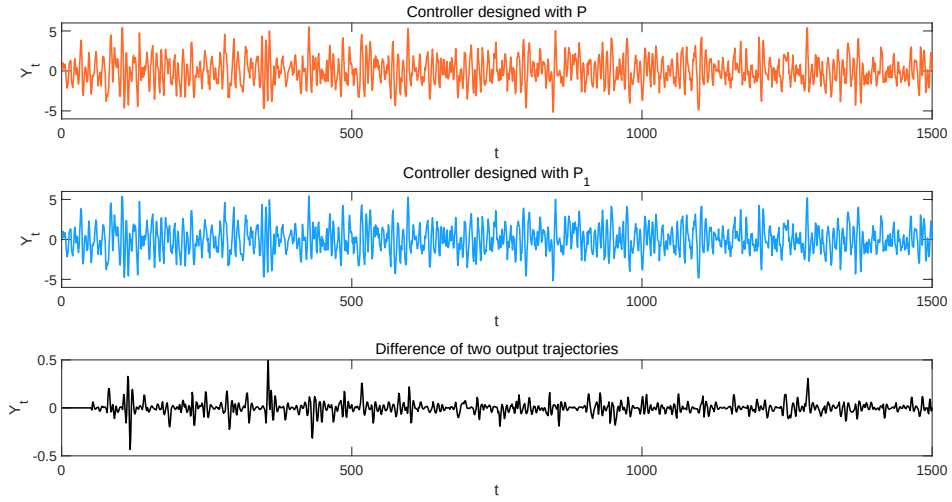

Figure 5.3: Output trajectories for the two control cases.

controller for $\omega = 2^{-6}$, with

$$P_2 = \begin{bmatrix} 0.1 & 0.9 & 0 & 0 \\ 0.1 & 0.2 & 0.7 & 0 \\ 0.1 & 0.1 & 0.2 & 0.6 \\ 0.1 & 0.1 & 0.2 & 0.6 \end{bmatrix} \tag{5.50}$$

There is a large gap between the true transition probability matrix and the one used for the current controller design. Then, performance of the current controller is assessed based on the proposed approach. Output and input trajectories for the system under the current controller are shown in Figure 5.4, while the control performance assessment results are shown in Figure 5.5. The left top figure shows the conventional LQG tradeoff curve designed for the centralized control systems. The other three figures show the time-varying MPC performance tradeoff curves and performance of the current controller for 3 different time intervals, respectively. Since all possible combinations of the future delay sequences are considered, the proposed time-varying MPC is more conservative and has smaller $E[U_t^T U_t]$ comparing with the conventional LQG control for centralized case. From the figure we can find that the

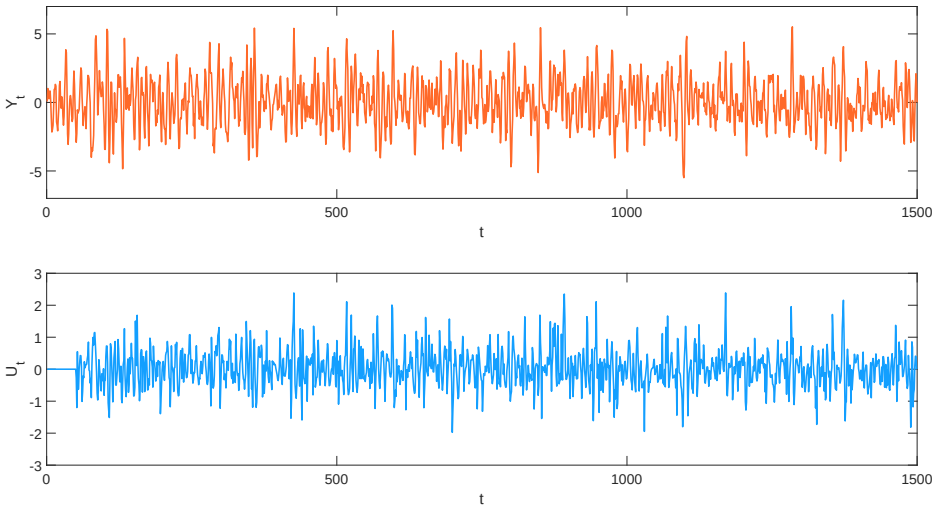

Figure 5.4: Output and input trajectories for current control system.

best achievable $E[Y_t^T Y_t]$ for a given $E[U_t^T U_t]$ in networked model predictive control is larger than that in the centralized case. Therefore, the benchmark control performance for the centralized case is not achievable by a networked model predictive control system with random communication delays. If conventional LQG tradeoff curve is used as the criterion for performance assessment, even if the networked model predictive control system is well designed, it is highly likely to show a poor control performance and may lead engineers to search for non-existent networked model predictive controllers. Further, although performance of the current controller varies with time, the distances from its operating points to the proposed time-varying MPC performance tradeoff curves for different time intervals are similar. Thus, the proposed time-varying MPC performance tradeoff curve can give consistent and more reasonable assessment results for a networked model predictive control system with random communication delays.

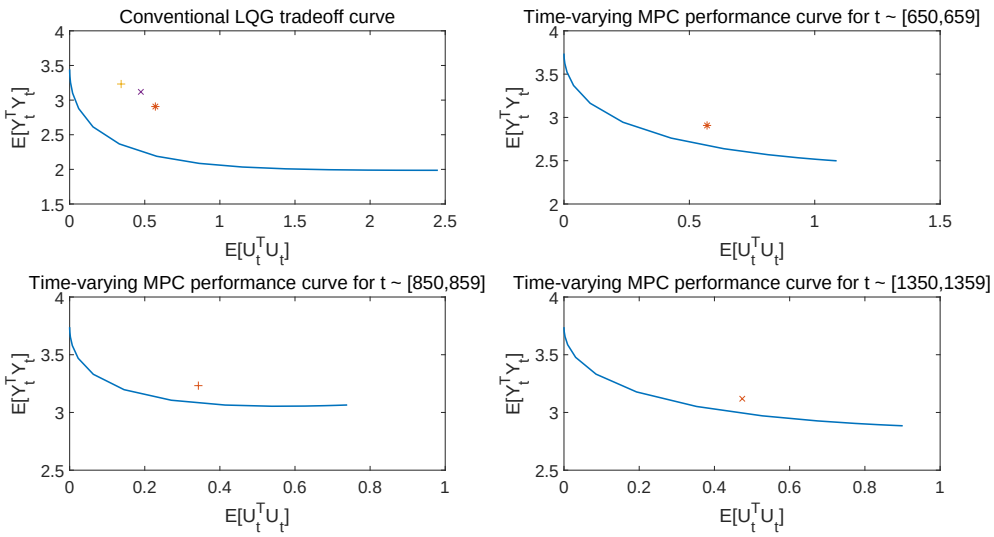

Figure 5.5: The time-varying MPC performance tradeoff curves for different time intervals.

5.5 Conclusions

In this chapter, a time-varying MPC performance tradeoff curve is designed for control performance assessment of networked model predictive control systems with random communication delays. Sensor-to-controller communication delay and controller-to-actuator communication delay are considered simultaneously. These two kinds of communication delays are both modeled as first order Markov chains with known transition probabilities. An explicit solution to time-varying MPC is derived, and the time-varying MPC performance tradeoff curve is proposed based on it. The obtained tradeoff curve can be used to evaluate how much potential of performance improvement an existing model predictive controller has by tuning or redesigning it. Finally, A numerical example is provided to demonstrate the effectiveness of the proposed work.

Chapter 6

Concluding Remarks and Future Works

6.1 Concluding remarks

The focus of this thesis is on finding the limits of control performance for DNCSs and NCSs with random communication delays. A number of distributed networked control and networked control solutions both numerically and analytically have been developed to optimize variance control objectives. Further, based on the proposed control algorithms, strategies for obtaining limits of control performance from process models or from routine operating data are provided for control performance assessment.

Chapter 2 proposes the limits of minimum variance control performance for DNCSs with random communication delays. A fixed network topology is presented for DNCSs where each subsystem in the network can communicate directly with all the other subsystems. Output communication delays and system time delays serve as the most fundamental performance limitations in distributed networked control, and are fully considered in the proposed distributed output feedback controllers design. An optimization-based solution to minimum variance control of DNCSs with time-invariant communication delays is developed. Then,

this control design is extend to study of the limits of control performance in terms of variance for DNCSs by considering boundary values of random communication delays.

However, minimum variance control is usually not practical for real process operation due to its demand for excessive control effort and poor robustness. As an alternative, a distributed LQG control framework is developed in chapter 3 to further consider input communication delays and control effort penalty. The optimal structures of distributed state feedback controllers and distributed observers are presented. And the non-applicability of separation principle in distributed networked control is illustrated. An algorithm is proposed for designing distributed controllers and distributed observers simultaneously, based on which the lower and upper LQG tradeoff curves can be obtained to characterize the limits of LQG control performance for DNCSs with random communication delays.

In Chapter 4, a practical LTV minimum variance benchmark is developed for NCSs with random communication delays, where the *a priori* knowledge of the interactor matrix is not required. Sensor-to-controller communication delay and controller-to-actuator communication delay are modeled as independent random variables. An explicit solution to the LTV minimum variance benchmark is derived for NCSs with the simple interactor matrix. Furthermore, this result is extended to the development of a practical LTV minimum variance benchmark for NCSs with the general interactor matrix by using OIM and RIM. The proposed benchmark is shown achievable by a physically implementable control and can be estimated from routine operating data directly.

MPC is widely applied in the synthesis and analysis of NCSs due to its ability to incorporate inequality constraints and compensate communication delays. In Chapter 5, a time-varying MPC performance tradeoff curve is proposed to characterize the limits of control performance for networked model predictive control systems with random communication delays. Sensor-to-controller communication delay and controller-to-actuator communication delay are considered as first order Markov chains with known transition probabilities. An explicit solution to time-varying MPC of NCSs is derived by minimizing the expectation of

a quadratic cost function over all possible future communication delays in the prediction horizon. Based on this control design, the time-varying MPC performance tradeoff curve is presented for control performance assessment of networked model predictive control systems. Furthermore, a strategy is provided for obtaining the time-varying MPC performance tradeoff curve from process model.

6.2 Recommendations for future works

Control performance assessment of DNCSs and NCSs is a relatively new research area. The results presented in this thesis address some of the fundamental issues under this theory. As stated in this thesis, investigating limit of control performance is just the first step of control performance assessment. Estimation of the benchmark control performance from routine operating data is necessary for industrial applications. Furthermore, communication delays and system time delays are the most fundamental limitations on the achievable control performance for designing automatic control systems over network. Considering more realistic performance limitations will complicate the problem and pose as stumbling blocks in applying these ideas. The emphasis in future research must be to develop control performance assessment techniques that are user friendly to industrial application and simple to understand. Future development in this and related areas should consider the following problems:

1. Estimation of the benchmark control performance from routine operating data normally relies on an explicit solution to the control problem. For this purpose, exploring explicit solutions to distributed minimum variance control and distributed LQG control has great theoretical and practical value.

2. Controllers and observers of different subsystems are centrally designed and then applied distributedly in this thesis. Although such a strategy can provide the best achievable control performance, some advantages of distributed networked control may be

lost in the meantime. Limit of control performance for designing subsystem controllers and observers distributedly is worthy of further investigation.

3. In practice, communication within a DNCS can be restricted to neighbouring subsystems or extensively exist between a majority of subsystems. Development of approaches for investigating limits of distributed networked control performance under different kinds of communication network topology is of interest.

4. The unitary interactor is an all-pass term, factorization of such a unitary interactor matrix does not change the spectral property of the underlying system. This property of the unitary interactor matrix is desirable for minimum variance control of stationary systems. NCSs are naturally non-stationary due to the presence of random communication delays. Instead of deriving a bound on the benchmark control of NCSs based on OIM and RIM, estimating the true LTV minimum variance benchmark using the unitary interactor matrix would have great industrial appeal.

5. Limits of control performance for DNCSs and NCSs with non-minimum phase zeros should be taken into account.

6. Hard constraints should also be taken into account in practice. This would require an optimization procedure, for which the convex optimization may provide the solution.

Bibliography

[1] B. Huang and S.L. Shah. *Control loop performance assessment: Theory and applications*. Springer-Verlag, 1999.

[2] T.C. Yang. Networked control system: a brief survey. *Control Theory and Applications*, 153(4):403–412, 2006.

[3] R.A. Gupta and M.Y. Chow. Networked control system: Overview and research trends. *IEEE Transactions on Industrial Electronics*, 57(7):2527–2535, 2010.

[4] P.D. Christofides, R. Scattolini, D. Munoz de la Pena, and J. Liu. Distributed model predictive control: A tutorial review and future research directions. *Computers & Chemical Engineering*, 51:21–41, 2013.

[5] R. Scattolini. Architectures for distributed and hierarchical model predictive control–a review. *Journal of Process Control*, 19(5):723–731, 2009.

[6] Y. Tipsuwan and M.Y. Chow. Control methodologies in networked control systems. *Control engineering practice*, 11(10):1099–1111, 2003.

[7] G.C. Walsh and H. Ye. Scheduling of networked control systems. *IEEE control systems magazine*, 21(1):57–65, 2001.

[8] B.T. Stewart, S.J. Wright, and J.B. Rawlings. Cooperative distributed model predictive control for nonlinear systems. *Journal of Process Control*, 21(5):698–704, 2011.

[9] X. Yin, K. Arulmaran, J. Liu, and J. Zeng. Subsystem decomposition and configuration for distributed state estimation. *AIChE journal*, 62(6):1995–2003, 2016.

[10] J. Nilsson, B. Bernhardsson, and B. Wittenmark. Stochastic analysis and control of real-time systems with random time delays. *Automatica*, 34(1):57–64, 1998.

[11] Z. Wang and F. Yang. Robust filtering for uncertain linear systems with delayed states and outputs. *IEEE Transactions on Circuits and Systems I: Fundamental Theory and Applications*, 49(1):125–130, 2002.

[12] X. Ge, F. Yang, and Q.L. Han. Distributed networked control systems: A brief overview. *Information Sciences*, 380:117–131, 2017.

[13] B.T. Stewart, A.N. Venkat, J.B. Rawlings, S.J. Wright, and G. Pannocchia. Cooperative distributed model predictive control. *Systems & Control Letters*, 59(8):460–469, 2010.

[14] Z. Wang and X. Wang. Optimal distributed control for networked control systems with delays. *arXiv preprint arXiv:1312.3543*, 2013.

[15] S. Tatikonda and S. Mitter. Control under communication constraints. *IEEE Transactions on Automatic Control*, 49(7):1056–1068, 2004.

[16] J.P. Hespanha, P. Naghshtabrizi, and Y. Xu. A survey of recent results in networked control systems. *Proceedings of the IEEE*, 95(1):138–162, 2007.

[17] W. Zhang, M.S. Branicky, and S.M. Phillips. Stability of networked control systems. *IEEE control systems magazine*, 21(1):84–99, 2001.

[18] G.C. Goodwin, H. Haimovich, D.E. Quevedo, and J.S. Welsh. A moving horizon approach to networked control system design. *IEEE Transactions on Automatic Control*, 49(9):1427–1445, 2004.

[19] R. Krtolica, Ü. Özgüner, H. Chan, H. Göktas, J. Winkelman, and M. Liubakka. Stability of linear feedback systems with random communication delays. *International Journal of Control*, 59(4):925–953, 1994.

[20] L. Zhang, Y. Shi, T. Chen, and B. Huang. A new method for stabilization of networked control systems with random delays. *IEEE Transactions on Automatic Control*, 50(8):1177–1181, 2005.

[21] G.P. Liu, J.X. Mu, D. Rees, and S.C. Chai. Design and stability analysis of networked control systems with random communication time delay using the modified MPC. *International Journal of Control*, 79(4):288–297, 2006.

[22] M. Jelali. An overview of control performance assessment technology and industrial applications. *Control Engineering Practice*, 14(5):441–466, 2006.

[23] S.J. Qin. Control performance monitoring–a review and assessment. *Computers & Chemical Engineering*, 23(2):173–186, 1998.

[24] T.J. Harris. Assessment of control loop performance. *The Canadian Journal of Chemical Engineering*, 67(5):856–861, 1989.

[25] L. Desborough and T. Harris. Performance assessment measures for univariate feedback control. *The Canadian Journal of Chemical Engineering*, 70(6):1186–1197, 1992.

[26] M.L. Tyler and M. Morari. Performance assessment for unstable and nonminimum-phase systems. *IFAC Proceedings Volumes*, 28(12):187–192, 1995.

[27] W.A. Wolovich and P.L. Falb. Invariants and canonical forms under dynamic compensation. *SIAM Journal on Control and Optimization*, 14(6):996–1008, 1976.

[28] G.C. Goodwin and K.S. Sin. *Adaptive filtering prediction and control*. Courier Corporation, 2014.

[29] Y. Peng and M. Kinnaert. Explicit solution to the singular LQ regulation problem. *IEEE Transactions on Automatic Control*, 37(5):633–636, 1992.

[30] B. Huang, S.L. Shah, and E.K. Kwok. Good, bad or optimal? Performance assessment of multivariable processes. *Automatica*, 33(6):1175–1183, 1997.

[31] T.J. Harris, F. Boudreau, and J.F. MacGregor. Performance assessment of multivariable feedback controllers. *Automatica*, 32(11):1505–1518, 1996.

[32] B. Huang, S.L. Shah, and H. Fujii. Identification of the time delay/interactor matrix for MIMO systems using closed-loop data. *IFAC Proceedings Volumes*, 29(1):6149–6154, 1996.

[33] B. Huang and S.L. Shah. Practical issues in multivariable feedback control performance assessment. *Journal of Process Control*, 8(5-6):421–430, 1998.

[34] A. Horch and A.J. Isaksson. A modified index for control performance assessment. *Journal of Process Control*, 9(6):475–483, 1999.

[35] B. Huang, S.L. Shah, and R. Miller. Feedforward plus feedback controller performance assessment of MIMO systems. *IEEE Transactions on Control Systems Technology*, 8(3):580–587, 2000.

[36] R. Kadali and B. Huang. Multivariate controller performance assessment without interactor matrix–A subspace approach. *IFAC Proceedings Volumes*, 37(1):535–540, 2004.

[37] B.S. Ko and T.F. Edgar. Performance assessment of multivariable feedback control systems. *Automatica*, 37(6):899–905, 2001.

[38] C.A. McNabb and S.J. Qin. Projection based MIMO control performance monitoring: I–Covariance monitoring in state space. *Journal of Process Control*, 13(8):739–757, 2003.

[39] B. Huang, S.X. Ding, and N. Thornhill. Practical solutions to multivariate feedback control performance assessment problem: reduced a priori knowledge of interactor matrices. *Journal of Process Control*, 15(5):573–583, 2005.

[40] H. Xia, P. Majecki, A. Ordys, and M. Grimble. Performance assessment of MIMO systems based on I/O delay information. *Journal of Process Control*, 16(4):373–383, 2006.

[41] F. Olaleye, B. Huang, and E. Tamayo. Performance assessment of control loops with time-variant disturbance dynamics. *Journal of Process Control*, 14(8):867–877, 2004.

[42] B. Huang. Performance assessment of processes with abrupt changes of disturbances. *The Canadian Journal of Chemical Engineering*, 77(5):1044–1054, 1999.

[43] Z. Li and R.J. Evans. Minimum-variance control of linear time-varying systems. *Automatica*, 33(8):1531–1537, 1997.

[44] B. Huang. Minimum variance control and performance assessment of time-variant processes. *Journal of Process Control*, 12(6):707–719, 2002.

[45] F. Olaleye, B. Huang, and E. Tamayo. Industrial applications of a feedback controller performance assessment of time-variant processes. *Industrial & engineering chemistry research*, 43(2):597–607, 2004.

[46] Q. Xu, C. Zhao, D. Zhang, A. An, and C. Zhang. Data-driven LQG benchmaking for economic performance assessment of advanced process control systems. In *Proceedings of the 2011 American Control Conference*, pages 5085–5090. IEEE, 2011.

[47] M.J. Grimble. Controller performance benchmarking and tuning using generalised minimum variance control. *Automatica*, 38(12):2111–2119, 2002.

[48] P. Majecki and M.J. Grimble. GMV and restricted-structure GMV controller performance assessment multivariable case. In *Proceedings of the 2004 American Control Conference*, volume 1, pages 697–702. IEEE, 2004.

[49] C. Dai and S.H. Yang. Controller performance assessment with a LQG benchmark obtained by using the subspace method. *Proc. Control*, 2004.

[50] R. Kadali and B. Huang. Controller performance analysis with LQG benchmark obtained under closed loop conditions. *ISA transactions*, 41(4):521–537, 2002.

[51] N.D. Pour, B. Huang, and S.L. Shah. Performance assessment of advanced supervisory–regulatory control systems with subspace LQG benchmark. *Automatica*, 46(8):1363–1368, 2010.

[52] R.H. Julien, M.W. Foley, and W.R. Cluett. Performance assessment using a model predictive control benchmark. *Journal of Process Control*, 14(4):441–456, 2004.

[53] J. Schäfer and A. Cinar. Multivariable MPC system performance assessment, monitoring, and diagnosis. *Journal of process control*, 14(2):113–129, 2004.

[54] Y. Zhang and M.A. Henson. A performance measure for constrained model predictive controllers. In *1999 European Control Conference (ECC)*, pages 918–923. IEEE, 1999.

[55] B.S. Ko and T.F. Edgar. Performance assessment of constrained model predictive control systems. *AIChE Journal*, 47(6):1363–1371, 2001.

[56] O.A. Sotomayor and D. Odloak. Performance assessment of model predictive control systems. *IFAC Proceedings Volumes*, 39(2):875–880, 2006.

[57] F. Xu, B. Huang, and E.C. Tamayo. Assessment of economic performance of model predictive control through variance/constraint tuning. *IFAC Proceedings Volumes*, 39(2):899–904, 2006.

[58] C. Zhao, Y. Zhao, H. Su, and B. Huang. Economic performance assessment of advanced process control with LQG benchmarking. *Journal of process control*, 19(4):557–569, 2009.

[59] B. Huang, S.L. Shah, and H. Fujii. The unitary interactor matrix and its estimation using closed-loop data. *Journal of Process Control*, 7(3):195–207, 1997.

[60] S.L. Shah, C. Mohtadi, and D.W. Clarke. Multivariable adaptive control without a prior knowledge of the delay matrix. *Systems & Control Letters*, 9(4):295–306, 1987.

[61] M. Rashedi, J. Liu, and B. Huang. Communication delays and data losses in distributed adaptive high-gain EKF. *AIChE Journal*, 62(12):4321–4333, 2016.

[62] J.B. Lasserre. Global optimization with polynomials and the problem of moments. *SIAM Journal on Optimization*, 11(3):796–817, 2001.

[63] D. Henrion and J.B. Lasserre. Gloptipoly: Global optimization over polynomials with Matlab and SeDuMi. *ACM Transactions on Mathematical Software (TOMS)*, 29(2):165–194, 2003.

[64] E.L. Kaltofen, B. Li, Z. Yang, and L. Zhi. Exact certification in global polynomial optimization via sums-of-squares of rational functions with rational coefficients. *Journal of Symbolic Computation*, 47(1):1–15, 2012.

[65] G. Chesi. LMI techniques for optimization over polynomials in control: a survey. *IEEE Transactions on Automatic Control*, 55(11):2500–2510, 2010.

[66] M.C. De Oliveira, J.C. Geromel, and J. Bernussou. Extended H2 and H norm characterizations and controller parametrizations for discrete-time systems. *International Journal of Control*, 75(9):666–679, 2002.

[67] A. Hassibi, J. How, and S. Boyd. A path-following method for solving BMI problems in control. In *Proceedings of the 1999 American Control Conference (Cat. No. 99CH36251)*, volume 2, pages 1385–1389. IEEE, 1999.

[68] C.D. Meyer. *Matrix analysis and applied linear algebra*, volume 71. Siam, 2000.

[69] S.J. Qin and J. Yu. Recent developments in multivariable controller performance monitoring. *Journal of Process Control*, 17(3):221–227, 2007.

[70] M. Morari and E. Zafiriou. *Robust process control*. Morari, 1989.

[71] L. Ljung. System identification. *Wiley encyclopedia of electrical and electronics engineering*, pages 1–19, 1999.

[72] K. Liu. Identification of linear time-varying systems. *Journal of Sound and Vibration*, 206(4):487–505, 1997.

[73] M. Bertha and J.C. Golinval. Identification of non-stationary dynamical systems using multivariate ARMA models. *Mechanical Systems and Signal Processing*, 88:166–179, 2017.

[74] X. Yin and J. Liu. Subsystem decomposition of process networks for simultaneous distributed state estimation and control. *AIChE Journal*, 65(3):904–914, 2019.

[75] J. Richalet. Industrial applications of model based predictive control. *Automatica*, 29(5):1251–1274, 1993.

[76] J. Wu, L. Zhang, and T. Chen. An MPC approach to networked control design. In *2007 Chinese Control Conference*, pages 10–14. IEEE, 2007.

[77] B. Huang and R. Kadali. *Dynamic modeling, predictive control and performance monitoring: a data-driven subspace approach*. Springer, 2008.

[78] L.R. Rabiner. A tutorial on hidden markov models and selected applications in speech recognition. *Proceedings of the IEEE*, 77(2):257–286, 1989.

[79] T. Knudsen. Consistency analysis of subspace identification methods based on a linear regression approach. *Automatica*, 37(1):81–89, 2001.

[80] R.R. Bitmead, M. Gevers, and V. Wertz. Adaptive optimal control the thinking man's GPC. 1990.

[81] M.A. Woodbury. Inverting modified matrices. *Memorandum report*, 42(106):336, 1950.

Appendix A

Mathematical Backgrounds and Derivations of Chapter 4

A.1 Calculation of LTV transfer function matrices

1. Commutativity law

$$V(k)W(k) = \sum_{i=0}^{n}\sum_{j=0}^{m} v_i(k)w_j(k-i)q^{-(i+j)}$$
$$W(k)V(k) = \sum_{j=0}^{m}\sum_{i=0}^{n} w_j(k)v_i(k-j)q^{-(i+j)}$$

Thus, $V(k)W(k) \neq W(k)V(k)$, and the multiplication of LTV transfer function matrices does not satisfy commutativity law.

2. Associativity law

$$
\begin{aligned}
&[W(k)V(k)]X(k) \\
=&\sum_{i=0}^{n}\sum_{j=0}^{m} v_i(k)w_j(k-i)q^{-(i+j)}(\sum_{p=0}^{l} x_p(k)q^{-p}) \\
=&\sum_{i=0}^{n}\sum_{j=0}^{m}\sum_{p=0}^{l} v_i(k)w_j(k-i)x_p(k-i-j)q^{-(i+j+p)}
\end{aligned}
$$

$$
\begin{aligned}
&V(k)[W(k)X(k)] \\
=&(\sum_{i=0}^{n} v_i(k)q^{-i})\sum_{j=0}^{m}\sum_{p=0}^{l} w_j(k)x_p(k-j)q^{-(j+p)} \\
=&\sum_{i=0}^{n}\sum_{j=0}^{m}\sum_{p=0}^{l} v_i(k)w_j(k-i)x_p(k-i-j)q^{-(i+j+p)}
\end{aligned}
$$

Therefore, $[W(k)V(k)]X(k) = V(k)[W(k)X(k)]$, and the multiplication of LTV transfer function matrices satisfies associativity law.

3. Distributive law

$$
\begin{aligned}
&[V(k)+W(k)]X(k) \\
=&\{\sum_{i=0}^{m}[v_i(k)+w_i(k)]q^{-i}+\sum_{j=m+1}^{n} v_j(k)q^{-j}\}(\sum_{p=0}^{l} x_p(k)q^{-p}) \\
=&\sum_{i=0}^{m}\sum_{p=0}^{l}[v_i(k)+w_i(k)]x_p(k-i)q^{-(p+i)}+\sum_{j=m+1}^{n}\sum_{p=0}^{l} v_j(k)x_p(k-j)q^{-(p+j)}
\end{aligned}
$$

$$
\begin{aligned}
&V(k)X(k) + W(k)X(k) \\
=&\sum_{j=0}^{n}\sum_{p=0}^{l} v_j(k)x_p(k-j)q^{-(j+p)} + \sum_{i=0}^{m}\sum_{p=0}^{l} w_i(k)x_p(k-i)q^{-(p+i)} \\
=&\sum_{i=0}^{m}\sum_{p=0}^{l}[v_i(k)+w_i(k)]x_p(k-i)q^{-(p+i)} + \sum_{j=m+1}^{n}\sum_{p=0}^{l} v_j(k)x_p(k-j)q^{-(p+j)}
\end{aligned}
$$

Then, $[V(k)+W(k)]X(k) = V(k)X(k) + W(k)X(k)$, and the multiplication of LTV transfer function matrices satisfies distributive law.

4. Inversion

Equating coefficients of both sides of equations (4.9) and (4.10), yields

$$
\begin{cases}
wl_0(k)w_0(k) = 1 \\
wl_0(k)w_1(k) + wl_1(k)w_0(k-1) = 0 \\
wl_0(k)w_2(k) + wl_1(k)w_1(k-1) + wl_2(k)w_0(k-2) = 0 \\
\vdots
\end{cases}
$$

and

$$
\begin{cases}
w_0(k)wr_0(k) = 1 \\
w_0(k)wr_1(k) + w_1(k)wr_0(k-1) = 0 \\
w_0(k)wr_2(k) + w_1(k)wr_1(k-1) + w_2(k)wr_0(k-2) = 0 \\
\vdots
\end{cases}
$$

Solving the above two equation sets yields

$$
\begin{cases}
wl_0(k) = wr_0(k) = w_0^{-1}(k) \\
wl_1(k) = wr_1(k) = -w_0^{-1}(k)w_1(k)w_0^{-1}(k-1) \\
wl_2(k) = wr_2(k) = w_0^{-1}(k)[w_1(k)w_0^{-1}(k-1)w_1(k-1) - w_2(k)]w_0^{-1}(k-2) \\
\vdots
\end{cases}
$$

Then, $WL(k) = WR(k)$, the left inverse of an LTV transfer function matrix is equal to its right inverse.

A.2 Detailed derivations of LTV minimum variance benchmark for NCSs with the simple interactor matrix

The LTV minimum variance control law and the corresponding LTV minimum variance benchmark are derived as follows. For the system shown in equation (4.1), the closed-loop output under the LTV control law $U_k = -C(k)q^{-d_{sc}(k)}Y_k$ can be written as

$$Y_k = (1 + q^{-d_s}\tilde{T}q^{-d_{ca}(k)}C(k)q^{-d_{sc}(k)})^{-1}Na_k \tag{A.1}$$

According to the properties introduced in Section 4.3.1, LTV transfer function matrices can be treated as matrices in both multiplication and inverse. Thus, we apply the well-known matrix inverse lemma [81] to equation (A.1) and yields

$$Y_k = [I - q^{-d_s}\tilde{T}(1 + q^{-d_{ca}(k)}C(k)q^{-d_{sc}(k)}q^{-d_s}\tilde{T})^{-1}q^{-d_{ca}(k)}C(k)q^{-d_{sc}(k)}]Na_k \tag{A.2}$$

Let us define

$$\begin{aligned} M(k) =& q^{-d_s}\tilde{T}(I + q^{-d_{ca}(k)}C(k)q^{-d_{sc}(k)}q^{-d_s}\tilde{T})^{-1}q^{-d_{ca}(k)}C(k)q^{-d_{sc}(k)} \\ =& \tilde{T}[(I + q^{-d_{ca}(k)}C(k)q^{-d_{sc}(k)}q^{-d_s}\tilde{T})q^{d_s}]^{-1}q^{-d_{ca}(k)}C(k)q^{-d_{sc}(k)} \\ =& \tilde{T}[q^{d_s}(I + q^{-d_s}q^{-d_{ca}(k)}C(k)q^{-d_{sc}(k)}q^{-d_s}\tilde{T}q^{d_s})]^{-1}q^{-d_{ca}(k)}C(k)q^{-d_{sc}(k)} \\ =& \tilde{T}(I + q^{-d_s}q^{-d_{ca}(k)}C(k)q^{-d_{sc}(k)}q^{-d_s}\tilde{T}q^{d_s})^{-1}q^{-d_s}q^{-d_{ca}(k)}C(k)q^{-d_{sc}(k)} \end{aligned} \tag{A.3}$$

From equation (4.6) it follows that

$$\begin{aligned} M(k) =&\tilde{T}(I + C(k - d_s - d_{ca}(k - d_s))q^{-d_s - d_{ca}(k-d_s) - d_{sc}(k - d_s - d_{ca}(k-d_s))}\tilde{T})^{-1} \\ & C(k - d_s - d_{ca}(k - d_s))q^{-d_s - d_{ca}(k-d_s) - d_{sc}(k - d_s - d_{ca}(k-d_s))} \\ =&\tilde{T}(I + C(k - d_{co}(k))q^{-d_{so}(k)}\tilde{T})^{-1}C(k - d_{co}(k))q^{-d_{so}(k)} \end{aligned} \tag{A.4}$$

where we define

$$Q(k) = \tilde{T}(I + C(k - d_{co}(k))q^{-d_{so}(k)}\tilde{T})^{-1}C(k - d_{co}(k)) \tag{A.5}$$

Further, the disturbance transfer function matrix N is divided to two parts based on the Diophantine equation:

$$N = F(k) + R(k)q^{-d_{so}(k)} \tag{A.6}$$

where, $F(k)$ is the LTV polynomial matrix consisting of the first $d_{so}(k)$ terms in the impulse response form of N, and $R(k)q^{-d_{so}(k)}$ is the remaining LTV transfer function matrix in N. In equation (A.6), coefficient matrices in $F(k)$ and $R(k)$ are consistent with those in N, and only the order of $F(k)$ varies with time. Substituting equations (A.4)-(A.6) into equation (A.1) yields

$$\begin{aligned} Y_k =&(I - M(k))(F(k) + R(k)q^{-d_{so}(k)})a_k \\ =&F(k)a_k + R(k)q^{-d_{so}(k)}a_k - Q(k)F(k - d_{so}(k))q^{-d_{so}(k)}a_k \\ & - Q(k)R(k - d_{so}(k))q^{-d_{so}(k-d_{so}(k)) - d_{so}(k)}a_k \\ =&F(k)a_k + L(k)a_k \end{aligned} \tag{A.7}$$

where

$$L_k = R(k)q^{-d_{so}(k)} - Q(k)F(k-d_{so}(k))q^{-d_{so}(k)} - Q(k)R(k-d_{so}(k))q^{-d_{so}(k-d_{so}(k))-d_{so}(k)} \tag{A.8}$$

In equation (A.7), $F(k)$ is a LTV polynomial matrix of q^{-1} with order $d_{so}(k)-1$, and each term in $L(k)$ has at least time delay $d_{so}(k)$. Thus, $F(k)a_k$ is independent of $L(k)a_k$, and we have

$$\begin{aligned} E[Y_k^T Y_k] &= E[(F(k)a_k)^T(F(k)a_k)] + E[(L(k)a_k)^T(L(k)a_k)] \\ &\geq E[(F(k)a_k)^T(F(k)a_k)] \end{aligned} \tag{A.9}$$

Since $F(k)$ is independent of the designed LTV control law $C(k)$, the term $F(k)a_k$ in the closed-loop output Y_k is feedback controller-invariant. Thus, the term $F(k)a_k$ provides the most fundamental measure of $E[Y_k^T Y_k]$, and $E[Y_k^T Y_k]$ is minimized when $L(k)=0$. So, the LTV control law $C(k)$ that minimizes $E[Y_k^T Y_k]$ satisfies

$$R(k)q^{-d_{so}(k)} - Q(k)(F(k-d_{so}(k))q^{-d_{so}(k)} + R(k-d_{so}(k))q^{-d_{so}(k-d_{so}(k))-d_{so}(k)}) = 0 \tag{A.10}$$

Substitute equation (A.5), equation (A.10) can be rearranged as

$$\begin{aligned} C(k-d_{co}(k)) =& \tilde{T}^{-1}[(F(k-d_{so}(k))q^{-d_{so}(k)} + R(k-d_{so}(k))q^{-d_{so}(k-d_{so}(k))-d_{so}(k)}) \\ & (R(k)q^{-d_{so}(k)})^{-1} - q^{-d_{so}(k)}]^{-1} \\ =& \tilde{T}^{-1}[(F(k-d_{so}(k))q^{-d_{so}(k)} + q^{-d_{so}(k)}R(k)q^{-d_{so}(k)}) \\ & (R(k)q^{-d_{so}(k)})^{-1} - q^{-d_{so}(k)}]^{-1} \\ =& \tilde{T}^{-1}[F(k-d_{so}(k))(R(k)q^{-d_{so}(k)}(q^{-d_{so}(k)})^{-1})^{-1}]^{-1} \\ =& \tilde{T}^{-1}R(k)F^{-1}(k-d_{so}(k)) \end{aligned} \tag{A.11}$$

where $\tilde{T}$ and $F(k)$ are invertible according to the assumptions made in Section 1.2.2. To get the LTV control law $C(k)$, substituting equations (4.11) and (4.12) into equation (A.11) yields

$$C(k' - d_s - d_{ca}(k' - d_s)) = \tilde{T}^{-1}R(k')F^{-1}(k' - d_s - d_{ca}(k' - d_s) - d_{sc}(k' - d_s - d_{ca}(k' - d_s))) \tag{A.12}$$

If we define $k'' = k' - d_s$, we can get

$$C(k'' - d_{ca}(k'')) = \tilde{T}^{-1}R(k'' + d_s)F^{-1}(k'' - d_{ca}(k'') - d_{sc}(k'' - d_{ca}(k''))) \tag{A.13}$$

Further, defining $k = k'' - d_{ca}(k'')$, we have

$$C(k) = \tilde{T}^{-1}R(k + d_{ca}(k'') + d_s)F^{-1}(k - d_{sc}(k)) \tag{A.14}$$

A.3 Parameters of the reactor-separator process

Table A.1: Steady state values, system parameters and controller parameters of the reactor-separator process

Parameter	Value	Units	Parameter	Value	Units	Parameter	Value
H_1	29.8	m	A_1	3	m^2	P_1	4.944×10^4
x_{A1}	0.4524	wt(%)	A_2	3	m^2	I_1	1420
x_{B1}	0.4809	wt(%)	A_3	1.5	m^2	D_1	6.611×10^4
T_1	440.47	K	ρ	1	kg/m^3	N_1	1.852
H_2	30	m	C_p	2.5	kJ/kg K	P_2	-210.8
x_{A2}	0.4336	wt(%)	x_{A0}	1	wt(%)	I_2	-843.2
x_{B2}	0.4917	wt(%)	T_{10}	313	K	D_2	0
T_2	438.05	K	T_{20}	313	K	N_2	0
H_3	32.7	m	k_A	0.8	1/s	P_3	-7.533×10^4
x_{A3}	0.2006	wt(%)	k_B	0.6	1/s	I_3	-4167
x_{B3}	0.6286	wt(%)	E_A/R	900	K	D_3	-3.273×10^5
T_3	444.13	K	E_B/R	1500	K	N_3	3.014
F_{f1}	5.4	kg/s	ΔH_A	-40	kJ/kg		
Q_1	1000	kJ/s	ΔH_B	-55	kJ/kg		
F_{f2}	5.04	kg/s	α_A	3.5	m		
Q_2	1000	kJ/s	α_B	1.1	m		
F_R	55.4	kg/s	α_C	0.5	m		
Q_3	1000	kJ/s					

Appendix B

Detailed Derivations of Chapter 5

B.1 Proof of positive semi-definite matrix

According to equation (5.31), we define

$$M = \sum_{\delta_{t-\tau_t+1}=0}^{\bar{\delta}} \cdots \sum_{\delta_{t+N}=0}^{\bar{\delta}} \prod_{i=t-\tau_t}^{t+N-1} \lambda^{\delta}_{\delta_i \delta_{i+1}} V_{pref}^T H_f^N|_{\tau_t}^T H_f^N|_{\tau_t} V_{pref}$$

where $\prod_{i=t-\tau_t}^{t+N-1} \lambda^{\delta}_{\delta_i \delta_{i+1}} \geq 0$ and $H_f^N|_{\tau_t}^T H_f^N|_{\tau_t}$ is a positive semi-definite matrix. Thus, we have $V_{pref}^T H_f^N|_{\tau_t}^T H_f^N|_{\tau_t} V_{pref} \geq 0$ for any possible V_{pref}, and subsequently we can obtain $M \geq 0$ for any possible V_{pref}. Then, in equation (5.34)

$$M = (U_{pref}^J)^T \Upsilon^N|_{\tau_t} \, U_{pref}^J \geq 0$$

for any possible U_{pref}^J. Thus, $\Upsilon^N|_{\tau_t}$ is proven to be a positive semi-definite matrix.